Spectral and Coherence Estimates on Electroencephalogram recordings during arithmetical tasks

Ana Filipa Teixeira Borges

Dissertação apresentada na Faculdade de Ciências
e Tecnologia da Universidade Nova de Lisboa para
obtenção do Grau de Mestre em Engenharia Biomédica

Coordenadores: Prof. Carla Quintão Silva

LISBOA

2009

À minha família querida

Acknowledgments

First of all, I would like to thank my thesis advisors. In particular, Prof. Carla Silva for her enthusiastic way of teaching, all her efforts and the way she believed in me to this work since the first moment and Prof. Giuseppe Baselli, for his endeavors attempts to make this work possible and supporting guidance both, during my stay in Italy and the work developed here. I thank also Professor Mário Secca for his efforts in bureaucratic procedures regarding my stay abroad.

I thank also Marcella Laganà and Roberta Carabalona for their help and the data they provide me in the *Polo Tecnologico della Fondazione Don Gnocchi*.

I am grateful also to Ana Carolina Sousa, the person responsible for the acquisition of the data in the *Instituto de Biofísica e Engenharia Biomédica*.

A special thanking word to John Peter for his valuable suggestions on the arithmetical protocol and to all the volunteers of this work.

To my cousin, Pedro Teixeira, a thanking word for introducing me in the *Latex* typesetting world.

So many thank's to my friends, you know who you are, I must say that more than the support and all the moments we shared, every singularity of their personalities has inspired me in a profound way, I like so much each one exactly the way they are. I would like to thank Iolanda and Mariana for all the time we lived together, friends can really be family.

I express my gratitude also to all my family and specially to my grandma and grandpa, even though they are far away I feel them all around.

A thanking word also to Enrico, for the way he is always present in my ups and nows and shares with me everything. I would like to thank also the Scofone family for their support.

I thank my little sister, she might think Science is for nerds but her presence and constant support are a source of inspiration and proud to me.

In the end but not the least, I deeply, deeply thank my mother, she gave everything I am and she is everything I want to be.

Contents

List of Figures

List of Tables

Acronyms

EEG Electroencephalography

MEG Magnetoencephalography

CNS Central Nervous System

CSF Cerebral Spinal Fluid

AP Action Potential

PSP Postsynaptic Potentials

ATP Adenosine Triphosphate

EPSP Excitatory Postsynaptic Potentials

IPSP Inhibitory Postsynaptic Potentials

fMRI functional Magnetic Resonance Imaging

SMR Sensorimotorrhythm

EOG Electrooculography

EMG Electromiography

ECG Electrocardiography

ADC Analogue-to-Digital Converter

SPECT Single-photon Emission Tomography

PET Positron Emission Tomography

MRS Magnetic Resonance Spectroscopy

HEG Hemoencephalography

TMS Transcranial Magnetic Stimulation

EROS Event-related Optical Signals

NIRS Near-Infrared Spectroscopy

BOLD Blood Oxygen Level Dependent

DTT Difusion Tensor Tractography

WVD Wigner-Ville Distribution

WT Wavelet Transform

HOS High-Order Statistics

CFT Continuous Fourier Transform

DFT Discrete Fourier Transform

FFT Fast Fourier Transform

WOSA Weighted Overlapping Segment Averaging Estimation

STFT Short Time Fourier Transform

FT Fourier Transform

CWT Continuous Wavelet Transform

OCD Obsessive-Cmpulsive Disorder

WM Working Memory

CC Corpus Callosum

MSC Magnitude Squared Coherence

ERSP Event-Related Spectral Perturbation

ITLC Inter-Trial Linear Coherence

ITPC Inter-Trial Linear Coherence

ERCOH Event-Related Cross-Coherence

ERP Event-Related Potential

ICA Independent Component Analysis

PCA Principal Components Analysis

Abstract

Activation in brain areas during mental calculation can be assessed by techniques such as Positron Emission Tomography (PET) and Functional Magnetic Resonance (fMRI), however this information does not regard synchronization of distant brain regions in a given frequency. Following the fact that brain networks have distinct resonance properties, a correlation between the specificity of frequency and a particular brain circuit is expected. A way of evaluating brain's functional connectivity is trough measuring coherence between Electroencephalographic (EEG) channels. This work focus on the analysis of spectral differences and coherence between electrodes, during arithmetic calculation. The selected frequency bands were theta (4-7 Hz), alpha (8-12 Hz), beta (12-30 Hz) and gamma (above 30Hz).

The coherence algorithm was previously tested in simulated data in diverse conditions and levels of confidence were obtained trough a surrogation procedure. Analysis of real data comprised two protocols, the former related to only one individual in a mental task using arithmetical computations as stimuli and the latter, a mental calculation task of backward counting with eyes closed applied to 15 healthy volunteers. In the first procedure it was made a stationary and dynamical analysis of the power and coherence. In the last experiment, participants were asked about what strategy they use for calculation and power and coherence computed firstly for the whole recording and after for each minute separately aiming to look for coherence differences in time.

Simulation permitted to conclude that the method is well-suited to identify coupling in the frequency regions of interest in EEG, even though limited for higher frequencies. In the first experimental approach, results showing distinct information can be acquired depending on the method. Finally, mental calculation spectral and coherence results were related successfully with previous findings in the field, consistent results were obtained for alpha and beta bands, meanwhile theta appears correlated with suggestive results. It was not possible to discern between different mental calculation strategies with the current experimental protocol.

Coherence measure is shown to be an useful method in understanding mental calculation processes, though more research and improvements of the technique are needed.

Chapter 1

Preface

"In a world divided by culture, politics, religion and race, it is a relief to know one thing that stands above them - mathematics. The diversity among today's mathematicians shows that it scarcely matters who invents concepts or proves theorems; cold logic is immune to prejudice, whim and historical accident. And yet, throughout history, different families of humans have distilled the essence of the cosmos to capture the magic of numbers in many ways." (Pervez Hoodbhoy)

1.1 Context

Since early days there is an interest in understanding the functions that contribute to form what we can call the human identity as a species. Exploring mental processes such as language, emotion and memory have always kept live the attention of the scientific community. Conversely, investigation of other specific higher cognitive functions like mental calculation (arithmetical thinking) only came into focus in the last decades and a permanent discussion of its underlying mechanisms persists nowadays.

The functional aspect of the brain, in the same way, was always correlated with the specific zones firstly denominated by Brodmann in the turn of the twentieth century. Nowadays, parallel to specific regional functionality there is a growing interest in explaining how functional aspects result from interaction between the different parts. This interesting excerpt illustrates the relevance of this study, comparing brain networks to personal computers:

"The number of neurons in the human brain is approximately equal to the number of transistors in a modern personal computer. Compared with the

> computer that operates in the GHz range, the brain has a much lower firing rate (below ca. 1000 Hz), but a massive advantage in the interconnectivity between its basic units: a single neuron can have up to 1000 connections to other neurons, and in the entire human brain, there are approximately 100 trillions of neuronal connections. While computers are certainly faster and more reliable in straight-forward 'number crunching' computational tasks, the brain outperforms computers in reliability and accuracy when dealing with complex tasks such as language understanding, object recognition or planning and strategy development. Thus, it is likely that the brain's advantage in these tasks must be in the cooperation of the units, rather than the processing speed in the units. Therefore, connectivity in the brain is probably one of the most fundamental and challenging fields of study at this time. Useful theories on 'how the brain works' will certainly have to account for how the brain establishes, organizes, maintains and modifies its internal connectivity structure in space and time." (T. Koenig et al,2005 *in* [114])

This theory that cognition bases emerge from dynamic connections mediated by synchrony over diverse frequency bands was recently advanced from several authors [104, 38, 114] and the need for the use of techniques with high-temporal resolution (EEG, MEG) for this line of research strongly emphasized [38]. Nonetheless, a full comprehension of large-scale integration of brain networks during mental processes is still impossible. Mental calculation is no exception, the comprehensive work done regarding brain functional connectivity of arithmetical thought is unsatisfactory to clearly establish a paradigm sustaining the hypothesis of binding trough frequency.

1.2 Scope and Work Developed

The work involved studying the theoretical implications and practical constraints of the instrument chosen to evaluate this brain functional connectivity following mental tasks: coherence among electroencephalographic (EEG) signals. The main motivation regarding the technique was that even if there is an extensive research on its principles and experimental applications it is still not sufficiently developed for appliance in clinical protocols. So, the main goals of this thesis were validating the coherence measure technique as an useful tool for quantifying relations among brain zones in mental calculation tasks. The specific relevance in the scenario of all neuroimaging techniques is emphasized by the intrinsic capacity of detecting brain networks segregated by frequency.

The main questions of this thesis are: Is EEG coherence appropriate to measure functional correlation of distant brain areas? What are the main limitations of the algorithm applied? What other approaches can be followed to study coupling in mental calculation processing? Can mental calculation's patterns be depicted trough spectral and coherence measures? Can we find different wiring patterns following distinct strategies n mental calculation? What are the main drawbacks of such a protocol?

1.3 Outline of the Thesis

This thesis work is organized in chapters, each chapter as a distinct goal. Following the present preface, Chapter 2 elucidates the principal aspects regarding brain anatomy, physiology and functional aspects, a brief introduction to the electrical properties of the brain signals and the network structure of the brain. The third chapter explains succinctly the questions regarding the technique of acquiring the signals - EEG; important constraints and the context among other techniques are highlighted. The theoretical background in EEG coherence is developed in the immediate subsequent chapter, reviewing some approaches and subtleties of the technique, most of them necessary for the experimental work. The concepts of this Chapter are developed extensively, they correspond to the author's efforts of understanding all the potentialities of the coherence technique in EEG data and must be faced as a preliminary guide. Once this project will be continued by a colleague, it is assertive to include it in such a way, unifying well-established knowledge with more recent advances. Chapter 5 makes a concise introduction to the actual knowledge about mental calculation processing in the brain. Indeed, the first five chapters have a focus on theoretical aspects which are assumed thereafter in the next chapters.

The experimental work comprises three distinct parts: a first chapter (Chapter 6) in which the coherence algorithm is validated trough simulated data and two following chapters (Chapter 7 and 8) relative to real datasets. The former presents the study done with a first set of data of one healthy volunteer of different approaches and the latter, the detailed description of the experiment done with 15 healthy individuals. All these three chapters expose independently their methods, results and discussion.

The last chapter (Chapter 9) is devoted to the main conclusions of the work, reviewing the limitations and possible future improvements.

Chapter 2

The Brain:Anatomy, Physiology and Functional Connectivity

This chapter intends to provide a basic introduction to the anatomical and functional characteristics of the field of study of the present project - the brain. An accurate study of methodologies for optimization of brain inspection is not possible without a notion of brain's architecture and also the origin's of the biosignal measured with the Electroencephalogram. As an extension, an approach to the brain signal characteristics that can be revealed with EEG coherence measures of coupling is presented too, namely the patterns of brain functional connectivity among different zones of which intensity can be correlated with the level of coherence among EEG data.

2.1 Anatomy and Physiology of the Brain

The Brain is the part of the Central Nervous System (CNS) with the greater degree of enlargement and specialization, externally protected by the skull and more interiorly by protective membranes called meninges [126]. The CNS is composed by seven main parts [27] reported in Table 2.1 and Figure 2.1:

Both, the spinal cord and the brain are immersed in a fluid designated Cerebral Spinal Fluid (CSF) that relieves the pressure, inevitably present if the brain would be merely sitting in the top of the skull. The brain has also a subdivision in three large regions (see figure 2.1): the hindbrain, the midbrain and the forebrain. The brainstem is constituted by the first two, excepting the cerebellum.

The Main Parts of the Central Nervous System (CNS)	
Spinal Cord	Caudal part responsible for receiving and processing information from the limbs and trunk
Medulla oblongata	Situated immediately above the spinal, controls essentially autonomic functions like digestion, breathing and heart rate
Pons	Juxtaposed to the medulla, carrier of the information between the cerebral hemisphere and the cerebellum
Cerebellum	Mass behind the pons, it is the coordinator of voluntary muscle movement and takes a role in the learning of motor functions
Midbrain	Located rostral to the pons, it is responsible for sensory-motor function such as eye movement and visual/auditory reflexes.
Diencephalon	Rostrally positioned relative to the midbrain, it is composed by the thalamus (where the major part of the sensory information is processed and relayed to the cortical areas) and the hypothalamus (regulator of autonomic, endocrine and visceral functions)
Cerebral Hemispheres	Composed in their outer portion by the cerebral cortex and innerly by the basal ganglia (regulator of motor performance), the hippocampus (memory storage) and the amygdaloid nuclei (autonomic and endocrine responses of emotional states)

Table 2.1: *The main parts of the Central Nervous System and short description of its main functions.*

2.1.1 Brain and Cognition

The cerebral cortex being the outer portion of the cerebral hemispheres consists of large sheets of mostly layered neurons that involve other core structures, being the cognitive functions confined within the 1.5-4.5 mm of thickness of the cerebral cortex. The structure of the cortex is composed by gray matter and presents a highly convoluted surface comprising *gyri* (ridges), *sulci* (valleys) and *fissures* (deeper sulci) [126], the goal of such formations is to pack more cortical surface into the skull [76]. The more accentuated features divide the cortex in the following lobes: frontal, parietal, temporal and occipital (see Figure 2.2, part a)). The lobes display varied functions in neuronal processing that can be clearly centralized in one lobe or comprise more than one [76]. There are several possible criteria for the division of the cortex in functional areas [27]. One possible subdivision is based on the cytoarchitectonics, Brodmann (1909) was the first to perform this division and attribute numbers to the distinct functional units [76]. His model is still

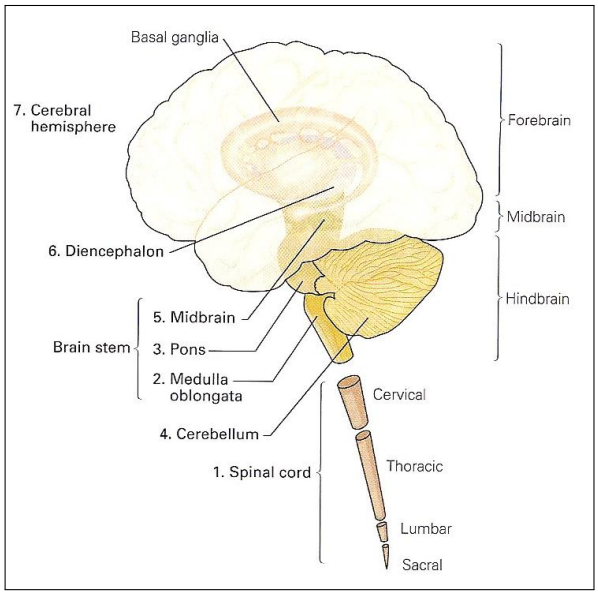

Figure 2.1: *The seven main parts of the Central Nervous System. (adapted from [27])*

prevalent with a lot of modifications suffered through the years, in Figure 2.2 part b) and c) one can see the division in the 52 distinct areas.

In a general way, the higher cognitive systems are often composed of networks whose individual units are located in distinct lobes, all the brain functions (sensory, motor or cognitive) rely on both cortical and subcortical components. The complex functional anatomy of the cortex will not be reviewed in an extensive way, merely the main functions will be highlighted. The frontal lobe is mainly divided in motor cortex and prefrontal cortex. The motor cortex has the precentral gyrus (also known as primary motor cortex (area M1) or Brodmann's area 4) and other areas responsible to contact with spinal cord and brainstem motor neurons. The prefrontal cortex is responsible for higher aspects of motor control, planning and execution of behavior and general tasks that include integration of information in a temporal scale. It is divided in several regions like e.g. the dorsolateral prefrontal cortex that has been implicated in working memory functions. In the parietal lobe, we have the somatosensory cortex composed by the postcentral gyrus and adjacent regions (Brodmann's areas 1,2 and 3 - see Figure 2.2), its main function is to receive the inputs from the thalamus and constitute information about pain, touch, temperature sense and limb prioception. The areas for visual processing are, on their turn, located in the occipital lobe. This latter includes the primary visual cortex (area V1 or Brodmann's area 17) that is responsible for receive the inputs of the lateral geniculate nucleous of the thalamus, starting the encoding of visual features like color, luminance, orientation and movement [76].

Traditionally, in a more strictly domain, there are some regions associated with specific functions, such as language has been related with Wernicke's area (posterior end of the superior temporal gyrus) and Broca's area (Brodmann 44 area) or face recognition

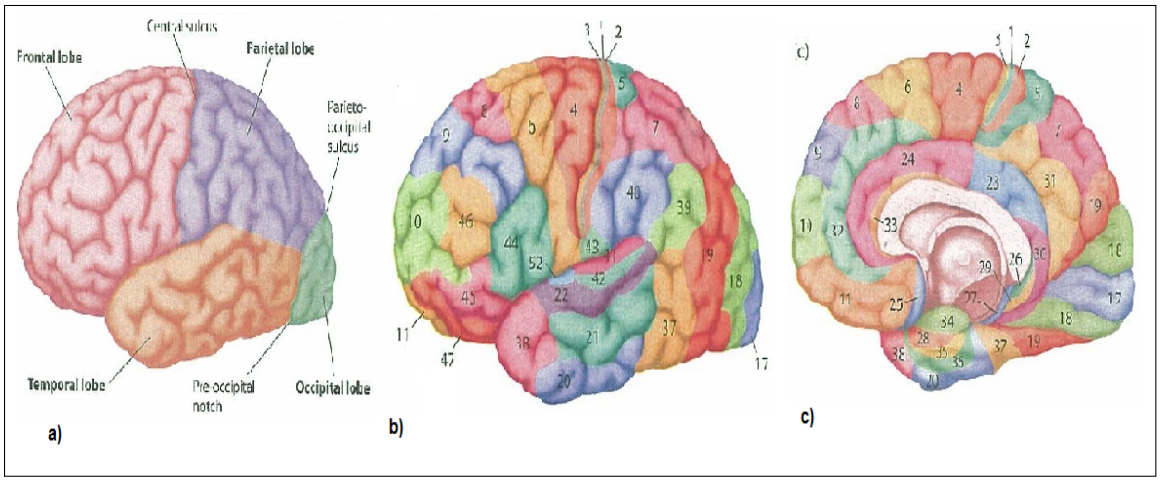

Figure 2.2: *Functional divisions of the cerebral cortex. In a) we can see the four main lobes in lateral view of the left hemisphere. Images b) and c) represent a lateral view of the left hemisphere and a medial view of the right hemisphere of the 52 Brodmann areas (one can see they are almost symmetrical). (adapted from [76])*

was connected to the right inferior temporal lobe just to cite some examples [40]. Moreover, there was a tendency to localize certain abilities in an hemisphere such as music and spatial processing in the right hemisphere and verbal and mathematical capacities in the left. Nowadays, however the general effort is to decentralize the focus on a hemisphere and try to locate sub-components of this higher tasks in specific regions in order to form a comprehensive picture.

2.1.2 Cytology of the Brain

Concerning now the ultrastructure, the neocortex (the evolutionary newest part of the cortex) has a multilayered structure formed by six distinct layers in the major part of the cases (see figure 2.3): the *molecular layer* (I) is the most superficial portion filled by the dendrites of deeper cells of the cortex; the *external granule cell layer* (II): the *external pyramidal cell layer* (III); the *internal granule cell layer* (IV); the *internal pyramidal cell layer* (V) and the *multiform layer* (VI) [27]. These layers have different constitutions and vary accordingly to the zone of the cortex. Of particular relevance are the pyramidal cells of layers III and V - these neurons are the major projection cortical neurons and their apical dendrites are the principal inputs of synaptic activity being in sum, the most expressive contribution for the EEG (see Figure 2.3).

The CNS is essentially composed by two different types of cells: the neurons and the glial cells - their individual and conjunct functionalities form the global brain activity. The proportion of neurons and neuroglial cells is 1 neuron for 10-50 glial cells

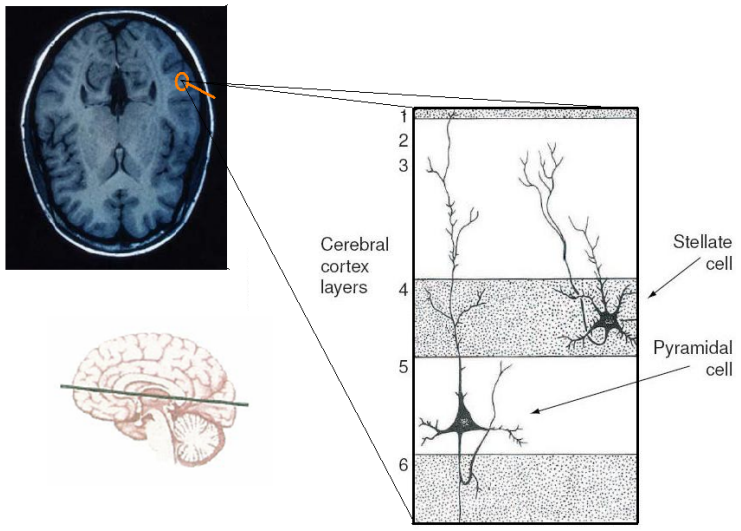

Figure 2.3: *Cortex viewed trough a MRI scan and schematic representation of the its ultrastructure, evidencing the pyramidal cells.*

and it is estimated that exist approximately 10^{11} neurons in the CNS [40]. The neurons are the units responsible for the integration and transmission of the nerve impulses and, even though the glial cells have important and diversified functions they do not have a direct role in the processing of information on the brain, the only known correlations are: active role in regulation of the extracellular K^+ which, as we will see below has an important role concerning neuronal information transmission and, additionally, their activity as myelin producers.

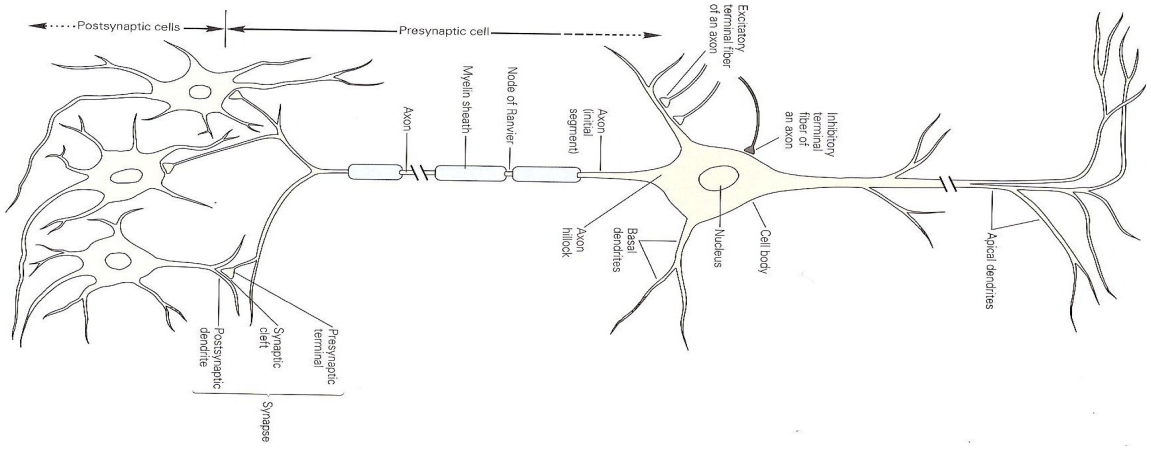

Figure 2.4: *The structure of the neuron.(adapted from [27])*

The neurons can differ in size and shape among mammalians although they have always present a differentiation in four zones (see Figure 2.4): the dendrites (arborizations from the cell body outwardly) form the sensory receptor area, the cell body

itself corresponding to the metabolic and integrator center of the cell, the diametrically opposed to the dendritic zone axon that covers a site where propagated action potentials are generated and is mainly responsible for the conduction of information into the final part - the synaptic endings. These latter are the terminal branches of the neuron composed by synaptic knobs where synaptic neurotransmitters are stored and consist in the last differentiated functional area of the neuron, performing the transport of the information for other neurons or muscles. Many axons are surrounded by a sheath of myelin (a protein-lipid complex that wraps around the axon) interrupted only by zones called nodes of Ranvier, the importance of such myelin coating is its insulating properties that make the current trough practically inexistent, originating the so-called saltatory conduction which is proved to be really efficient as it yields a 50 times faster conduction when compared to the fastest unmyelinated neurons.

Concerning the morphology, one neuron may be classified in unipolar, pseudo-unipolar, bipolar or multipolar (see fig. 2.5). Although, the last are commonly the ones found in the nervous system. Moreover, it is in this group in which are present the cortical pyramidal cells, their importance will be emphasized in the next Chapter.

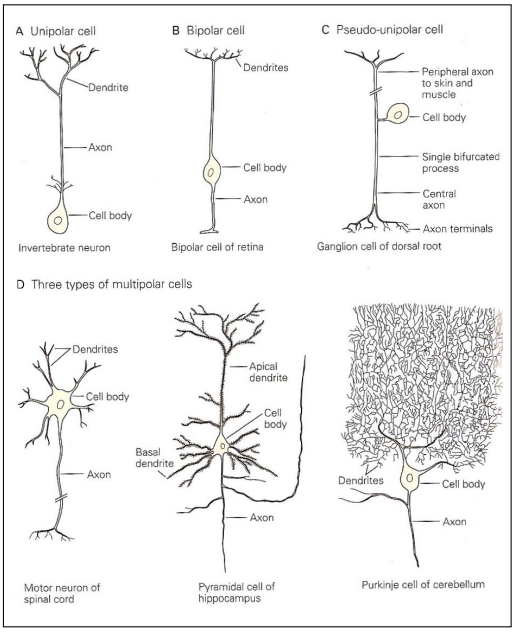

Figure 2.5: *Classification of neurons in agreement with the number of processes originated in the cell body. A - Unipolars; B - Bipolars; C - Pseudo-unipolars and D - multipolars.(adapted from [27])*

2.2 Neurophysiological Background of the Brain Signals

First of all, it is well established that the brain has an intrinsic electrical activity consistent with its functions. This electrical activity is rapid and transient and yields the information to be conducted along great distances in the brain. The question is what is the precise origin of this brain's patterns. Albeit an explicative model was not fully developed, there were made several attempts such as physiological approaches and computational modeling of the neural networks.

On a cellular context, this activity has a neuronal origin and is expressed mainly in the generation of action potentials (AP) and postsynaptic potentials (PSP) excitatory and inhibitory. Both are related to changes of potential in the neuronal membrane, being the formers activated when the membrane's potential surpasses a threshold and the latter in cases a subthreshold is exceeded [26]. The measured EEG is the reflection of these potentials in the surface of the cortex and on the surface of the scalp and actually, only the PSP have a significant contribution to the signals obtained in the Electroencephalogram.

In a general way, the macroscopic insight provided by EEG can be correlated with the electrical activity of a large amount of dipoles (the electrical field of cell's membrane is approximated to that of a dipole) parallel-oriented and synchronized so, the only cortical cells which obey to that pattern and though supply that information are the pyramidal cells (see previous section for cortical layer's information). As it is easily deduced, if the cells bodies and dendrites of the neurons were positioned randomly the global influence of the synaptic currents would be null. Considering instead that some group of cells have a special arrangement, a difference of potential can be generated. These cells, the pyramidal neurons have, as it was said primordially, a behavior approximated to a dipole: the inputs of the synapses of the apical dendritic arborizations cause a depolarization of the dendritic membrane - consequently, a bilateral subthreshold current flow is initiated between the dendrites and the cell body. The two poles correspond to the extracellular medium of the soma - *source* (+) and the top of the apical dendritic tree - *sink* (-). On the contrary, the non pyramidal cells do not contribute expressively to the EEG due to the constrained arrangement of their dendritic zones and body cells that form a closed-field situation and as so, at a considerable distance their net potential is zero [126].

Controversially, the AP have a small contribute as argued in [26] for the scalp recording, the signal is sensitively a summation of excitatory and inhibitory postsynaptic potentials since the two, have a role in the modulation of the processing of neuronal information. These PSP's influence the signal accordingly to their character (+ ou -), orientation and their position relative to the electrode's zone [126]. Moreover, the reason

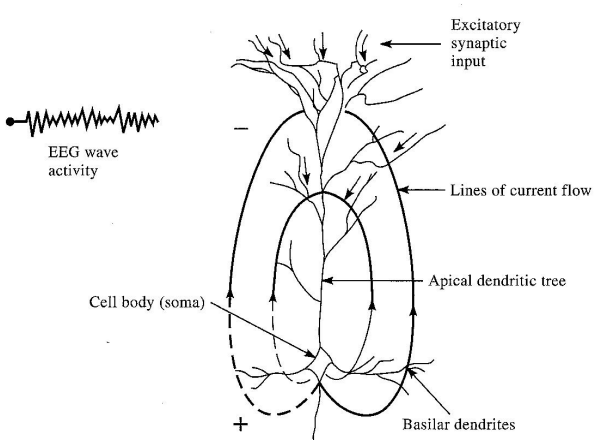

Figure 2.6: *Generated potential field in a pyramidal cell due to a excitatory synaptic input in the dendritic tree, note that for inhibitory stimulation the current flow would spread inversely. (adapted from [126])*

why the EEG's signal corresponds to populations of synchronized neurons is because small contributions of reduced groups of neurons do not construct signals possible to measure in the scalp as the transmembranar currents of the neurons would cancel out and not sum effectively [89].

For a better comprehension of the EEG signals' origins an introduction of the bases of this potentials is needed. Briefly, they are mainly modulated by the flow of ions in the cell membranes, the principal ions involved are the K^+, Na^+, Cl^-, Ca^{++} and other large organic anions, the voltage-gated channels of these ions contribute to form the electrical signals. The neurons resting state usually have a potential of nearly -70 mV [26].

The mechanisms underlying the maintenance of this potential are based in the balance between the passive flow of ions trough non-voltage dependent channels and active ion pumps. The neurons are specially rich in ions like Ca^{2+}, Na^+, Cl^- which concentrate themselves preferentially in the exterior of the cells and K^+ and other organic anions in the interior. The Na^+/K^+ pump maintains the intracellular concentration of these ions. The potential is held in that negative value because recurring to the hydrolysis of a molecular of ATP, for each three ions of Na^+ that are transported outwards only two ions of K^+ enter the neuron, causing the difference. Further, this pump contraries the passive flow of this two ions which is also a factor that contribute for the resting potential due to the greater permeability of the membrane to the K^+ that flows to the outside the cell when compared to the Na^+ entering [27].

Concerning the action potentials, they initiate with a depolarization of the cell membrane, followed by a repolarization and a brief hyperpolarization until the previous

resting level is achieved, they last $\sim$ 2 ms but can last between 1-10 ms [27]. In the depolarization, the point where its rate start to increase is designed firing level or threshold and it is the value minimum for the generation of the action potential [40]. The threshold is dependent of the membrane's resistance and capacitance and also of the intracellular axial resistance along the axon [27]. The AP are governed by the all-or-none law i.e. they do not occur for subthreshold stimuli and maintain their shape even with stronger stimuli [40]. The existence of AP is regulated basically by the voltage-gated K^+ and Na^+ channels. When the depolarization occurs, these channels open and augment the permeability of the membrane to the ions, the Na^+ voltage-gated channels open first so the potential increases suddenly, the subsequent repolarization happens due to the open of the K^+ voltage-dependent channels and simultaneously closing of Na^+ channels. Finally, because of the delayed closure of the K^+ channels, the efflux of K^+ lasts a while causing a hyperpolarization before the recovering of the resting potential [40].

The hyperpolarization is also called refractory period, the action potentials are spread in the axons unidirectionally because of the existence of this period. The persistent openness of the K^+ voltage-dependent channels after restoration of the resting potential and the fact Na^+ channels have a few milliseconds inactive period after their aperture make impossible to generate an AP, guaranteeing only one sense of flow.

Considering now the generation of postsynaptic potentials, it is well-known that the neurons communicate with each other by means of synaptic junctions. The proportion of synapses in the forebrain is estimated in a number of 40,000 for each neuron. The synapses' clefts establish the connection between a portion of a presynaptic cell with a portion of the so-called postsynaptic cell. The transmission of information can be chemical (through intermediary neurotransmitters), electrical (trough physical contact of the cells by means of low-resistance bridges) or both, yet it is almost always chemical. In all cases, the transmission yields a potential in the postsynaptic cell that can be excitatory or inhibitory, that nature and the quantity of the formed potentials will be decisive to determine if an action potential is generated or not, permitting this condition a great versatility of the neuronal response which is such a desirable feature for a complex system like the brain. Extremely connected with that fact is the diversity of neurotransmitters and the way they combine - yielding also a strong level of plasticity to the transmission mechanism, the neurotransmitters stimulate directly or indirectly the open or closure of ion channels that will regulate postsynaptic potentials. As these potentials are low in voltage, in order to form an action potential conducting information there is a need for an integration of the potentials originated by diverse synapses, this integration may be spatial and/or temporal. The former is intended such as a summation of synaptic knobs acting simultaneously, controversially the latter relates to subsequent stimuli applied causing

new excitatory postsynaptic potentials (EPSP) in the temporal range before preliminary ones have occurred. The EPSP formed are though not all-or-none responses but show a dependency on the stimuli integrated. The temporal scale which this postsynaptic potentials follow is in the millisecond range, indeed all the EPSP and IPSP have at least a delay of $\sim 0.5ms$ (the minimum delay of a synapse) but, can be longer if there are many synapses on the chain. Moreover, there were reported cases of cortical neurons with latencies situated in a time of 100-500 ms [40].

A diametrically opposed view on the way cortical neurons form its postsynaptic potentials was first introduced in the early eighties with the work of Abeles [2] and it is based in the hypothesis of neurons acting as coincidence detectors instead of being temporal integrators. In [89] it is outstanded this vision with a competing character and not replacing at all the classic alternative of neurons as an integrate-and-fire. In their work, Koenig et al, suggests the prevalence of a mode depends on time, indeed if the mean interspike interval is shorter when compared with the time of integration, the coincidence detection would be the main process activated and, on the other hand, if it is longer the process of summing the potentials in a greater window would be preferred. The neuronal transmission would have in the former case a more rapid contour, being lesser than 5 milliseconds. Further, it hints the relevance of EEG data on the correlation of synchronized brain patterns and function, standing in the fact that the EEG signal obtained is a glimpse of the synchronization of assemblies of neurons and diverse studies developed with this technique concerning functional states or functional roles of cooperation between various areas in the brain have demonstrated an association between this synchronization and function, giving this idea a great support to the importance of synchronism in neuronal processes and consequently further pertinence to the studies in which this characteristic is highlighted as is the case of the present study. Several subsequent studies support this perspective as though expose some fragilities of it, some examples are the works in [108, 75, 8, 110] and recently [64].

2.3 Brain's Functional Connectivity

2.3.1 Introduction to Brain Networks

The biological neural structures and, particularly, the human brain have evolved in the sense of execution of high-level processes which make them natural systems with high complexity of behavior and underlying capacities of adaptability, learning and perceiving. The brain can be seen as a complex network composed of millions of sub-networks that are connected from a micro-level to a large-scale degree [61].

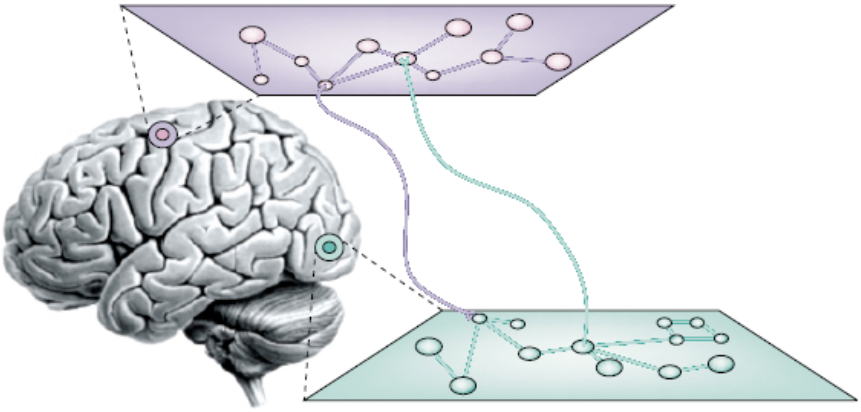

Figure 2.7: *Brain as a network. (reproduced from [38])*

The general idea that the brain works as a single unit composed by a group of different specialized centers (functional areas) appeared earlier than the nineteenth century, compounding a theory that was called *Holism*. However, in the precedent century a lot of studies on brain functions were done having in account the concept of localization in detriment of integration of activity, indeed attention was mostly centered to attribution of functions to specific zones and the primordial idea fell almost completely in oblivion. Controversially, later it was shown that it was right, actually studies based on individual components was proved insufficient for understand brain networks [65]. On such a context, the desirable diversity, specificity and adaptability of evolved structures seem to be acquired by the union of two important aspects: a great computational capacity inherent of the extremely large amount of neuronal intermediaries and a precisely designed connection network between all brain [99].

Based on that duality, it is easily perceived that for true and full comprehension of the mechanisms beneath higher level brain functions, an in-depth analysis of its global properties is needed. A detailed and profound knowledge of each functional parts separately is insufficient. Besides that, it was established that our brain's structure seems to obey to some principles of minimization, indeed the geometry of the brain reflects clearly a reduce of wiring cost and a minimization of global energy consumption simultaneously with the maintenance of maximal communication bandwidth [111].

Contemplating now other side of the problem, regarding to the dynamic activity in the cortical brain, it was noted in [104] that the work of the brain as a whole could not be entirely due to its anatomical connections, due its inherent topology but instead synchronization would depend on other factors. This observation born from the fact that there is an ever-changing systematic probability of synchronization and also, an internal coordination at the temporal scale not only in response of a stimulus. These discoveries were firstly supported by observations of visual cortical neurons that fire synchronously

with a precision of the order of millisecond [13].

The concept that synchronization of the neuronal cells can be a phenomenon related to the binding of information on the brain, as we can see, started to be discussed some decades ago and is nowadays an important subject of research. The binding problem, in a neuroscientific cognitive environment, refers to the way the brain proceeds a signal integration, segregated in space and time, causing an experiencing of singularity *i.e.* a feeling of perceiving an unique sensation. This crossing of information in the brain networks seems to be yielded with the support of two processes that were already introduced: the "binding by convergence" or "labeled line coding" and the "dynamic binding" accordingly to the designations in [104]. The former is related merely with the grouping of information by simple unification of axonal projections (the second designation assents on the fact each intermediary signal always the same conjunction of inputs) and the latter admits that neuronal responses that somehow conjunctively show their saliency in contrast to others are assumed to be bounded and even though, not linked anatomically they reveal themselves like belonging to the same level in the processing hierarchy.

Moreover, several studies conducted to the evidence that these mechanisms of dynamic coupling are ways of express such higher level brain functions like perception, cognition, consciousness and behavior [121]. Large-scale synchrony in the brain is pointed as the ultimate way brain orchestrate complicate expressions such as emotion, thought, perception and action that constitute our minds [38].

Chapter 3

Methods of Acquisition of the Signals of the Brain - EEG Acquisition

"Porque eu sou do tamanho do que vejo, E não do tamanho da minha altura."
Alberto Caeiro

In the previous section, I exposed some introductory remarks on the human brain, the cerebral cortex, the process of neuronal transmission of information across this highly-elaborated machine. On its turn, this chapter will concern with how we can extract, record and pre-process this extremely complex signal. In a nutshell, the basis of Electroencephalography will be studied, presenting also a brief discussion on the relevance of this technique on the current purposes.

3.1 First Steps and Recent Developments- Brief Review of Electroencephalogram History

Early in the second half of the XIX century, the first measurements of the electrical brain of cats and rabbits were made by a scientist named Richard Caton. He used a galvanometer to measure the currents and his work consists in the first approach in the study of the brain potentials, others followed his work namely, Beck in 1890, was the first to report brain rhythmic activity [26].

The first publish on the experiment of a human electroencephalogram was made

in 1929 by the German psychiatrist Hans Berger [10]. The importance of this finding was although limitedly recognized until a British neurophysiologist named Edgar Douglas Adrian showed this new technique with proved validity in the spring of 1934. Since that date, the EEG showed that has capacity to be consider nowadays an important resource in neuroscience clinical and research branches, it contributed expressively for new concepts in the epilepsies knowledge, other pathologies like brain tumor localization and clinical states like brain dead confirmation only to mention some earlier perspectives of utilization. Until mids of the twentieth century some of the most important research on EEG was concentrated mainly in observing the electrical activity of the brain, exploring the significance of brain waves and developing styles of recording the electroencephalogram [11].

Subsequently, a strong need for automation and the revolution of power computation yielded to the development of EEG quantitative techniques. Initially, these methods relied mainly in a frequency-related analysis. Progressively, in the eighties, nineties decades other concepts started to be applied to EEG analysis such as information theory-based methods and non-linear approaches [116].

Recently, the EEG was utilized also in a background of human-machine interaction concretely some brain waves recorded with the EEG (such as the mu rhythm or the P300) were used as channels of communication for those in disabled conditions [54].

Concluding, Electroencephalography opened an intense field for neuroclinical research, some examples of application more related with this dissertation will be given in section *4.8*. An important mark in its history is also its multimodal utilization with fMRI which will be referred in section *3.5*.

3.2 EEG Signal

The EEG signal is a temporally well-defined measure of the electrical fields of the brain amplified by a factor sensitively equal to 1000 [61]. The aspect of an EEG signal can be variate, composed by transients, spikes or apparent random events and rhythms.

Due to its high complexity, the electroencephalogram is not easy to analyze or classify. In addiction, the EEG is commonly in a range of $10 \sim 300\mu V$ and as though is prone to physiological or electrical noise [116]. In fact, the recording system, movements from the heart, muscles or eyes can affect strongly the electroencephalogram and filters must be applied to remove this contributions or an analysis considering its background noise must be followed (see further sections).

The signal can be described basically on the following characteristics: noisy and pseudo-stochastic, highly non-linear and essentially non-stationary (stationarity of a signal is the characteristic of preserving the same statistical properties such as mean, variance and frequency in time [127]).

3.2.1 EEG Rhythms

There were identified several rhythms in the electroencephalogram being related with different cognitive or physiological states of the brain (see Figure 3.1). A lot of studies contributed for the nowadays division of the EEG in the following frequency bands (although it is still somehow arbitrary and not standardized [101]): *delta* (0.1-4 Hz), *theta* (4-8 Hz), *alpha*(8-12 Hz), *sensorimotorrhythm SMR* - also called mu rhythm - (normally seen in the range 9-11 Hz in healthy individuals, sometimes mixing with β frequencies in 20 Hz [28]), *beta* (15-40 Hz) and *gamma* for above 40 Hz. Further, beta band can be splitted in smaller bands: *beta 1* (12-16 Hz or 15-18 Hz), *beta 2* (18-24 Hz) and beta 3 (24-30 or 30-40 Hz) [58].

This rhythmic activity in δ band is common during deep sleep (it shows high coherence in the scalp and elevate amplitudes (75-200 μV)), moreover it was recently addressed as important in large-scale cortical integration and developing a role in attention and language processing. On the other hand, α activity is observed in individuals awake specially in relaxing states with eyes closed in the posterior parts of the brain (this waves tend to suddenly disappear when some type of focused attention happens like a visual or mental task), when alpha's amplitude is high a proportional deactivation of cortical pattern is related, specially attached to highly perceptual tasks, memory and attention processes. SMR or μ rhythms may arise in the central part of the head and are implicated with activity of the sensoriomotor cortex only, being blocked when a motor function takes place. Sometimes, it is impossible to distinguish this rhythm from the strongest occipital alpha waves at the same frequency. The β rhythms usually appear in simultaneous with alpha blocking as are related with increased states of alertness and with the focused attention, functionally speaking their low amplitudes in the primary motor cortices are intimately associated when some movements are performed. Finally, *gamma* has been recognized for its association with higher levels of cognition like information processing (it was associated with visual awareness since the research performed by [13] in the cat visual cortex in late 80's), it gained a role in the binding of information problem and the onset of voluntary movements [26, 61].

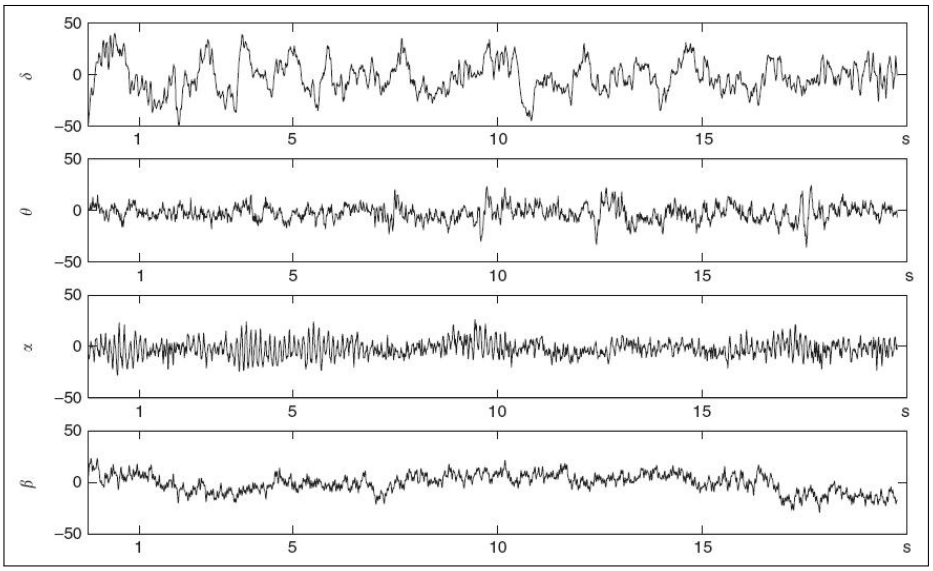

Figure 3.1: *The rhythms δ, θ, α and β of the brain.(adapted from [26])*

3.2.2 Variability of EEG

In the context of subject susceptibility, the electroencephalographic signals show significant variability between individuals, also gender, age, handedness and behavioral state of the subject influence the contribution of the different rhythms to the electroencephalogram. Factors like neuro-pathological cases, metabolic disorders or influence of drugs, can also constitute alterations to the normal EEG pattern. Differences among sexes were reported [44], namely neuroanatomical differences and a pronounced functional asymmetry in males, also handedness should be taking into account as it influences the lateralization of functional patterns in the brain (see [58] for some examples of studies). The degree of maturation of the EEG, implicated with age is also extremely important when elaborating conclusions because alterations among the human-scale of life and lead to wrong interpretations (see [26] for details on maturation of the EEG).

3.3 Protocols in EEG Acquisition

This section aims in studying the basis of EEG recording, an introductory view of the apparatus of Electroencephalography and main deals in acquisition and preprocessing are persecuted. There is a mention to the panoply of the ways of recording an EEG, nevertheless this project only contemplates a type of procedure so the subject is presented briefly. The EEG recording system can be divided in three distinct stages following the division showed in [116]: electrodes and head stage, preprocessing and quantitative EEG

and data storage - I will follow this logical division in my exposition. The figure below illustrates all the phases of the process.

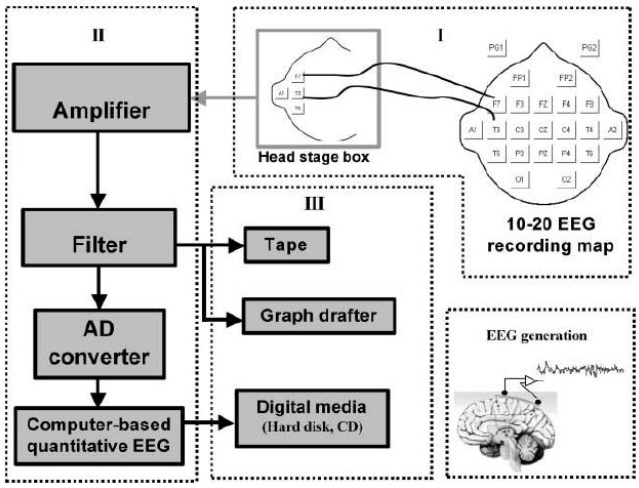

Figure 3.2: *Schematic representation of the EEG recording system divided in 3 parts - Electrodes and Head Stage (I), Preprocessing (II) and Data Storage (III). (extracted from [116])*

3.3.1 Electrodes and Head Stage

Accordingly with the information provided in the last sections, the electroencephalogram reflects the electrical activity of the surface of scalp, it furnishes a measure of the potential difference between two electrodes. A pair of electrodes is connected to a channel amplifier constituting a derivation (see subsequent section), trough a certain montage. This one can be *referential (unipolar)* - if the measured difference is always relative to one active electrode situated under the region of the brain we desire to study and the other, the reference electrode situated in a part of the body such as the earlobe, the nose, the mastoid, the chin, the neck or the scalp center and the *bipolar* recording setup – this considers the electrodes active and performs the difference between them. Besides these conventional montages, there are others that permits to individualize better the information of each channel, that is the case of the *common average reference* recording that subtracts to the channels the computed average of all recording electrode signals. With this performing the signal is not subjugated by local contamination although, instead is sensitive from artifacts in the whole brain. In fact, the system reference is made by means of connect all the electrodes to a common point trough equal high resistances [126]. Pragmatically, it can be implemented by linking the referential-ears, for using a common usual clinical example [58].

At last, there is a claimed reference-free technique called *Source derivation* or *Laplacian* recording. A more profound review on other strategies as well as the possible advantages and drawbacks of each of them is contemplated in [86, 29, 6] and will be stud-

ied better in the development of this thesis regarding problems in coherence identification (see section *4.7*).

Electrodes

The scalp electrodes are electrical potential sensors capable of detecting charges in a surface cortical surrounding area of 6 cm^2 and as deep as several millimeters [116]. The designation sensor is used for transducers that convert a physical measurand to an electric output [126] and such is this case in which a biopotential is converted in an electrical measure.

There are a lot of different types of electrodes such as needle and sphenoid electrodes but in clinical routine the ones commonly used due to the not invasive character are the surface electrodes. In order to obtain a meaningful signal is desirable that the connection scalp-electrode maintains an impedance nearly to 5 kOhms [26] so, to optimize the results usually the electrodes are cleaned with alcohol and a gel is applied in the contact to augment the conductivity and help electrodes remaining in the right position.

The 10-20 system

For a correct interpretation of information and also because of the need of comparing intra and inter-subject trials there were developed standardized ways of position and label the electrodes on the scalp. The actual system utilized is the International 10-20 system developed by Herbert Jasper in the fifties decade. This system is based on proportion and not in absolute values as though, it can be adapted to individual parameters.

Basically, accordingly with this system four anatomic points are chosen and the electrodes are positioned in proportional distances referenced to that marks. Indeed, there are used the point where the nose meets the fore head (nasion), the small salience of the skull at the back of the head (inion) and the small depressions in the front of the ears (preauricular points). The letters that label each electrode are also representative of the underlying brain areas: frontal pole (FP), frontal (F), parietal (P), central (C), temporal (T) and occipital (O) [58]. The labels are completed with the information of the lateralization of the electrodes: it is used even numbers for electrodes on the left, odd numbers for the ones in the right and *z* or *0* for the central line. The electrodes distance all 10 or 20% from the total distance between two landmarks (see figure 3.3) and that is the reason of the designation attributed to the system. Posterior extended versions of the former model were developed, being introduced further electrodes for a better coverage. Some

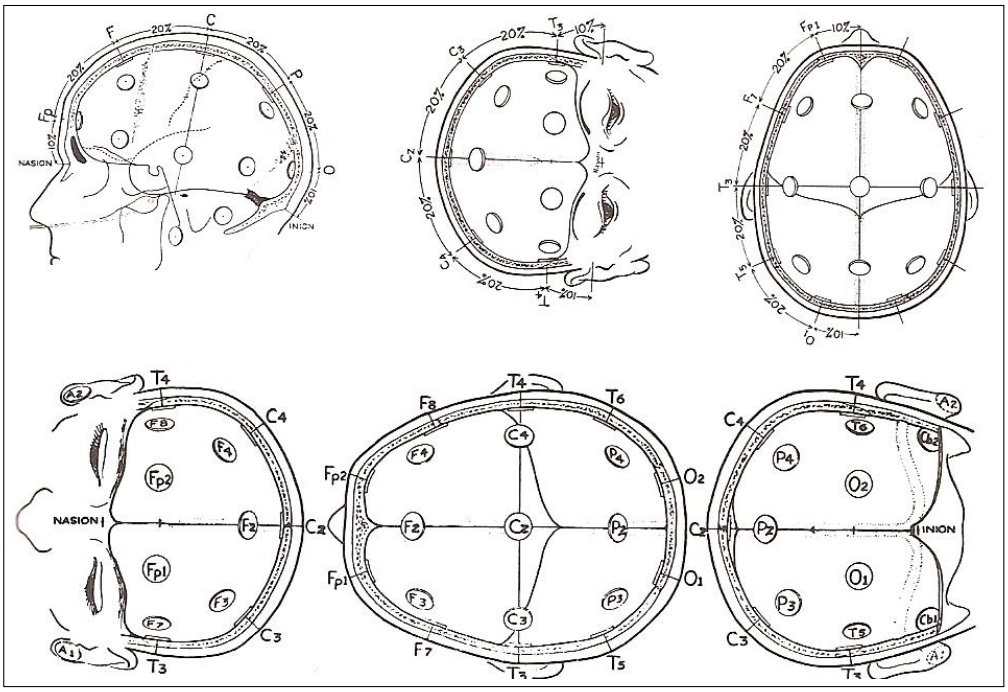

Figure 3.3: *The position of electrodes in the 10-20 system. (adapted from [126]*

electrodes were also re-labelled, namely T7/8 for T3/4 and P7/8 for T5/6 although this new adoption is not always followed [58].

Besides the electrodes of the 10-20 system usually are utilized also electrodes to monitor eye movement (EOG), electrocardiographic (ECG) and electromiographic (EMG) signals which must be segregated from the electrical activity provenient of the brain and treated as artifacts [26].

It is interesting to observe also the relation between the position of the electrodes and the regions of the brain and the underlying Brodmann areas. The Table 3.4 below resumes this information in an expressive way.

3.3.2 Preprocessing

The biosignals in which the signals from the brain are included have a signal frequency bandwidth situated in the range of 0.5-100 Hz with amplitudes typically located between 10-300 μV [116]. As any other equipment for measuring biopotentials, the Electroencephalograph has an amplification and filtering system. The amplifier must obey to some characteristics to suit the intrinsic properties of the EEG signal such as the ones mentioned earlier. More precisely it requires: a low level of noise, high common

Lobe	Gyrus	Brodmann Area	Site (Left/Right)
Frontal	Superior	10	Fp1/2
	Inferior	47	F7/8
	Medial	9	F3/4
	Medial	8	Fz
	Precentral	6	C3/4
	Superior	6	Cz
Temporal	Medial	21	T3/4
	Medial	37	T5/6
Parietal	Inferior	7	P3/4
	Precuneus	7	Pz
Occipital	Medial	19	O1/2

Figure 3.4: *The cortical areas and Brodmann areas underlying each electrode in the 10-20 system. [58])*

mode rejection ratio (typically, between 80 and 120 dB [79]) to minimize the artifacts due to common-mode voltages intrinsic in the utilization of bipolar electrodes, high input impedance (at least 10MΩ in modern amplifiers) to avoid excessive loading which would cause distortion, low output impedance relatively to the load impedance in order to maintain maximal fidelity, limited bandwidth to augment the signal-to-noise ratio, high gain (∼1000 or greater) in order to amplify the extremely low voltages of the electroencephalografic signal and yield its recording and processing, must have isolation and protection circuitry to protect the patient from microshocks and macroshocks and yield a quick calibration[126, 116]. It is relevant to refer that this necessary amplificatory stage produces the undesirable consequence of adding noise to the signal, filtering the signal and affecting the phase relationship between the diverse frequency components contained in the signal [101].

Regarding the filtering system, a routine electroencephalogram is usually sampled at a frequency of $\sim 250Hz$ which accordingly with the Nyquist law covers the interval of frequencies between 0-125 Hz. Sometimes, it may have a slight higher sampling rate in order to optimize the signal resolution. The DC component is uninteresting and as it was referred anteriorly the source impedance is high and the leads between the EEG apparatus and the patient are long making this technique susceptible to electrical noise specially the one originated from the power supply of 50 or 60 (USA) Hz, so it used a notch filter to remove this undesirable contribution. Further, the filters permit to select different bands of interest such as the ones introduced in the *EEG Signal's section.* The filters implemented in the modern circuits are based on operational amplifiers that use RC circuits for implement high-pass, low-pass and band-pass filters (see figure 3.5) [79].

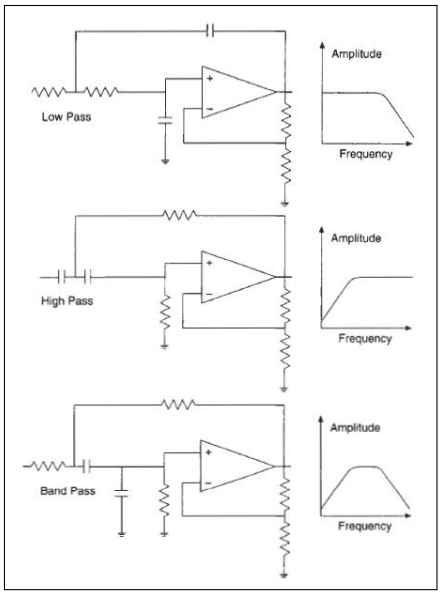

Figure 3.5: *Different types of basic filters and respective frequency response. (extracted from [79])*

3.3.3 Data Storage

In the early days of Electroencephalography, the EEG was recorded on a paper or saved in an analog tape [116]. Nowadays the analog EEG fell in disuse and it was entirely replaced by the digital EEG saved in hard disks or compact disks that is extremely more valuable for a quantitative analysis of the data. Due to the limitations of the computer memory and hardware there is a need to convert the analogue values to digital ones using for the effect a analogue-to-digital converter (ADC). This device is a restraining factor of the resolution of the Electroencephalogram, it is characterized by the amplitude resolution and the rate of digitization (sampling frequency) being the former given in 12 or 16 bits AD-conversion and the latter that being limited to the Nyquist theorem yields a resolution of the inverse of the sampling frequency[101].The ADC is composed by a converter, a clock that imposes the converting rate and the control logic, all bits are converted in parallel using highspeed precision comparators associated with a precision resistor network [79].

3.4 EEG in the context of other Brain study techniques

There are several techniques in the contemporary days used for making inferences of brain activity (*i.e.* for brain mapping) , offering each of them different advantages and drawbacks. As a matter of fact, the field of functional neuroimaging had become a leader argument of research in neuroscience and as a proof of that we have nowadays techniques of brain insight like *Functional Magnetic Resonance Imaging* (fMRI),

Single-photon Emission Tomography (SPECT), *Positron Emission Tomography* (PET), *Magnetoencephalography* (MEG), *Magnetic Resonance Spectroscopy* (MRS), *Hemoencephalography*(HEG), *Transcranial Magnetic Stimulation* (TMS), *Event-related Optical Signals*(EROS), *Near-Infrared Spectroscopy* (NIRS) as well as continuous and event-related *Electroencephalography* EEG [58][103].

3.4.1 EEG and an overview of the Hemodynamic Response based techniques

There are a lot of tools in brain imaging concerning principles related to the hemodynamic response, an explanation of each of them is not the goal of this thesis, I will merely focus in the fMRI, PET and TMS which are according with [103] the principal tools which have been used for studying functional connectivity as by means of correlation analysis of data of the formers or by conjunct use of the latter with other neuroimaging methods and though could be alternative solutions to the EEG coherence tool.

EEG and fMRI

Firstly, although the hemodynamic response based techniques seem promissory due to its better spatial resolution and capacity of yield information above the scalp EEG (they can study structures like the cerebellum or the subcortex) still, even if with the approximated resolution of one cubic millimeter of the fMRI which contains a great amount of pyramidal cells, the electrodes in the EEG can reach a total of more neurons [58].

Considering now the topic of computation of coherence for having insights of brain functional connectivity the further consideration is extremely relevant, having in mind that high cognitive performance of the brain requires the rapid integration of information through several sensorial and behavioral domains along widely distributed brain zones [39] it is important to have estimations of coherence with high resolution in time and as though the EEG with its excellent temporal resolution is a strong candidate for these studies. Indeed, the electroencephalogram has in its favor two powerful allies: simple to analyze in the frequency domain and truly precise in time. This characteristics support its utilization in functional connectivity studies of the brain in detriment of the fMRI - the BOLD signal has an obscure physiological origin and offers poor temporal resolution and as though correlation studies using this approach are not the better procedure. It is important also to emphasize that Electroencephalography permits a measure of neural activity in real time and not relies, like other neuroimaging techniques like fMRI and PET

in a measurement that is subject to the lag of the hemodynamic response [61].

As an extending advantage, the EEG rhythms play a role in information process along the brain and specially the highest information content is correlated with high-frequency rhythms (like gamma) that are originated from small neuron groups which are not so easily accessed by the other imaging techniques.

Further, Electroencephalography sums also others advantages namely, the fact that is by itself and comparing to others absolutely non expensive, its facility and portability being extremely utile when studying sensible populations like individuals with mental disorders and children that can be easily frightened by the magnetic resonance apparatus [58].

To conclude, EEG is a valuable technique due to its low-cost noninvasive and expedited procedure and portability, high precision in the temporal domain as well as a long story of seventy-five years of research on the maturation of this technique.

Still, there are other recent and not so explored methods for assessment of brain functional connectivity like the correlation analysis of PET or fMRI data or the combination of TMS with neuroimaging, although as it argued in [121] for studying brain coordination and self-organizing processes only the methods of EEG and MEG offer sufficient temporal resolution.

Towards a multimodal approach

This analysis would not be complete although without refer that its conjunct utilization with different techniques has been proven to be an enriched way of acquire information, making the research on co-registration technologies a promising field of work, even though still not clinically spread due to high economic cost and intrinsic difficulties such as the diminution of the quality of MR images by EEG and the potential risks for the patient and interference of the EEG signal by the MRI [95]. Besides all,it is pertinent to emphasize the importance of the alliance of these techniques combining high temporal resolution (EEG) with high spatial resolution (MRI). There are a lot of work done uniting this two like: texturing 3-dimensional reconstructions of the brain with the EEG using data from simultaneous MRI scan, combined functional MRI (fMRI) and EEG data with the linear inverse estimation method to the generation in real-time of spatio-temporal series of brain activity, linkage between the MRI T2-weighted image, the EEG coherence and power spectrum in traumatic brain injury, localization accurately performed of epilepsy by this combination for citing a few examples highlighted in [116]. Further, it is also important to notice that there are in general three diverse ways to combine EEG and

MRI: converging evidence, direct data fusion and computational neural modeling. For an example of application of a simultaneous EEG-fMRI the review in [95] introduces some of the key points of the methodology. Concerning the multi-modal scanning of EEG-PET it yields a lesser extent of artifact problems and it is shown to give consistent results, also the use of TMS combined with other functional neuroimaging technique was shown useful for study functional coupling. In the group of functional imaging, nowadays a recent technique is gaining prominence, its name is *Diffusion Tensor Tractography* (DTT) and yields better resolution above the voxel - based on the diffusivity principles of water molecules it permits to reconstruct the paths of white matter fibers and as though, can provide an insight of functional relation among different areas [103].

Still, considering the predominant role of temporal dynamics in the brain, alone it is natural to benefit from the EEG tool in a study of the functional connectivity of the brain.

3.4.2 EEG and MEG

These two techniques permit to obtain information of brain electrical activity, *i.e.* are the electrophysiological methods of mapping the brain. Magnetoencephalography (MEG) is a relatively new technology which is based on measuring the magnetic field generated by the pyramidal neurons. Once this magnetic field is perpendicular to the electric field, the sensors must be positioned tangentially to the apical dendrites. MEG offers above all its advantages the one that it does not require so much knowledge on the geometry of the head and volume conductive properties to modeling the signal. In fact, the head tissues are not magnetic and though have nearly the same magnetic permeability (μ) consequently the magnetic field can merely depend on the locations and orientations of the sources and the sensors. On the other hand, in the EEG there is an attenuation of the signal due to the skull and a distortion due to the so-called "shunting effect", phenomenon of a wide distribution of the electrical fields in the head surface caused by the difference in the electrical conductivity between the spinal fluid and the overlying skull [103].

Nevertheless, EEG is sensitive to the tangential and radial sources which is a clear advantage regarding the MEG that only detects electrical information concerning the tangential sources. MEG also implies extremely higher cost and it is more sensible to artifacts produced by head's movement, characteristics that make the EEG a extremely valuable option.

In addiction, sometimes it is assumed that MEG offers intrinsically better spatial

Detectability of cortical neuronal activity by EEG, MEG and PET/fMRI

Cortical neurons	Arrangement		Orientation to head surface		Synaptic input	
	Aligned	Random	Radial	Tangential	Excitatory	Inhibitory
EEG	Yes	No	Yes	Yes	Yes	No[a]
MEG	Yes	No	No	Yes	Yes	No[a]
PET/fMRI	Yes	Yes	Yes	Yes	Yes	Yes?

Yes, detectable; No, undetectable; ?, Controversial.
[a] Might be possible by analyzing the power change of rhythmic activity.

Figure 3.6: *Comparison of detection of cortical neuronal activity by EEG, MEG and PET/fMRI. (reproduced from [103])*

resolution than EEG conceals but this may not be true. Hence, due to the significant distance between the magnetometer coils and the sources MEG information shows a great extracranial coherence (field spread effects to the sensors), even in the cases the underlying sources are completely non correlated [94].

As a conclusion, both techniques cannot be seen as competitive between each other because in a certain way they salient different aspects of the neocortical dynamics, there are examples of studies that they have showed different aspects (see [103] for review of some) which means they can offer complementary information. In the work of [94] it is concluded that EEG coherence is preferentially sensitive to large-scale source distributions covering a significant part of gyral crowns and MEG coherence to small isolated dipole layers in sulcal walls, being always both affected by volume conduction (MEG in a lesser extent when electrodes are far away from each other), suggesting that the two tools yield information from different sources and that MEG does not cover a so wide field as the EEG. In that context, an important factor when choosing the preferred tool is to understand in what type of cortical sources it is the information we want to study, without knowing that it is difficult to decide *a priori* what is the best approach [103].

As a conclusion, Electroencephalography is a valuable way of studying brain functional relations and although showing some counterparts, it is a much lesser expensive and more mature technique, extracting information of a great number of sources.

3.5 EEG Temporal and Frequential Analysis

In the earlier days of Electroencephalography, its analysis relied mainly in visual inspection of the recordings made on paper. With the development of technology and the digital EEG this technique was on and on substituted or used with the aid of automatic ways of extract information [26]. Nowadays, this inspection is still a lot used for detection of transient features in an electroencephalogram trace.

In parallel, during the last decades were developed an extensive group of EEG quantitative methods, this process was evolving also in a consequence of the progresses in achieving superior power computation. EEG analysis methods can be generally classi-

fied into linear and nonlinear approaches. The conventional EEG analysis is based on the measure of the spectrum and has naturally, the implication of stationarity of EEG process although, EEG signal is non stationary and nonlinear in the most part of the cases and especially in pathological states of the brain.

Analysis evolved also in a way that provide relevant advantages in the way it can provide fine details on frequency and also where the dynamic changes of frequency occur in a temporal scale. The simplest of these approaches is the Short Time Fourier Transform (STFT) which permits increasing time resolution but not much, for more accurate computations it can be used or the Wigner-Ville Distribution (WVD) that is the FT of the autocorrelation function of a given signal with respect to a delay variable and offers a significant upgrade in time and frequency resolution. The Wavelet Transform that utilizes a scalable function instead of a fixed-scale window function provides an adaptive time-frequency analysis method outstanding selectively what we prefer to have more accuracy – time precision for transient waves, frequency accuracy for slow waveforms. This methods will be more in-depth highlighted in chapter 4.

Considering now the Nonlinear Methods, they assent basically in three subdivisions: Methods on Information Theory-Based Analysis, Methods on High Order Statistics and Chaotic Measures. All of these consider that EEG signals are random processes and enclosed in the first group exist (for measure of order/disorder of a time series) an extensive study of formalisms for calculation of Entropy Values and, for extracting relations of interdependence between different cortical areas, we may use the computation of Mutual Information. On the topic of High-Order Statistics (HOS) we must salient its importance relatively a first-order statistical analysis (power spectrum) once it provides information also in phase coupling (synchronization), it most commonly used calculations are the bi spectrum (which is the FT of the third-order cumulant) and bi coherence. Afterwards, to conclude the descriptions of Chaotic Measures can include nonlinear dynamic computations such as dimension estimation (correlation dimension, information dimension, capacity dimension and multifractal spectrum), Lyapunov exponent spectrum, Poincare maps, Kolmogorov-Sinai Entropy and Approximate Entropy [116].

In a synopsis, quantitative techniques have evolved from conventional frequency analysis (decomposing into delta, theta¸ alpha, beta and gamma frequency Bands) to diverse time, spectral and altogether time-frequency linear or nonlinear approaches. All lines of investigation are valuable tools, even if the nonlinear methods can exploit novel fine details of the EEG recordings, the traditional time or frequency analysis are the most generalized as clinical tools. In a comprehensive way, all types of analysis permit to obtain distinct measures regarding information on time, frequency or time-frequency, altogether they help to disentangle the complex mechanisms underlying mental processes.

Chapter 4

Coherence on Electroencephalography

"The real voyage of discovery consists not in seeking new landscapes but in having new eyes."**Marcel Proust**

The idea of this chapter is to cover all the basic theoretical details this work involved. Some parts are developed in an extensive way, sometimes with more detail than the absolutely necessary for the experimental work. The main goal was, having in mind that the present project will be continued by others, to give a solid background from which to start from, an ideal framework adapted for the present case-study. The specific theoretical considerations of each chapter are not presented here. Synthetically, the ultimate goal is to make an approach to the coherence tool in EEG applications.

4.1 Brief Historical Remarks on EEG Coherence

Studies on EEG Coherence started to being developed around forty years ago, D. O. Walter (1968) was the first to publish a work on relationships between EEG signals. Before that, studies on the subject were limited by the lack of adequate mathematical algorithms, computational power and software [127]. Consequently, the first full paper was published in 1970 by *Gersh and Goddard's* and was referred to studies on coherence and partial coherence for infer the positions of epileptic *foci*. Since then and specially round ten years later, a lot of coherence applied studies was performed in the clinical field (studies of epilepsy, dementia, multiple sclerosis...) and in the cognitive context (studies

of networks involved in working memory operations, linguistic functions and binding problem approaches) (more in-depth analysis in *EEG Coherence contributes in Neurocognitive and Clinical findings*) as well as it was widely studied in created models and simulated data.

As a matter of fact, it is greatly valuable in the area of brain functional connectivity, a field of extremely growing interest in the present days.

4.2 Concept of EEG Coherence

In the context of EEG analysis surges the concept of coherence of an EEG signal, this is one well-established standard tool to analyze the linear relationship between two signals using the correlation between their spectra. Thus, in formal terms the general concept of EEG coherence can be defined as the cross-spectral density of the signal pair divided by the square root of the product of the power spectra of the two signals. The coherence value can also be seen as a correlation coefficient in the frequency domain. A dualism exists between these two computations: coherence (frequency domain) versus correlation (time domain). It can be obtained by the following expression, in which we compute coherence $C_{xy}(f)$ at a frequency f for signals x and y with the cross-spectrum of signals x and y being designed by $W_{xy}(f)$ and the power spectra of both signals by $W_{xx}(f)$ and $W_{yy}(f)$[16].

$$C_{xy}(f) = \frac{W_{xy}(f)}{\sqrt{W_{xx}(f)W_{yy}(f)}} \tag{4.1}$$

This expression is also designated coherency according to some authors [43, 86].

Another expression of coherence arises from the fact that generally we are leading with a complex signal and as though coherence can be divided in an magnitude coherence $|C_{xy}(f)|$ and a phase coherence λf. The phase coherence represents the phase lead or lag of o signal over the other.

$$C_{xy}(f) = |C_{xy}(f)|e^{j\lambda f} \tag{4.2}$$

Integrated implicitly on this last equation, there is a valuable derivate of coherence, use commonly instead of the former - the *Magnitude Squared Coherence* yielded naturally by:

$$MSC = |C_{xy}(f)|^2 = \frac{|W_{xy}(f)|^2}{W_{xx}(f)W_{yy}(f)} \tag{4.3}$$

This expression is so frequent that is sometimes taken as simply coherence like in the review of [97].

The complex cross-spectrum of the signals is defined by the following expression [15]:

$$W_{xy}(f) = \int_{-\infty}^{\infty} R_{xy}(\tau) e^{i2\pi f\tau} d\tau \tag{4.4}$$

This is the Fourier Transform of the cross-correlation function below (the auto-spectrum is omitted as it is a particular case of the former):

$$R_{xy}(\tau) = E[x(t)y(t+\tau)] \tag{4.5}$$

Here, E represents the mathematical expectation, *i.e.* given a process h the expectation operator *E(h)* is the average value of *h(t)* in a period of time with infinite duration.

This previously definition yields the exact values of the auto and cross-spectra however, it is only statistically fully reliable for an infinite signal so an approximated estimation of some type must be performed. The reason underlying this fact is that biological data needs to be sampled in order to be possible make computations over it in a process referred as *population signal* [16]. In this context, the auto spectral density function (also called power spectra) for a generic signal x and the cross spectral density function for the two generic signals x and y can be deduced by the product of the complex Fourier Transform ($X_x(f)$) of a signal x at a frequency f with its conjugate and by the product of the complex Fourier Transform of a signal x at a frequency f with the conjugate of the complex Fourier Transform($X_y(f)$) of the signal y at the same frequency.

$$W_{xx}(f) = X_x(f)X_x(f)^* \quad \text{and} \quad W_{xy}(f) = X_x(f)X_y(f)^* \tag{4.6}$$

As a normalization estimator, the amplitude range for a coherence function is between the extreme cases of 0 (random relations of power and phase between signals) or 1 (linear relation of phase and power between the two signals).

Moreover, EEG Coherence can be also conceptualized by three phases: passing the signals trough a narrow band filter tuned to the given frequency, computing the Pearson-product moment correlation of the filtered signals and squaring the result correlation coefficient [97].

Regarding now a purely mathematical point of view, the coherence function can also be seen as a statistical measure that yields the likelihood of stochastic signals, with provenience from the same source, for a given frequency(ies) band(s). The main reason of this statement is the fact that all coherence estimations usually rely on sampled epochs of the biologically relevant signal so, as a consequence have an intrinsic statistical character [102].

The definition of coherence although, extremely simple in theory has some drawbacks in adapting to experimental procedures, in fact the requirement of stationarity of the signals for the validity of the expression raise field for a lot of different implementations in practice (see further sections). To overcome this problem, we can split the entire signals in single parts (n parts of equal size), obtaining discrete signals x_k and y_k that will further be used for estimation of the auto-spectra and cross-spectrum. The final computation of coherence will be in that case acquired by (this procedure will be highlighted in the following sections):

$$\tilde{C}_{xy}(f) = \frac{\left|\sum_{k=1}^{n} \overline{\hat{x}_k(f)}.y_k(f)\right|^2}{\sum_{k=1}^{n} |\hat{x}_k(f)|^2 . \sum_{k=1}^{n} |\hat{y}_k(f)|^2} \tag{4.7}$$

Another valuable observation is that coherence is commonly different from synchrony, this one relates to signals that oscillate at the same frequency with the same phases also. In other words, coherence does not depend on direct information on phase relation (*i.e.* synchrony between two signals) but, it concedes a way of measure the stability between them [127].

In a certain way, coherence is an indirect measure of phase synchrony [31]. Phase synchrony is a measure of the constancy of the phase shift between two signals during a specified time interval. The idea underlying this computation is based in the phase synchronization of chaotic oscillators. The phase synchrony coefficient (phase locking value) of two oscillators l and m, in a window of N samples can be obtained by [50]:

$$PLV_t = \frac{1}{N} \sum_{n=1}^{N} e^{j(\Phi_1(t,n) - \Phi_2(t,n))} \tag{4.8}$$

This measure accordingly to [50] can be efficacious for a more powerful interpretation of connectivity, indeed a distinction between the relative importance of phase and amplitude covariance is available with this approach, acquisition that is not possible with the *MSC*.

The classical concept of coherence can also be extended to a framework of two variables - time and frequency - as we will see in the subsequent sections, assuming the following form [128]:

$$MSC(\tau, f) = |C_{xy}(\tau, f)|^2 = \frac{|W_{xy}(\tau, f)|^2}{W_{xx}(\tau, f) W_{yy}(\tau, f)} \tag{4.9}$$

Where the time-frequency cross spectrum and the auto-spectra are calculated analogously with the time-independent case.

A deeper inspection of the algorithmic theoretical implementations of this concept is the goal of the next sections as well as, a discussion on its value in the application of Electroencephalography.

As a general purpose on the choice of the algorithm to use, three major facts should be evaluated: trade-offs in time-frequency resolution, computational complexity as well as time and interference between harmonics which may lead to artifacts [80].

4.3 EEG Coherence as a measure of Brain Functional Connectivity

Coherence can traduce the degree of information flow between groups of neurons generators of the EEG signal [127]. As a result, coherence can be a way to approach the way which functional networks can cooperate with each other during neurocognitive processes or pathologic states. Thus, it is a high-resolution way to quantify the degree of dynamic connectivity between the diverse areas in the brain.

Further, it is relevant to observe that exists a dependency of coherence profile on frequency and brain state *i.e.* the fact that a pair of EEG signals is coherent or incoherent depends on the frequency value [94], the notion of distribution of values of coherence among a range of frequencies is always present.

This simple idea of the interaction among different electrode channels may reflect some sort of interaction between the the brain regions involved is a form of evaluating *Brain Functional Connectivity* and is an intuitive idea that was first thought early after the starting of development of EEG techniques. Historically, it was first verified with the help of correlation analysis but then, with the starts of extremely great evolution of computational power and computational algorithms such as the Fourier Transform the analysis on the frequency domain prevailed, eliciting measures of variance between signals by means of its spectral properties (coherence).

On a first observation, it is important to state that high coherence values point out naturally for a simultaneous activation of populations of neurons (even if it does not give information about the synchronization of the source) and a low value of coherence indicates that the signals measured appear to exist strictly independently. On the other hand, coherence values must depend on any factor that influences covariance of the signals in their distributed localizations and so, activity induced by cortical-cortical, thalamo-cortical or corticopetal connections may contribute a lot for high coherence values [71].

A lot of work was done in correlating the neuronal synchrony observed in the adjacent neurons of the cat's and monkey's visual, auditory, somatossensory and association cortices with the phenomenon of the feature binding of the visual system, in particular was demonstrated that a great amount of coherence in the β band is the basic binding mechanism underlying visual perception. Further, coherent brain activity is also thought to display a role in switching from distinct behavioral states, in a certain way providing a transition between different modes of information processing not restricted merely to visual perception process. It is like if a given quantity of neurons shares the same dynamic functional state in order to integrate in the globalism of a perceptual process. Another valuable discover is that synchrony within the α and the θ bands may induce the start of flowing information across the brain network acting like a "gating mechanism". Moreover, certain types of bursts in oscillatory activity can be a way of regulating the change of state as well as directing the information for a specific pathway [26].

On a global perspective however what is extremely important to retain is that the regions of the brain which are activated by a given cognitive operation reveal an increase or decrease in coherence estimations, in a determinate range of frequencies, indeed coherence variations on a given domain of frequency are related to the difficulty and nature of the mental task taken.

4.4 Methods of Coherence Estimation

During the last decades were developed an extensive group of quantitative methods for signal analysis with application in a lot of areas including analysis in Electroencephalography, this new achievements evolved extremely correlated with the progresses did in obtaining superior power computation. Considering the fact that EEG signal analysis is strongly based on the measures of the spectrum, which is also like has been noted above extremely connected with the concept of coherence, I will introduce some fundamental background on that subject and proceed further, trying to cover the most fine subtleties of the matter.

The spectral analysis in a general way tries to determine the spectrum of a given stochastic and stationary signal. The spectrum of a signal is its distribution of the different frequency components in the frequency domain. A distinction between the concepts of spectral analysis and spectrum estimation is essential - the first term is reserved for an exact estimation of the spectrum content and the second is applied for practical cases like the estimations on EEG data on the present work. Although, it is necessary a fully comprehension of the bases of spectral analysis to elaborate a spectrum estimation and

considering that a brief review is provided in the following sections.

We can designate two distinct ways to approach the solution of this problem of determination of the frequency content of a signal: a *non-parametric* methodology and a *parametric* one. The former is associated with the direct use of the signal itself for making the estimation and contrarily, the latter's concept is based on an indirect estimation as it proceeds by estimating first a group of parameters which yield the determination of the spectrum. Further, included in these two groups can be a panoply of techniques regarding information on a *linear* or *non linear* level. This thesis work only uses non-parametric linear strategies so I will focus only on this methodology. In addition, it will also be distinguished methods of stationary and dynamical analysis, i.e. strategies given information only in the frequency domain or in the time-frequency domain.

Another important distinction that must be clear before the full exposition of concepts is that coherence analysis may concern a continuous time or be time-locked to a given event, being called in that case event-related coherence. A relevant hint is the actual discussion around this latter type of approach, which previously was thought not to reflect event-related synchronization of ongoing EEG oscillations [78].

4.5 Stationary analysis: Fourier Approaches

This section is organized following firstly a brief review of theoretical concepts regarding Fourier analysis and evolving in the subsequent parts to more pragmatical constraints of practical implementation.

4.5.1 Continuous Fourier Transform

The basis of Fourier spectral analysis is the Continuous Fourier Transform (CFT, designated also forward Fourier Transform, analysis or decomposition). The CFT of a function *x(t)* for a frequency F can be given by the following expression:

$$X(F) = \int_{-\infty}^{\infty} x(t) e^{-j2\pi Ft} dt \tag{4.10}$$

Alternatively, it can be also depend on a angular frequency $\omega = 2\pi F$:

$$X(\omega) = \int_{-\infty}^{\infty} x(t) e^{-j\omega t} dt \tag{4.11}$$

There are a group of conditions, called *Dirichlet conditions* [55] that guarantee the existence of the Fourier Transform of a signal. The first and the second ones assume that *x(t)* has a finite number of finite discontinuities and a finite number of maxima and minima respectively. The third one points that x(t) must be absolutely integrable for a frequency $\omega \in \mathbb{R}$ which is expressed below:

$$\int_{-\infty}^{\infty} |x(t)|dt < \infty \tag{4.12}$$

and at last there is a weaker condition that is always verified if the third is true (being the converse not necessarily valid) - *x(t)* having finite energy:

$$\int_{-\infty}^{\infty} |x(t)|^2 dt < \infty \tag{4.13}$$

We must notice although that these are just sufficient conditions for the existence of the Fourier Transform not being necessary for its obtainment, there are several functions not included in this group which have Fourier Transform, naturally a periodic or a constant function cannot obey to the principles in equations 4.12 and 4.13. So this Fourier approach was enlarged to surpass this limitation in a way it includes those other functions so-called generalized functions (see [45] for more details).

On the other hand, the inverse transform (also called synthesis) yields the expression of the signal *x(t)* as a linear superposition of sines and cosines characterized by their frequency F or ω:

$$x(t) = \int_{-\infty}^{\infty} X(F) e^{j2\pi Ft} dF \tag{4.14}$$

$$x(t) = \frac{1}{2\pi} \int_{-\infty}^{\infty} X(\omega) e^{j\omega t} d\omega \tag{4.15}$$

An exchange between the time domain and frequency domain can be made naturally without a loss of gain of information.

It is important to note that the expressions of CFT and its inverse can vary among different books and reviews, sometimes the signals in its exponentials appear changed, the factor $\frac{1}{2\pi}$ may be in the forward transform and not in the inverse, even the same factor can be replaced by $\frac{1}{\sqrt{2\pi}}$ in both transforms or no factor been applied to none of them when the angular frequency ω is substituted by $2\pi f$. All expressions are valid, there is just a need for care when handling with them [45].

A central question in the Fourier analysis is that a signal cannot be simultaneously limited in frequency and in time. A band-limited signal is infinite in time domain and vice-versa, an infinite signal in one domain can be or not finite in the other although.

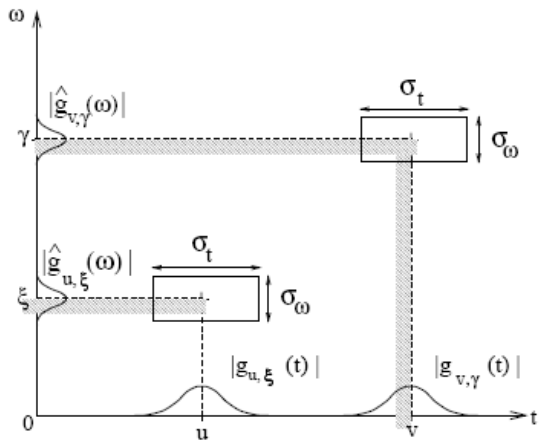

Figure 4.1: *Schematic representation of the Heisenberg inequality.*

Constraining the signal in time leads to a spreading in frequency and subjugating the same signal to restrictively low frequencies elongates the function in time making it smoother. This balancing between the two domains is known as the *Uncertainty Principle* and is a physical constraint in all the methods we will discuss in this thesis based in the above *Heisenberg inequality* (see Figure 4.1) that stipulates the time-frequency trade-off between $\delta\omega$, the bandwidth and δt, time scale [34]:

$$X(t) \longleftrightarrow X(\omega) \Longrightarrow \delta\omega\delta t \geq \frac{1}{2} \tag{4.16}$$

4.5.2 Discrete Fourier Transform

The Fourier Transform is applied to discrete-time signals as well as continuous, yielding always to a continuous spread of the transform in frequency which makes computational operations on it not feasible [55] and so there was a need to develop a Discrete Fourier Transform (DFT). This transform is the central tool for spectral analysis of stationary signals and noise and also the characterization of nonstationary signals [80].

Considering now that a signal is sampled in a range of a finite time $k = 0, 1, 2...N-1$ in which k instead of representing an instantaneous temporal reference designates the number of counts of intervals, being N the total number of samples, the *Discrete Fourier Transform* would take the form:

$$X(k) = \sum_{n=0}^{N-1} x(n)e^{-j\omega_k n} \tag{4.17}$$

Or,

$$X(k) = \sum_{n=0}^{N-1} x(n) e^{-jkn((2\pi/N)} \tag{4.18}$$

The symbols n and k are used in order to make a distinction and do not confound with the continuous time (t) and continuous frequencies (f and ω). The measure $\omega_k = k\frac{2\pi}{N}$ is called the natural frequency. The conjunct of sines (imaginary part of the signal) and cosines (real part) with an amplitude equal to one that form the time domain signal are called the basis functions of the Discrete Fourier Transform, each one corresponding to a determined frequency in the frequency space.

Analogously to the continuous case, considering that the sines and cosines of the expression 4.18 are orthogonal we can obtain also the inverse discrete transform (DFT^{-1}) given by the following expression:

$$x(n) = \frac{1}{N} \sum_{k=0}^{N-1} X(k) e^{i2\pi kn/N} \tag{4.19}$$

A pertinent observation is that although this passage is made without any loss, when analyzing its results in a signal, we have to deal carefully because even if the discrete Fourier theory is consistent, the biological signals have a non continuous character and as a consequence an immediate equivalence may be sometimes misleading [45].

The signal of N samples in the time domain when transformed gives origin to independent complex coefficients of $\frac{N}{2} + 1$ samples. The number N of samples usually is a power of two integer or when it is not, the signal's length can be adapted in order to satisfy that feature. The reason for that fulfillment is bifolded: first, the digital data storage uses binary addressing and second, for the computation of the Fast Fourier Transform (see below) its convenient a power of two [105]. Re-emphasizing, the Discrete Fourier Transform is an extremely important tool of the Fourier Analysis because of the condition that in digital signal processing of biological signals we have to work with finite and discrete data. (although the Fourier transform itself is important for theoretical analysis and comprehension, pragmatically we basically need the Discrete Fourier Transform in computation). A more profound review of the characteristics of this transform will be made below, when discussing the computation of power spectrum.

The Discrete Fourier Transform, although named in this way is nothing more than the coefficients of the Fourier Series of a discrete signal real periodic or assumed to be periodic [16] (see [45] for a more profound approach to this analogy).

4.6 Spectrum Estimation

The classical methods for non-parametric spectrum estimation are the methods implemented by Bartlett (1948), Blackman and Tukey (1958) and Welch (1967). All these computations are based in the *periodogram* that was introduced by Schuster in 1898 [55].

The periodogram, in its essence is basically the squared modulus of the Fourier Transform, it can be expressed by the following relation for a segment of signal with N samples:

$$P(\omega) = \frac{1}{N}|X(\omega)|^2 \tag{4.20}$$

Here, the $X(\omega)$ is given by *(4.8)* the following sum considering the case we are dealing with a discrete signal of finite length that is continuous in the frequency space.

$$X(\omega) = \sum_{\tau=0}^{N-1} x(n)e^{-i\omega\tau} \tag{4.21}$$

However, the more common computation of the periodogram is the one used in the FFT, with a version of $P(\omega)$ sampled in frequency at intervals of $\omega_k = k\frac{2\pi}{N}$ - obtained by the use of the DFT shown in Equations 4.17 and 4.18)

$$P(k) = \frac{1}{N}|X(k)|^2 \tag{4.22}$$

To report the resolution of the periodogram estimated in 4.22 we must start analyzing the characteristics of the Discrete Fourier Transform. Considering that we have a signal with a sampling interval of Δ, the discrete frequencies for the number of sample k will be:

$$f_k = \frac{k}{N\Delta} \tag{4.23}$$

The resolution in the frequency domain is the inverse of the duration of the signal being treated in the time domain, as though it can be deduced by means of the following expression:

$$\Delta f = \frac{1}{N\Delta} \tag{4.24}$$

The sampling has to obey to the Nyquist's theorem that establishes that the frequency $f_{Nyq} = \frac{1}{2\Delta}$ correspondent to the sample $k = \frac{N}{2}$ is the maximum threshold that can be detected with the considered sampling period Δ. In case exist frequencies that exceed the Nyquist frequency, the resulting spectrum is adulterated by a spurious effect known commonly by the designation *Aliasing*. Usually, in practice is used a sampling frequency that is at least the quadrupole of the maximum frequency of the input signal.[16]

A natural way of increasing resolution comes implicitly with the equation 4.24,

if we use longer input signals, frequency resolution will improve as the space between spectral lines Δf is minimized. Although, this feature cannot be expanded in extensively being the limiting factor assent on the hardware profile, it is naturally impossible to have infinite space memory to archive all ideally long acquired signals. So, the natural finiteness of the data sequence represents the major limiting factor for spectral resolution.

Another issue on the subject of resolution as to deal with a concept called *spectral leakage*. In its essence it is related with the fact that considering a signal it can have frequencies that perfectly match a frequency of the group of the basis functions (the basis functions are the sins and cosines implicit in the transform) or instead, show a frequency (or frequencies) that are intercalated by two values of the basis functions. In the latter situation, the spectrum would no longer be a single point but it would suffer from some spreading, appearing like a peak with tails - this is due to the fact that the spectral energy contained on that precise frequency would be distributed to the nearest two frequencies possibly causing errors of interpretation of the data in the time domain. On this topic it is relevant to notice that exists a clear distinction between two different concepts of the length of the data: the length of the input signal (originally limited by available memory space, referred above) and the length of the Discrete Fourier Transform, this one can be extended by an augment of the number of samples by new ones valued zero in a process called *zero padding*, this artificially increase of the number of samples in the frequency domain yields a better resolution in frequency although the spectrum is unaltered. Spectral leakage is also a consequence of the necessity of windowing the data (turning it finite), this concept and its applications are developed in the next section.

Although a panoply of different strategies for optimize the determination of the spectrum and reducing the variance associated to the estimation, in every way is present a form of frequency smoothing (windowing) and temporal smoothing (sampling). As though, the basis of the this two necessary processes when leading with finite data are developed in the following sections.

4.6.1 Windowing - Frequency smoothing

A window is somehow a function that is convolved with the time domain signal and has the capacity of selecting a piece of the input signal exalting some of its features, there are several types of windows, the most utilized ones will be introduced shortly in this exposition. The concept of window surges naturally in the context of the Blackman-Tukey method. Windowing is necessary also for reducing the nefast effects caused by spectral leakage (see Figure 4.2) [46].

To understand better how a window smooth the sequence data, we must consider that every signal that has frequencies that do not match with the ones of the basis set and so exhibits discontinuities in the borders of its periodic extensions (like it was seen previously and is represented in 4.2). The role of the window is smoothly brought to zero or near zero the discontinuities of these boundaries transforming the periodic extension in an apparently continuous sequence [46].

As the computation of the Discrete Fourier Transform requires an assumed notion

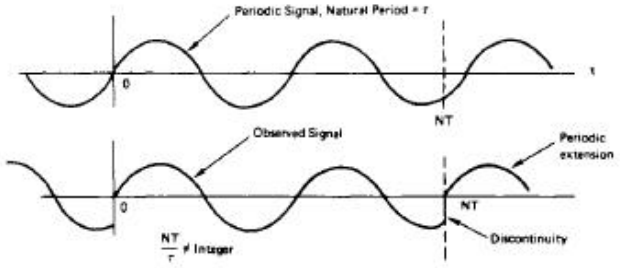

Figure 4.2: *Evidence of discontinuities in a periodic extension, phenomenon that causes spectral leakage.(adapted from [46])*

that the signal is infinite (some samples valued zero), the first use of a window in signal processing would be for truncating the signal in a segment containing all non-zero valued points and also eventually some zero ones.

In practice, for the appliance of a window we can pick the periodogram obtained in 4.20 and convolve it with the window function $W(\omega)$, producing a smoothed spectrum. This computation is patent in the following expression [46]:

$$P_{win}(\omega) = \int_{-\infty}^{\infty} I(k)W(\omega - k)dk/2\pi \tag{4.25}$$

Synthetically, represented by:

$$P_{win}(\omega) = I(\omega) * W(\omega) \tag{4.26}$$

Here, the symbol $*$ stands for convolution.

There were developed a lot of different windows with different characteristics. In a general way, a window must obey at least to the following three requisites: narrow bandwidth in the frequency domain, low side lobe levels in the frequency domain and no severe reduction of the signal-to-noise ratio [12].

The appliance of windows for extraction of the signal treated as infinite must be balanced to overcome the problems of spectral leakage exposed above. As the input signal is multiplied by the the window function, we will no longer have an exact spectral peak with infinitesimally narrowness for a given frequency but a main lobe surrounded by sec-

ondary lobes with lesser amplitude in a variate extension depending on the characteristics of the window applied, this is due to the fact that a multiplication in the time domain is a convolution in the frequency domain and as though some kind of distortion of the spectrum is produced [105].

Examples of classic windows are the Blackman-Tukey (also designated Hanning), the rectangular (Dirichlet), the Hamming, the triangular (or Bartlett), their expressions in the time domain are exalted below [46]:

Classic Windows and respective expressions	
Hanning	$w(n) = 0.5(1+\cos[\frac{\pi n}{N-1}])$ if $\lvert n\rvert \leq 0$ or $w(n) = 0$ otherwise (4.27)
Rectangular (Dirichlet)	$w(n) = 1$ if$\lvert n\rvert \leq 0$ or $= 0$ otherwise (4.28)
Hamming	$w(n) = \alpha + \beta\cos[\frac{\pi n}{N-1}]$ if $\lvert n\rvert \leq 0$ or $= 0$ otherwise (4.29)
Triangular (Bartlett)	$w(n) = 1 - \frac{\lvert n\rvert}{N}$ if $\lvert n\rvert \leq 0$ or $= 0$ otherwise (4.30)

The spectral leakage can be greatly minimized if the windows involved have a low peak sidelobe level relatively to that of the main lobe and a rapid asymptotic rate of falloff of the same sidelobes. On the other side, on the window selection it is also involved a selection of the effective bandwidth of the spectral line and likewise, how greater is the window's bandwidth worser is the frequency resolution.

The results produced vary, there is not one window that is perfect in the sense that has an ideally thin main lobe and the amplitude of the surrounding lobes extremely small. As an example, the Blackman window has the lowest amplitude tails but the widest main lobe. On the other hand, the rectangular window has the opposite effect: a narrow main lobe but large tails. A more balanced position between these two features is the Hamming

one. In a general way, we can say that windowing provide a compromise between spectral leakage, controlled by the amplitude of the tails and, frequency resolution, influenced by the width of the central lobe [105].

Considering that windowing "rejects" a portion of data (the boundaries are forgotten), a loss of important information is possible so, sometimes it is used an overlapping of different partitions to guarantee that we would not fail to detect short-duration tone-like signals in that discontinuities. Further, it has been seen that for good windows transforms performed with 50% of overlapping are essentially independent [46].

Concluding, as is pointed out in [46], the appliance of a window have effects on the detectability, resolution, dynamic range, confidence and facility of implementation of a estimator.

4.6.2 Averaging the data - Temporal Smoothing

Another procedure that is correlated with the process of windowing is the one of averaging segments of the input signal. In a general way, for extracting the individual segments a window is applied accordingly. The most simple approach to this problem is when a rectangular window is applied, a process known by Bartlett procedure. A more global method involving other types of windows was presented by Welch in 1967 [16].

Focusing now on the subjugate idea of this process, it consists of dividing the original signal into equally lengthened segments, computing posteriorly the periodogram of each one and resume the result into an averaged periodogram estimate. In practice, the input signal of N samples is fragmented into K segments of L-lengthened frames, the value of L must be an integer power of two for reasons explained in the section *The Discrete Fourier Transform* . The computation of the averaged periodogram can be elicited than by the following expression, in which j refers to the number of the periodogram:

$$P(\omega) = \frac{1}{K}\sum_{j=1}^{K}\left[\frac{1}{L}\left|\sum_{n=0}^{L-1} x(n+(j-1)L)e - j\omega n\right|^2\right] \tag{4.31}$$

4.6.3 Welch's Overlapping Segment Averaging (WOSA) Estimation

Allying those types of spectral smoothing with the concept of overlapping the segments of the recorded signals, a generalized view of spectral estimation extensively approached in [15] called WOSA (*Weighted Overlapping Segment Averaging Estimation*) opens a pathway for a combination of an enormous amount of strategies for computing coherence. Briefly, this estimation can be resumed by the following stages:

♢ Dividing each finite series of the signal in question in N overlapping segments;

♢ Multiplying each segment by a weighting function (like any of the windows exposed in the section *Frequency Smoothing*);

♢ Determining the Discrete Fourier coefficients for each segment using an algorithm like the FFT;

♢ Multiplying the DF coefficients of one series by the complex conjugate or the coefficients of the other, yields respectively, the power spectra and auto spectra of the two series, which must be naturally aligned in a the temporal scale (see Equations 4.6);

♢ Afterwards, an average of the complex coefficients found among the N epochs is performed and we obtain a cross-spectrum estimate.

The new feature in this whole process is the overlapping procedure. It is actually not totally new because we saw above how it is relevant for the detectability of short-duration tones when windowing. The importance of this process is also that, overlapping to a certain extent may permit good frequency resolution in a way it makes possible to compute more averages and counterbalance the demand for longer segments and in a greater number. An integral extension of overlapping i.e. performing it with a degree of 100% does not give, although better estimators in fact, when a certain level is attained the correlation between signals becomes greater and no gains emerge (a degree of 50% overlapping or near is desirable). An exposition in [15] for a few example cases shows some values for these limits of overlapping. The work of [30] reviews the performance of this methodology.

4.6.4 Statistical Properties of the Fourier Approaches

In determinations of coherence, non-zero results between independent signals may appear. The calculation of the mean (related with bias) and variance of this resulting coherence distributions is a way to approach the consistency of the coherence estimator applied [31], once a measure of the error is associated. Consequently, when performing a spectral measure attention must be provided to the statistical properties of the signal and also those produced by the estimator applied in the computation as both, are a source of bias and variance in the estimation. Coherence can only be a valuable and meaningful tool when it is accurately estimated and for judge on that is necessary to know the statistics of the estimator to provide a consistent result [15].

Important features in spectral analysis are resolution, bias and variance, an ideally improvement of these three parameters is needed but is limited by the fact that they are commonly interdependent and due to that a compromise between them is essential

[16].

For basic spectral estimates usually a validation of statistical power trough analytical methods can be followed but, a more complex measure such as coherence need an heuristic way of validating the algorithm's estimators such as testing on simulated data with known spectral characteristics to evaluate the rightness of the estimator and then when desirable apply to the neurophysiological data [31].

In the experimental part of this thesis (Chapter 5) a more profound background will be given in simulation data for assess significant levels of coherence estimates.

4.6.5 Thomson's method - Multitaper's approach

Another group of strategies for spectral estimation that have shown to provide improved biased estimations when compared to Welch's periodogram estimates are the multiple-taper methods also known as Thomson's spectral estimation procedure in honor of his work in this algorithm estimation [119][120].

This methodology consists in using an alternative for the window w_n (also called data taper) as the ones described in subsection *Windowing - Frequency smoothing* for the estimation of power spectrum performed below:

$$W(f) = \left| \frac{1}{N} \sum_{n=1}^{N} x_n \omega_n e^{i2\pi f n} \right|^2 = |X(f)|^2 \tag{4.32}$$

This alternative is an orthogonal family of tapers called Slepian sequences (Fourier transforms of the discrete prolate spheroidal wave functions (DPSWF)). These last can provide estimates that for N-lengthened sampled data and a bandwidth W, determined by the user, give the first $K = 2NW - 1$ sequences optimally concentrated in the interval of $[-W, W]$ [47]. A reader interested in some background about the Slepian sequences may recall [119] which also introduces how to compute these sequences.

The simplest way of determining the spectrum relying in this approach is explicit in the following formula where $u_n^k n = 1, 2, 3.. - N$ is the *kth* Slepian sequence:

$$W_{MT}(f) = \frac{1}{K} \sum_{k=1}^{K} \left| \frac{1}{N} \sum_{n=1}^{N} x_n u_n^k e^{i2\pi f n} \right|^2 = \frac{1}{K} \sum_{k=1}^{K} |X(f)|^2 \tag{4.33}$$

The coherence expression yielded with this method is identical to the one presented in section 4.2, for the generic input sequences x_n and y_n it assumes the form:

$$C_{MT}(f) = \frac{\sum_{k=1}^{K} x_k(f) y_k^*(f)}{\sqrt{|\sum_{k=1}^{K} x_k(f)|^2 | \sum_{k=1}^{K} y_k(f)|^2}} \tag{4.34}$$

The product NW permits to balance the variance and resolution of the multitaper's estimation, the number of tapers used to are as we have seen previously *2NW-1*. Briefly, increasing NW augments the number of estimates of the power spectrum and so variance is minored. On the other hand, the implicit increased of the taper's bandwidth produces also a grow of the level of spectral leakage and the estimation is though more biased. The ideal trade-off of this two parameters is highly dependent on the data we want to analyze.

This estimate can provide a good trade-off of bias-variance because both are reduced: variance is reduced in this procedure due to the averaging across trials and tapers that are statistically independent and bias is optimized because the Slepian sequences are ideally concentrated in frequency.

Compared to WOSA method, multitaper's methods are the most computationally expensive mainly due to the cost of computing the Slepian sequences, the computation of large datasets is though not so straightforward.

4.7 Dynamical analysis

As it was already exposed above the EEG signal is characterized for being dynamic, mostly nonstationary, sometimes transient (typically having spikes and bursts) and normally noise corrupted. Traditional frequency analysis does not appear to be the most appropriate for a correct extraction of information as normally exist time-varying features. A more robust approach would be a time-frequency analysis. Here, I will enunciate the most important principles regarding two techniques of time-frequency decomposition: the Short-term Fourier and Wavelet approaches.

4.7.1 Short-time Fourier and Gabor analysis

The simplest form to obtain information also on time is trough the *Short Time Fourier Transform* (STFT) [116], being represented by the following expression:

$$STFT(\omega, t) = \int_{-\infty}^{+\infty} x(\tau) g(\tau - t) e^{-i\omega\tau} d\tau \tag{4.35}$$

In this formula the *g(t)* represents the window function. The main underlying idea is to select a piece of the signal *g(t)* with length $2T_{win}$ and assume that that piece is stationary, being the FT applied to each of the short-terms [80].

In case the window *g(t)* is a Gaussian function, the STFT is designated Gabor transform [34].

With this approach the problem of stationarity is somehow solved or at least, the stationarity in the wide sense is no longer needed. That concept is replaced by an assumption of stationarity among intervals in which the Discrete Fourier Transform is applied, being this criterion although not necessarily plausible to assume [93]. This methodology however, has implicitly some drawbacks that depending on the data can be very relevant.

For the STFT Transform use in the determination of coherence it is necessary to project some limiting parameters namely the segment length, the window length and the level of overlapping which constraint the implicit resolution of the measure. Consequently, in the light of this constrictions a knowledge about the time-frequency range we are interested is required primordially, in order to design the algorithm for that same time-frequency resolution. This constraint of prior knowledge is a pitfall of this approach and moreover, this time-frequency resolution is also hardly bounded by the uncertainty principle in the sense we have a trade-off between the window's width and frequency and time resolution - the wider the window, the better is the frequency resolution in detriment of the allocation in time, being the opposite equally true [93].

4.7.2 Wavelet analysis

A lot of adaptations have been made to the classical Fourier-analysis methods in order to obtain also a certain resolution in time by development of orthonormal sliding windows such as the *Short Time Fourier Transform*, nevertheless they offer rigid constraints on time and frequency resolutions and are in certain cases not optimal solutions. The Gabor approach, as it was pointed out above, is limited because cannot adapt to a different range of frequencies, a slow signal requires a wider window and a transient a very

narrow one so, a window modulation is compulsory for signals rich in diverse frequencies and this transform is not able to perform it due its fixed window width.

On the contrary, the wavelet method on the context of time-frequency analysis permits a great flexibility as we will see below that can be desirable, once an EEG signal is usually characterized for being highly non-stationary and possessing different frequencies. In fact, wavelets can sum an elevate temporal resolution with a good frequency resolution, particularly in the case of complex wavelets we can have a fortunate union of amplitude and phase information and time parameter as an additional one.

Moreover, the Wavelet Transform can be in some way compared with the Gabor Transform, the reference [12] salients expressively their similarity. Such an equivalence requires specific characteristics of the wavelet method, nevertheless, one point of view is certainly true: both use basis functions with finite duration to effectuate the estimation, the Wavelet is different simply because its length of the support is a function of frequency and its not fixed as in the STFT. In a certain way, the Wavelet Transform makes a coverage of the time-frequency plane utilizing rectangles of different dimensions and the same area, distinct from the homogeneous ones of the Gabor Transform estimation [93, 63]. This time-frequency tiling can be adapted specifically for each signal, in a way it can extract almost in an optimal mode its time-frequency content. This concept is linked to the one of choosing the best bases that will be developed further [59].

Contextualizing briefly the applications of this Transform namely in the case of

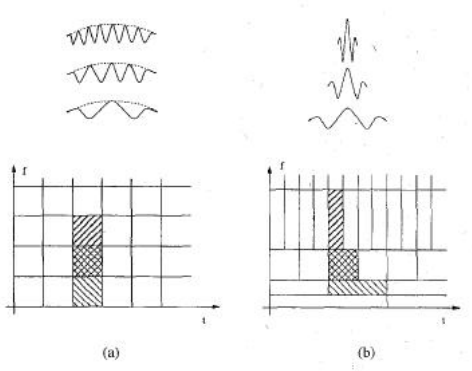

Figure 4.3: *Time-frequency tiling of the Gabor Transform (a) and of the Wavelet Transform (b). (adapted from [17])*

measures like coherence and bicoherence wavelet-based, it was already studied in fields as plasma physics [124], geophysics [67, 73] and aerodynamics and has been more recently also adapted for the analysis of electroencephalographic signals ([5, 31, 93] to cite some examples). Although the transform's origin is much older, it only knew an application to signal analysis when the geophysical engineer J. Morlet, in the end of the 70's decade, trying to unite good time and frequency resolution in the same transform picked a windowed cosine wave (like a Gaussian window with its width adjusted in order to the lateral peaks have half of the amplitude of the central ones) and spreading or compressing it, he observe

that could obtain a lower frequency in case of the former or a higher frequency one for the latter. Further, shifting this functions permitted a temporal inspection. He applied this transform mainly in seismic data analysis [42, 82, 21]. Despite these formulations made by Morlet e Grossmann which open field for broader applications, the underlying idea of wavelet decomposition was not new as it was connected intimately with other approaches in the context of spatial-frequency decomposition like the *Wigner-Ville Transform* and others that even with a different designation had the same formalism [69], however this approach is the only one which can furnish the phase spectrum and consequently be adequate for the computation of coherence [31].

Background concepts

This section aims to provide a summary of the most important concepts of the Wavelet Transformation and its potential vantages regarding the procedure of measuring coherence between two electroencephalographic signals. A more vast review of the methods developed until now is first elaborated, followed by an attempt to focus on the most important details for the next Chapters.

In a pragmatical point view of implementation there are two different groups of wavelet decomposition. The former consists in the *Continuous Wavelet Transform (CWT)* or wavelet frames that with its orthogonality property has also a characteristic redundancy of information at large scale because the wavelet spectra at consequent times is extremely correlated, contrasting with the latter that being represented by the orthogonal, semi-orthogonal and biorthogonal bases has a non-redundant character. The choice of the group of methods is not direct, the fastness of the algorithm used to implement is a crucial issue but, in a general way, according to the reference [123] the redundant approach may seem specially suitable for signal analysis, feature extraction and detection of more smooth and continuous changes in wavelet's amplitude [122]. On the other hand, the non-redundant sub-group is more effective in cases orthogonality of the represented data is highly relevant, being remarkably useful also in performing data reduction because it gives the most compact representation of the signal [122].

In deductions of spectrum and spectrum derivates that enroll the use of nonorthogonal wavelet functions, implementations can be made supported by both the Discrete or the Continuous Wavelet Transform (CWT). On the contrary, such implementations made with orthogonal basis recur strictly to the Discrete Wavelet Transform [122]. Formal expressions of these two transforms will be exposed bellow.

The Wavelet Transform is a standard time-frequency analysis tool that uses a

scalable function ψ instead of a fixed scale window function utilized by the diverse adaptations of the Fourier methods (see above), that flexibility consists in its main advantage. It is basically the integral of the correlation between the signal and the wavelet functions $\psi \in L_2(\mathbb{R})$ that must satisfy the *admissibility condition* $\int\limits_{\mathbb{R}} \frac{|\hat{\psi(f)}|^2}{|f|} df < \infty$ that guarantees the possibility of inversion of the *Continuous Wavelet Transform* and naturally, in the case of the coherence must be also subject of other *a priori* conditions such as: first, the used wavelet function must be a complex one because the coherence estimator is significantly sensitive to fluctuations of linearity in phase, the wavelet spectrum should be unimodal in a way it will not be so much discrepantly centralized from the traditional bands and at last, $\psi \in L_2(\mathbb{R})$ (the Hilbert space of square integrable functions) requires that $\lim_{|x|\to\infty} \psi(t) = 0$ and $\lim_{|f|\to\infty} \hat{\psi(f)} = 0$ not being specified for the case of coherence what is the preferable rate of decay [5]. Being established the preliminary conditions the CWT assumes the form:

$$W_\psi x(a,b) = |a|^{-1/2} \int\limits_R \overline{x(t)} \psi^*(\frac{t-b}{a}) dt =< x(t), \psi_{a,b} > \tag{4.36}$$

Although, in a practical point of view, we are more interested in a Continuous Wavelet Transform of a discrete sequence. Considering a sequence of this type named x_n with n from 0 to *N-1* equally spaced with a period of Δt, the transform would take the form [32]:

$$W_x(a,b) \approx \sqrt{\frac{\Delta t}{a}} \sum_{n=0}^{N-1} x_n \Psi^* \left[\frac{(n-b)\Delta t}{a} \right] \tag{4.37}$$

Each distinct correlation of $< x(t), \psi_{a,b} >$ yields an indication of how perfectly the wavelet function fits at every scale a, the signal being studied. Here the $\psi_{a,b}$ play the same role as $e^{i\omega t}$ in a Fourier development but, once the correlation is made not with complex sinusoids with a characteristic frequency but with the diverse scales of a single function, we can obtain a time-scale representation of the signal [92].

The wavelet cross spectrum of two signals x and y (or cross-wavelet periodogram), analogously with the Fourier theory can be approximated by the following expression:

$$S_{xy}(t,f) = W_x(t,f) W_y^*(t,f) \tag{4.38}$$

In this context, the family of wavelets $\psi_{a,b}$ is therefore a set of elemental functions of one unique admissible "parent" wavelet $\psi(t)$ that assumes the following form:

$$\psi_{a,b}(t) = |a|^{-1/2} \psi \left(\frac{t-b}{a} \right) \tag{4.39}$$

The values of a and b are real values and a is not null, they represent respectively the reciprocal frequency (with an increasing in a the wavelet becomes more narrow) and the time resolution (varying b provides a displacement in time), a and b can be furthermore considered the scaling and shift parameters [20]. The $|a|^{-1/2}$ factor guarantees that the functions $\psi_{a,b}$ have a constant norm in the space $L_2(\mathbb{R}$ of square integrable functions) [17].

In both expressions, a necessary conversion between the parameters a (reciprocal frequency) and b (time resolution) and a more pragmatical and conventional denomination is present. Indeed, relating the former with f (frequency given in Hertz) and t (time given in seconds) we have that $f = \frac{f_0}{a}$, being f_0 the frequency associated with the amplitude wavelet's spectrum maximum and $t = b.\Delta t$, in which Δt is the sampling interval [32].

Turning again for the formulation of the algorithm for the CWT of a discrete series x_n, the fastest way to compute the implicit convolutions is to effectuate it in the Fourier space with the help of the FFT [122]. Using as resource the DFT (Equations 4.18 and 4.17) we can obtain the N convolutions at the same time in the Fourier space.

The transform described above is continuous and consequently redundant for an algorithmic implementation in a practical sense of computation. A discrete one may be implemented by means of using only for the parameters a and b discrete values for the computation of the Wavelet Transform. It exists more than one ways to implement an algorithm for a Discrete Wavelet but, an important type with relevance in coherence analysis was first described by Meyer and Stromberg. In this case the wavelet family in (4.39) would take the form of the expression below given the transformation of continuous values to a finite sequence of discrete ones proportionated by $a_j = 2^j, b_{j,n} = 2^j n$:

$$\psi_{j,n}(t) = 2^{-j/2}\psi(2^{-j}t - n)\text{with}(j,n) \in \mathbb{Z}^2 \tag{4.40}$$

This expression forms a basis of the space $L^2(\mathbb{R})$ (this is the Hilbert space of measurable, square-integrable one-dimensional functions) as well as its correlation with the signal of interest has the nomination of *Dyadic Wavelet Transform* [69, 92].

The form of the function remains always unaltered, the dilation only provides a shrinking or stretching of the wavelet's support,this dilatation is controlled by the parameter j as the parameter n yields the spatial localization. A powerful insight vision of a signal is possible as the shrunk versions and long versions of the wavelet can be united to proportionate a detailed view at every single scale, different singularities are viewed as the former may match the oscillations of high frequency and the latter elements low frequency [63, 69]. An example of this versatility of changing the support is present in the scheme figure 4.3.

Concentrating now on the mother wavelet function, there were developed a lot of different functions concerning diverse applications of course not restricted to the medical field. Nevertheless, it was still not developed a wavelet optimized for coherence studies of neuronal processes, the most applied and broadly used in this subject as well as in other fields in which was previously utilized is the *Morlet Wavelet* (see Figure 4.4) and consists of a modulated Gaussian complex function with a smooth spectrum, it assumes the following expression in the time domain:

$$\psi_M(t) = \pi^{-1/4} e^{-t^2/2} . e^{i2\pi f_0 t} \tag{4.41}$$

Having as Fourier transform the form below, where the $\epsilon(\omega)$ is the Heaviside step function:

$$\Psi(\omega) = \pi^{-1/4} \epsilon(\omega) e^{-\frac{1}{2}[2\pi(f-fo)]^2} \tag{4.42}$$

The Morlet Wavelet performs the time-frequency localization using its envelope, in the meanwhile detects the frequency components with the help of its complex exponential [32].

An important observation, although, is that even if the wavelet function ideally should be chosen with characteristics that approach the features we are trying to find, in the determination of the power spectra accordingly to [122] this option does not represent a critical factor.

It is however important to notice that this wavelet was not designed to be applied in EEG-applications and we shall look for more types that could fit better the desirable characteristics in this case.

For the computation of wavelet coherence there is not also any standard proce-

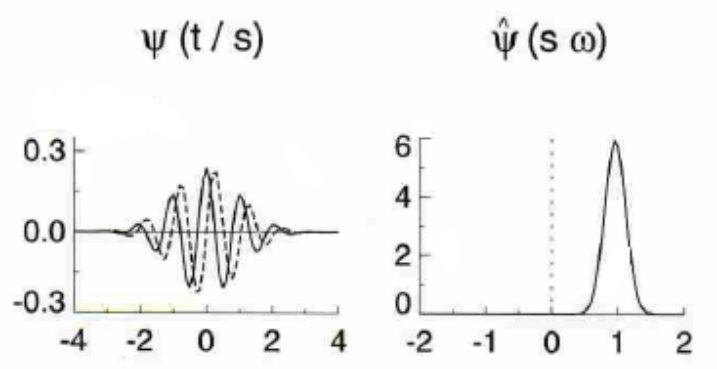

Figure 4.4: *Example of wavelet base: Morlet wavelet. On the left, representation of the real (solid line) and imaginary part (dashed line) of the time-domain wavelet. On the right, one can see the correspondent frequency-domain wavelet (adapted from [122]).*

dure, the reference [124] deduces it by means of computing auto and cross-spectra using integration for a short period of time. On the other hand, in [5] an approach based on the repetitive character of a neurophysiological experiment produced an expression which was called *Estimated Wavelet Coherence* and represents a measure of linear dependence

between two sets or it can be designated also as an ensemble of wavelet transforms in which variables a and b remain unaltered.

$$\tilde{\Gamma}^2_{uv}(a,b) = \frac{\left|\sum_{k=1}^{n} \overline{W_\psi u_k(a,b)}.W_\psi v_k(a,b)\right|^2}{\sum_{k=1}^{n} |W_\psi u_k(a,b)|^2 . \sum_{k=1}^{n} |W_\psi v_k(a,b)|^2} \tag{4.43}$$

This method was applied successfully to a case of study of associative learning perceived by coherence computation, in this example of study Wavelet Coherence revealed itself more valuable than Classical Fourier Coherence as it could show high values of coherence and temporal evolution of this values in the γ band, situation that was not detected by the latter.

Nevertheless, even if it can provide a frequency-adaptive tiling of the time-frequency plane, it has also some drawbacks: namely, it is still somehow uncertain how to visualize the huge amount of data it provides, its statistical properties are still not fully understood and in a lesser extent, the fact that it is not able to detect coherence when the delay between signals is greater than the frequency and duration of them (which occurs due to the fast decay with time of the wavelet) [5].

The superiority of the wavelet approaches in coherence is still an ongoing discussion and accordingly with [12], classical and wavelet procedures can yield the same results depending on the data profile. Still in concordance with the same author, wavelet coherence seems more adequate for signals with mixed higher frequency bands and a rapid temporal fashion.

4.8 EEG Coherence Significance and Drawbacks in EEG Coherence Studies

The origins of the measurable coherence can be multiple: it is generally due to neocortical source correlation (which are naturally *physiologically* interesting), volume conduction properties of the head and reference electrodes effects. These last ones explain differences between intracranial and scalp electroencephalographic data, such as the amplitude ratio of two to six in the alpha and delta rhythms during sleep between measures made directly in the dura and those from the scalp reported in [95].

Values of high coherence between different brain zones were interpreted as an evidence of anatomical connection, functional coupling, information exchange and functional

and temporal co-ordination among the underlying cortical sources [6].

Another counterpart of the estimation is the fact that being coherence a measure of linear dependency among two variables, if its value is high it is a sign that the signals underlying that brain zones can be approximated by a linear transformation, do not meaning that the neocortical dynamics is strictly linear [94].

Concerning the fact that actually, measures of EEG coherence are performed to study the interaction that might justify functional connectivity among different areas of the brain, the greatest problem for this interpretation is that the signal obtained in one channel regards information not just from a single source. In fact, all the EEG channels, specially the nearest ones are subject to a phenomenon called *volume conduction* and attention to high coherences among these electrodes is necessary in order to avoid misleading conclusions due to the artifacts of the referred phenomenon [43].

The problem of volume conduction effects on EEG coherence estimates has been sufficiently severe that only in the 1990's, it was started to be taken in a fiducial form that large or even moderate extracranial coherence could be associated inherently in a reliable way with brain source coherence, the distortion causes always illusive higher values of coherence [86].

A lot of different approaches were followed in order to remove the confounding effects of volume conduction. Since, create different montages of electrodes, developing techniques of current source densities instead of electric field measurements [86] or using only the imaginary part of the cross-spectrum [43]. This last strategy is based on the evidence that since volume conduction is an instantaneous phenomenon, when computing the power spectra of two channels, theoretically there is not any lag between them for volume conduction activity, meaning with this that only the real part is affected. Although this can be a good attempt in some cases for minoring the misleading effects of volume conduction, its utilization is not free from a lost of statistical power once interesting information related to the real part risks to be discarded [97].

Another situation that can provoke erroneous high or low coherence values is in cases where the number of epochs averaged is reduced causing statistical errors [86], this is extremely related with the signal processing analysis already covered in the anterior sections.

Moreover, other important factor that has been proven to affect the EEG coherence results is the utilized method of derivation of the signal. When a reference-based method is involved, ideally the amplitude of the reference signal should be near zero and using different reference signals implies obtaining different estimations for spectral parameters [29].

As an example case of EEG study of different derivation in an EEG test where resting state and a motor task (finger movement) was performed, the appliance of non-reference techniques and Laplacian approaches yielded significant contrasting results when trying to find conclusions about mu desynchronization in finger movement [6].

In the work done in [35] there are evidence on experimental data that reference-free techniques (such as dura image and Laplacian recording) yield smaller scale values of EEG dynamics than the group of reference-based methods applied.

Although, all the techniques were consistent in showing expressively a relatively lower coherence pattern in the α band for sequences with the eyes open due to the phenomenon of *alpha blocking* (reviewed in the chapter 3) [35]. In this study conclusions is also highlighted the necessity of using different methods, indeed each strategy has distinct sources of error and proportionate insight for unequally sized neural populations so a conjunct approach could yield optimized results.

Finally, it is important to retain that although volume conduction constitutes the major drawback in interpreting if the inter-areal coordination observed has a physiologically fundamental, it is possible to develop models that allow *a priori* recognition of what may be true and false events of synchronization [121].

4.9 EEG Coherence in Neurocognitive and Clinical findings

The brain coordination trough coupling patterns is a feature of extremely relevance in the complex brain network, being as though characteristic of determined cognitive states and conclusive in pathologic situations. The fact that the EEG coherence varies according to changes in mental state or in some pathologies allows this tool to be applied in various cases. This section only aims to review the literature of some of the utilizations.

Studies of coherence up to now spread into a panoply of different cognitive states and diseases. EEG coherence was used and yielded interesting results in creativity [106], bilingualism [112], Alzheimer [74], working memory [61], Obsessive-compulsive disorder [91], Attention-Deficit/Hyperactivity Disorder [4] among many other subjects.

Chapter 5

Simulation Data

Although the algorithms for estimation of power spectrum coherence were based in functions based on a standard software, they were not developed to be used in an EEG paradigm so, before passing to real EEG data there is a need for testing them in data with known properties e.g., simulated data. This type of data must be thought to mimic inherent characteristics of the data we are interested to analyze. It must be present however that the goal of this work was not to simulate EEG data but easily provide a benchmark of simple data with merely some characteristics which an EEG record potentially has. The main objective is to validate the algorithms created and support the conclusions on real data from the next Chapters 7 and 8.

5.1 Experimental Paradigm

The work on simulated data can be divided in two stages regarding the nature of the data, the former utilized for testing two sinusoidal functions composed by a cosine with frequency of 10 Hz and the latter by a mix spectrum of sines with frequencies of 6, 10, 14, 22 and 43 Hz. All the simulated data was elaborated using *MATLAB v. 7.1.0.246(R14) Copyright 1984-2005 The Mathworks, Inc.* The sinusoidal functions used in simulation sets have typical frequencies of the EEG bands (see Chapter 3).

The algorithms for estimation of the coherence and phase among the signals are founded in the Welch's Averaged Periodogram method (see Chapter 4 for concepts). The implementation was made with recourse to the Matlab in-built function *mscohere()* .

The data was tapered with Hanning windows of 512 points (corresponding to 2 seconds), coherence was computed in epochs of 256 samples with 50% of overlap. Results with other windows such as a Hamming were compared but I could not find any distinct

particularities. The added white noise used in all sets of simulated data created was reproduced using the function *rand()*.

Additionally, coherence based in another estimation method (Thomson method see 4) was performed but the first method was chosen because it is a more standardized method.

5.1.1 Apart on Confidence Intervals

We must take in consideration that inherent to every estimation of coherence there is an error associated with the practical calculation of this measure, a good example of that are non-zero values of coherence arising from known uncoupled pairs of signals [68]. Bearing this fact in mind, there is a need to set a threshold level that allows to consider that two series are significantly coupled.

The resampling methods were born from the necessity of obtaining statistics of interest and confidence intervals in situations where it is difficult to use traditional methods based in exact analytic solutions, they permit to effectuate a statistical inference without constraint *a priori* the probability distribution of the series [25]. As it was evidenced in [68], for series which have narrow-band constituents in two close frequencies the coherence estimator might produce a broad peak and bias the hypothesis test for zero coherence, being this particularly true in the case of short epochs. An EEG series such as the ones used in the following chapters possibly are in these conditions and as though is appropriate to use a technique that are frequency dependent and consider the characteristics of the data if the goal is to obtain an optimal threshold.

For the estimation of threshold values I followed two methods of surrogation. The first consisted in a FFT surrogation, it was first proposed for testing nonlinear properties [52] and has a basic tripartite procedure: finding the Fourier coefficients, replacing their phases by random numbers in the correct range (modulus left unchanged) and applying the inverse Fourier Transform to return to the time domain. The second was a permutation of the temporal order of the samples in order to generate a set with the exactly same samples but destroying any temporal information although maintaining the mean, variance and histogram distribution.

The reason for following two procedures was that different strategies to create the surrogates can originate distinct sampling distributions and as though also different thresholds, once again the work of [68] revealed that FT surrogates produce higher thresholds for zero coherence than the method of permutation, yet this last did not show a significant variation among frequencies behaving almost likely a constant threshold. I

tried both approaches but I could not find a significant difference among them, though the method of permutation was in a few cases unstable, producing locally higher thresholds. However, having in mind the work done in [68] I decided to use FT surrogation as this procedure was the most successful in avoiding false coherence episodes at nearby frequencies but originated trough different mechanisms. In the work of [68], this was recognized as important to distinguish processes in cardiac and respiratory information, I assume that it could also be valuable for electroencephalographic data.

To reach statistical significance 100 surrogate pairs were created. The threshold for each frequency was found at the percentile of the coherence sampling surrogate distribution correspondent to a significance level of 0.05 %, coherence results above this frequency-dependent threshold reject the null hypothesis of no coherence.

To simulate all the conditions proposed I created each set of data and applied the coherence estimator and the calculation of the confidence levels through surrogation, Appendix 1 has some exemplary functions I implemented to follow this purposes. Every condition is explained in the following section.

5.2 Cosine Based Data

This section briefly explains each of the four conditions and resumes the results, discussing them in the end.

5.2.1 Phase modulation

This stage involved testing the algorithms in a situation where the phase associated with the 10 Hz cosine was changing between 0 and 100% by 10% of the value of a white noise with an uniform distribution from -1 to 1. The following expression enunciates it (m represents the modulation, $\omega = 2\pi 10$):

$$\boxed{cos(\omega t + \frac{m}{\pi} W_n)} \tag{5.1}$$

Coherence depends strongly on the phase consistency between two signals so studying how a growing level of noise influences the measure is recommended.

In Figure 5.1 and Table 5.1 we can see an example of the results displayed graphically and the magnitude values of the peak of interest for each level of noise studied.

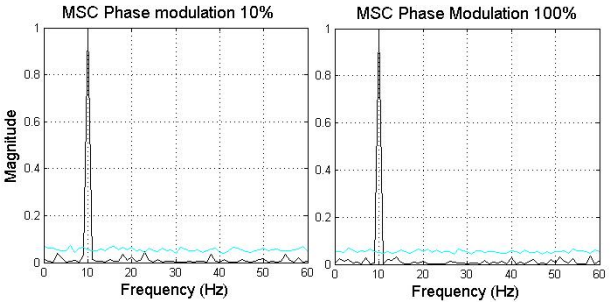

Figure 5.1: *Magnitude Squared Coherence (Welch method) with 10 of modulation (left) and 100 modulation (right). Confidence levels estimated trough FFT surrogation.*

5.2.2 Integral Phase Modulation

For this simulation the simple white noise of the phase was substituted by the expression $W_n(t-1) + W_n(t)$. The simulated data generated obeyed to the expression:

$$\boxed{cos(\omega t + \frac{m}{\pi}(W_n(t-1) + W_n(t)))} \tag{5.2}$$

The goal of performing such a simulation is to test the robustness of the algorithms face to a situation where there is no temporal dependency between two subsequent instants, to test if the episodic coherence observed is not due to a previous influence.

The main results are summarized in Table 5.1.

5.2.3 Amplitude Modulation

In this case, I tested the algorithms depending on an ascending value of amplitude accordingly with the following relation:

$$\boxed{(1 + mW_n)cos(\omega t)} \tag{5.3}$$

Also amplitude influences the output result of coherence and needs to be tested, the graphics of Figure 5.2 illustrate some of the results.

In addition, results are also displayed in Table 5.1.

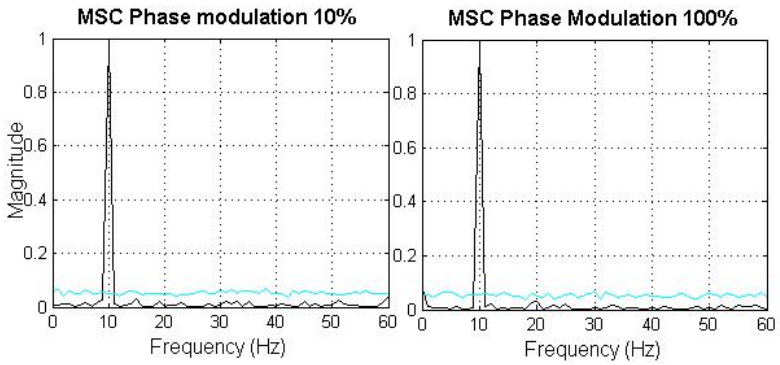

Figure 5.2: *Magnitude Squared Coherence (Welch method) with 10 of modulation (left) and 100 modulation (right) for amplitude modulation. Note that maximal noise seems that does not influence the broadness of the peak. Confidence levels estimated trough FFT surrogation.*

5.2.4 Modulation with additive noise

For the latest simulation, a simple situation condition of adding uniform noise progressively from 0 to 100% was used like the expression below suggests:

$$\boxed{cos(\omega t) + mW_n} \tag{5.4}$$

This type of condition simulates the noise that does not influence any feature in particular, it contributes merely as a background noise (see Table 5.1 for results).

WN [%]	Phase	I. Phase	Amplitude	Additive case
0	1.0000	-	-	-
10	1.0000	1.0000	1.0000	1.0000
20	1.0000	0.9999	1.0000	0.9999
30	0.9999	0.9999	0.9999	0.9998
40	0.9999	0.9998	0.9999	0.9998
50	0.9998	0.9996	0.9998	0.9996
60	0.9997	0.9995	0.9998	0.9993
70	0.9997	0.9991	0.9998	0.9990
80	0.9995	0.9989	0.9996	0.9989
90	0.9992	0.999	0.9996	0.9985
100	0.9992	0.9984	0.9995	0.9979

Table 5.1: *The magnitude coherence results for the cosine simulated data in the four conditions.*

5.2.5 Brief Discussion

The Table 5.1 resumes the magnitude of the peaks obtained by simulation procedures. In a preliminary analysis, one can easily conclude that the algorithm successfully

detected the coherence peaks in each of the four conditions. Looking more attentively, we can also observe that only for the condition of phase modulation it successfully detects coherence in all the cases, the others work well always except in the absence of noise. Regarding the broadness of the peaks, there are not any significant changes with increasing noise. The attenuation in magnitude due to the effect of noise in the different conditions is also minimal, we can observe that it grows with ascending white noise but this attenuation does not overcome 0.21%.

For all this reasons, we can conclude the algorithm is adapted for a situation of a simple sinusoidal function with noise.

5.3 Mix Spectrum Data

Here the former four conditions described above were applied, this time to the signals composed a sum of sines such as these presented below:

$$0.7sin(2\pi 6t + \frac{m}{\pi}W_n) + sin(2\pi 10t + \frac{m}{\pi}W_n) + 0.6sin(2\pi 14t + \frac{m}{\pi}W_n) + 0.8sin(2\pi 22t + \frac{m}{\pi}W_n) + 0.4sin(2\pi 43t + \frac{m}{\pi}W_n)$$

In the figure (5.3) I show the coherence values calculated for each one of the conditions for the case of 100% noise.

In the stage of **phase modulation**, I found that coherence could be identified for all frequency peaks, although it failed to calculate level of coupling in the cases with 0% noise yielding a magnitude 1 for all frequencies as Table 5.2 and Table 5.3 show. For the **integral phase modulation** case this was not true, it failed to detect the higher frequency peak (43 Hz), inspecting Table 5.2 and Table 5.3 once again we can depict that it was equally in this condition that the attenuation of coherence value relatively to 1 was superior if we just consider all the frequency peaks instead of 43 Hz. Considering now the **amplitude modulation** and the **additive case**, in both the algorithm calculated accurately the coherencies and interestingly, the attenuation suffered due to noise was minored progressively with crescent level of noise in the amplitude or general signal. However, for the case of **additive noise** the attenuation was more expressive even with low levels of noise, being maximal at 10% (5.34%). More conclusions on this results can be found in the discussion.

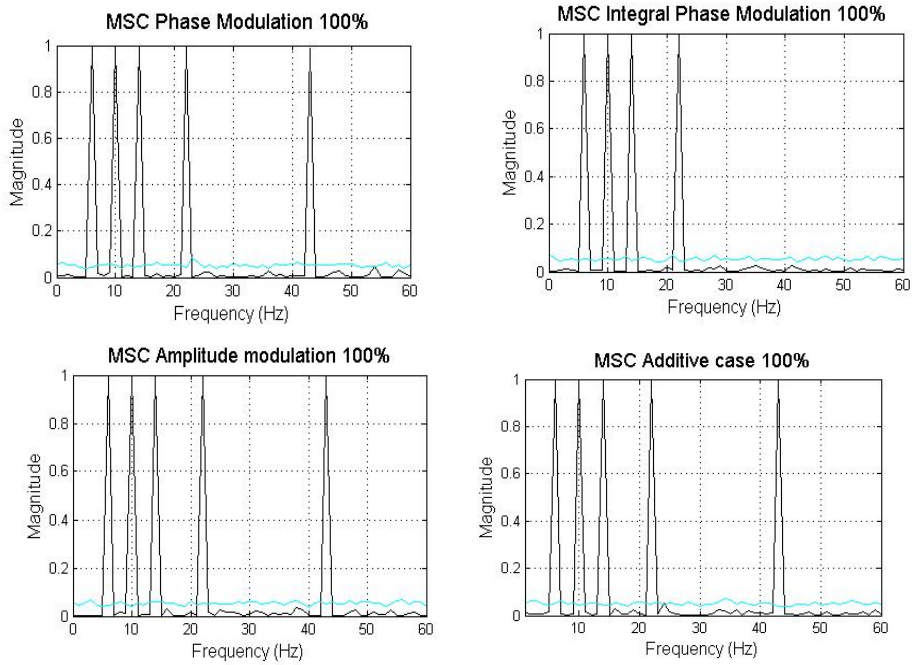

Figure 5.3: *Magnitude Squared Coherence for the four conditions with the maximum level of noise: phase modulation (top,left), integral phase modulation (top, right), amplitude modulation (left,bottom) and additive case (right,bottom).*

5.4 Interpretation and Discussion of the results

Interpreting the overall results, one can assume that the coherence estimation performed is able to correctly identify possible coupling between two noisy signals. In cases in which the noise existent in the series affects the amplitude or the whole signal, the tendency is to have more accurate estimates (less biased and attenuated) with a growing level of noise. This is valid only for the case of the mix spectrum, for the basic cosine data the tendency is the opposite for all conditions. An important point though, is that even when attenuation is higher, it never happens to have significant levels of coherence among the series when they are supposed to be uncoupled, the assessment made with the surrogation procedure showed that noisy background never overcome the frequency-dependent threshold estimated.

A counterpart of this method however is its inherent inadequacy for use with pure sinusoids or mix of sinusoids. Indeed, it was only useful in the condition of phase modulation with cosine data. A possible reason for this is easily understood if we think in the algorithm that it was used for the estimation (see details of WOSA method in Chapter 4). Indeed the coherence estimate is based on averaging the segments, if they are from pure sinusoids an average would lead inevitably to the value 1, recalling Equations 4.3

	Phase					I. Phase				
WN [%]	6	10	14	22	43	6	10	14	22	43
0	-	-	-	-	-	-	-	-	-	-
10	1	1	0.9999	1	0.9999	0.9964	0.9979	0.9947	0.9967	-
20	0.9997	0.9998	0.9995	0.9997	0.9999	0.9967	0.9984	0.9947	0.9973	-
30	0.9997	0.9998	0.9995	0.9997	0.9999	0.9961	0.998	0.9946	0.997	-
40	0.9993	0.9997	0.9992	0.9995	0.9984	0.9957	0.9981	0.9946	0.9963	-
50	0.9999	0.9995	0.9986	0.9993	0.9969	0.996	0.9981	0.9946	0.9981	-
60	0.9988	0.9994	0.9979	0.9989	0.9948	0.9953	0.9981	0.9934	0.9969	-
70	0.9981	0.999	0.997	0.9984	0.9937	0.9958	0.9981	0.994	0.9962	-
80	0.9974	0.9986	0.9969	0.9983	0.9924	0.9953	0.9936	0.9933	0.9965	-
90	0.9962	0.9983	0.9956	0.997	0.9907	0.9951	0.998	0.9933	0.9963	-
100	0.9974	0.9979	0.9943	0.9976	0.9869	0.9954	0.9977	0.9932	0.9964	-

Table 5.2: *Magnitude of coherence values of the conditions of Phase modulation and Integral phase modulation for the mix spectrum data.*

and 4.6 we can draw this conclusion:

$$|C_{xy}(f)|^2 = \frac{|W_{xy}(f)|^2}{(Xx(f)Xx(f)^*)((Xy(f)Xy(f)^*)} = \frac{(Xx(f)Xx(f)^*)((Xy(f)Xy(f)^*)}{(Xx(f)Xx(f)^*)((Xy(f)Xy(f)^*)} \equiv 1 \tag{5.5}$$

The fact that it does not detect coherencies between pure sinusoidal signals is naturally irrelevant for an EEG analysis and considering that accuracy improved with amplitude and additive noise this could be advantages for an electroencephalographic recording, where so much sources of noise can be present such as the noise picked by the electrodes (although the executer tries to maintain the impedance low) and the amplifier.

The algorithm also demonstrated a limitation in detecting higher frequencies such as 43 Hz, this does not although forces us to conclude the algorithm will fail detecting coherencies in EEG data, it only reflects a constraint on the analysis.

Regarding now the estimation of the significant thresholds, it is important to refer that considering [3] the number of trials used to ensure statistical significance might be small (100 surrogates) although meaningful results with such a value were obtained by others [68]. For future research a comparison should be made before picking one value, at this point there is no sufficient information to assume 100 surrogates are few.

Finally, based on the information of the simulation that this method of estimate coherence can possibly be used on measuring coherence among EEG signals and estimate frequency-dependent thresholds, it shows however a possible limitation for higher frequencies ($\geq$ 43Hz).

	Amplitude					Additive case				
WN [%]	6	10	14	22	43	6	10	14	22	43
0	-	-	-	-	-	-	-	-	-	-
10	0.9981	0.9989	0.9964	0.9985	0.9925	0.9811	0.9901	0.9731	0.9837	0.9466
20	0.9998	0.9999	0.9997	0.9999	0.9995	0.9992	0.9997	0.9989	0.9993	0.9977
30	0.9997	0.9998	0.9995	0.9997	0.999	0.9982	0.9993	0.9978	0.9988	0.9950
40	0.9997	0.9993	0.9992	0.9994	0.9985	0.997	0.9984	0.9974	0.9975	0.9903
50	0.9991	0.9996	0.9988	0.9994	0.9978	0.9953	0.9976	0.9934	0.9960	0.9853
60	0.9988	0.9995	0.9985	0.9993	0.9971	0.9922	0.9969	0.9901	0.9944	0.981
70	0.9985	0.9993	0.9983	0.9990	0.9958	0.9898	0.995	0.9866	0.9916	0.9742
80	0.9984	0.999	0.9977	0.9987	0.9951	0.9901	0.994	0.9861	0.9926	0.9554
90	0.9977	0.999	0.9970	0.9984	0.9941	0.9862	0.9927	0.9739	0.9883	0.9537
100	1.0000	1.0000	0.9999	1.0000	0.9999	0.9998	0.9999	0.9998	0.9999	0.9994

Table 5.3: *Magnitude of coherence values of the conditions of Amplitude modulation and Additive noise for the mix spectrum data.*

Chapter 6

Mental Calculation

"That arithmetic is the basest of all mental activities is proved by the fact that it is the only one that can be accomplished by a machine."

Arthur Schopenhauer

Mental calculation is a complex higher cognitive function hard to unravel as an isolated phenomenon.Only in the last decades attention has been given to this delicate higher function which holds in its essence an unique trait - unlikely for example language problem-solving, arithmetical skill permits to resolve a simple problem both from retrieving facts from long-term memory or doing the calculation *per se*. A comprehensive picture of mental calculation may be perceived as an interaction of diverse cognitive mechanisms with different roles, acting in different stages and with distinct regional patterns of which the wholly colors remain unknown.

6.1 Mental calculation substrate

A general model proposed [14] resumes that in order to make a calculation, we have to follow through subsequent stages: perceive and process numerical information, process operational signs specific to the calculation, retrieve of arithmetic facts and execute the retrieved calculation. The mechanism of retrieval of arithmetic facts can be rather challenging to disentangle in the whole scenario, indeed a high variability of strategic approaches can be used in a calculation and the specific neuronal networks associated with each strategy are difficult to distinguish.

A comprehensive use of diverse neuroimaging techniques is mandatory for under-

standing the brain patterns of activation of single functional areas as well as simultaneous group activation, considering the complementary information provided by techniques such as fMRI, PET, MEG and EEG (see chapter 3 for review). Moreover, experiments in healthy individuals as though in the ones with injured arithmetic capacities such as acalculia are both promising.

6.2 Comprehensive state-of-art

Regarding the state-of-art of the experimental work done in finding neural correlates of arithmetical calculation or other related cognitive functions , there are not an agreement between all findings. It is important to refer that this brief review is not intended to cover all the research in the field but give an introduction of some main findings that correlate with the present work.

The mental calculation process can involve retrieval, nonretrieval and both strategies. The retrieval strategies were seen as finding, stored in memory, the so-called arithmetic facts (e.g. 3+2, 2x5), these are recalled by a somehow semantic network like they were words [24]. This view of mental arithmetic is though intimately related with the brain areas traditionally addressed to language like the inferior frontal gyrus (Broca's area), the posterior part of the superior and the middle temporal gyri (Wernicke's area), the basal ganglia and the thalamic nuclei. This is a classic view which exhibits left lateralization of mathematical abilities. There are studies that point for a relation between language and arithmetic skills and reveal the left hemisphere as dominant, some examples are [118, 49].

Although from early days [41], there are a lot of authors defending the perspective of an important role also of the right hemisphere. The fMRI work of Burbaud [90] found consistent with previous similar works by others an activation of left prefrontal cortex as well as in the inferior-parietal cortex bilaterally during mental subtraction . More specifically, in the work of [129], although a clear fMRI activation pattern of left lateralization was depicted in simple calculations, this factor decreased when confronted with a higher complex calculations suggesting a bilateral functional activity. Zhang et al [129] related this finding also with a previous study in which the right prefrontal lobe was only activated in a situation of high memory load. The main conclusions were that mathematical computations depended on task specificity and that both hemispheres have a role in the calculation.

Assuming the bivalent characteristic of arithmetical thinking of relying on retrievable memorized facts and make resource of computing, there were also studies that

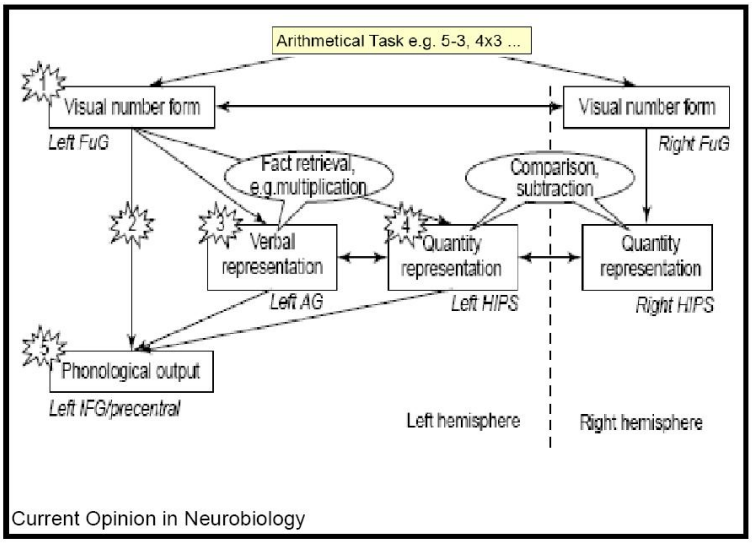

Figure 6.1: *Schematic diagram represents the actual opinion on pathways of digit processing in the brain. It results from a combined information of diverse neuroimaging techniques in healthy and pathological subjects. Abbreviations: AG - angular gyrus; FuG - fusiform gyrus; HIPS - horizontal segment of the intraparietal sulcus; IFG - inferior frontal gyrus. (adapted from [98]).*

tried to differentiate between these two as well as establish the common neural background. In a study with a dual task, activated left subcortical structures were related with retrieval procedure (rote ability of using multiplication tables) and bilateral inferior parietal lobe connected with much more demanding tasks in terms of numerical manipulation such as subtraction and division [23]. In agreement with this findings are the coincident pattern found between an addition/multiplication test and a test involving language comprehension, contrasting with activation in the parietal cortex exclusive of the subtraction/division test developed in [56]. Rote arithmetic operations revealed a left-prominent pattern (activating the inferior frontal gyrus and angular gyrus) and exact calculation a heavier activation of both parietal cortices also in other fMRI and behavioral studies [98, 36]

Important findings were also possible in experiments involving not healthy individuals. Interestingly, a patient with acalculia and agraphia with a lesion in the left prefrontal cortex was able to do simple arithmetic calculus (without carrying) nonetheless he could not perform multiplications properly [48]. The recent study of Funnell et al [70] with a patient with a split-brain reinforced the idea that right hemisphere is able to perform successfully subtractions and approximate calculations, although left hemisphere language-dependent systems are dominant for calculation. A lesion in the corpus callosum disables any interhemispheric flow and so the segregation between the specific abilities of each hemisphere is more likely to happen, emphasizing though these theories.

An important aspect that can introduce high variability when testing mental calculation is mathematical skill's heterogeneity. Some experiences ([88, 72]) tried to access the relevance of this factor and the general conclusion was that perfect performers have regionally different patterns of activation when compared with less skilled.

Influence of age was also studied, up-to-date studies are somehow contradictory, meanwhile the fMRI work of [60] shown only insignificant differences among adults and children in simple arithmetic, another study [96] revealed greater activation of left parietal cortex in older children contrasting with stronger activation of prefrontal cortex in a more younger group.

The evidences of inter-individual differences must be taken into account in every study of this field, although one can try to minor their influence using larger and more homogeneous populations, the truth is that there is in the present era a limited knowledge to control the arising confounds.

6.3 Mental calculation in EEG studies

Concerning EEG neuroimaging data, there are fewer reports of arithmetical neural correlates and particularly, few of them use coherence as the evaluating measure. A possible relation between decrease of power in the upper alpha band in the left parietal cortex and long-term retrieval is well-founded in [37]. In addition, it was also reported an augment in calculus relative to the basal situation in the theta band higher in the right prefrontal cortex. Reviewing implications of the alpha and theta bands in cognitive processes, Sauseng et al [87] emphasizes their connection with working memory processes, particularly reporting findings relating theta power with memory performance, memory retrieval, its modulation by memory load and its role in encoding. Analogously, upper alpha seem especially important in long-term memory and its modulation by memory load was a common finding among diverse experiences.

Moreover, during a test with progressively more difficult arithmetic tasks (from merely reading numbers to addition with decimal numbers), significant differences in delta, theta and beta power were found, being the first two allocated to diverse areas meanwhile beta rhythm increased in the frontal lobe [117]. Regarding the theta band, the only significant increase was frontal and in the more complex task.

Throughout the experimental work, other more specific findings will be highlighted.

Chapter 7

Mental Calculation: Interval Stimuli task

In this chapter, a first study of a calculation task will be made on a healthy subject. The analysis will focus on event-related spectral and coherence measures, all the necessary theoretical details are explained. The main findings of each method will be compared in terms of what are the possible advantages, evidencing what type of information can be obtained with an EEG recording of successive stimuli. The aim is not focus on the data but on different strategies to compute spectral and coherence information, their possible advantages and pitfalls. This can be viewed as a first approach to analysis of real EEG data.

7.1 Experimental Protocol and Paradigm

The data available for this work is from a healthy individual. The recording contemplates a period when the performer remained relaxed with its eyes open, a sequence that he was still relaxed with the eyes closed and two final sequences when he was subject to a mental arithmetic test first with a stimulus being applied in intervals of 3 seconds and afterwards in intervals of 2 seconds.

The four electrodes used in this experiment were positioned accordingly to the 10-20 system, they all belong to the medial line - FZ, CZ, PZ and OZ (see figure 7.1). The mastoid was utilized as a reference and the channel FpZ was connected to the ground. All the acquisitions were performed with a sample frequency pair to 256 Hz.

The mental test applied is a common test [1], clinically used, for assessment of

[1]This specific test was performed in Fondazione Don Gnocchi, Milan.

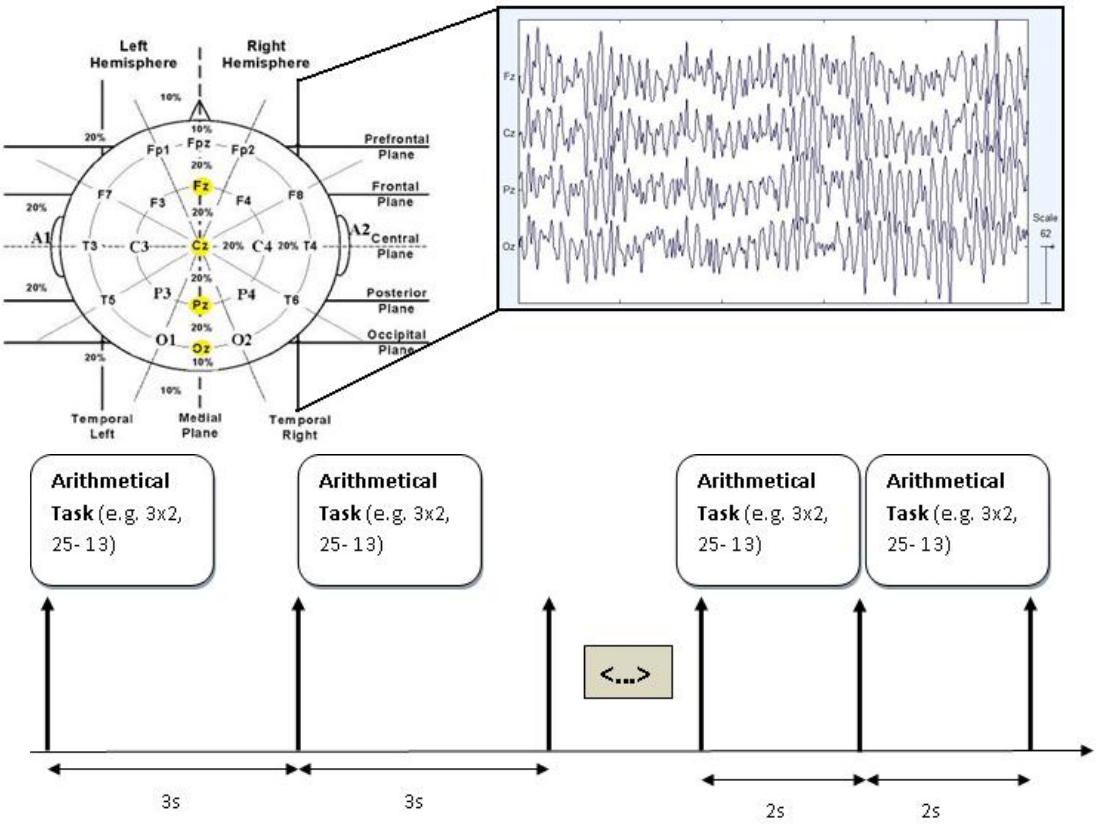

Figure 7.1: *Experimental setup: on the top we see the configuration of the electrodes used in this protocol with a placement according to 10-20 system (adapted from [19]) and an exemplary group of obtained brain waves. On the bottom, a schematic representation of the two applied tasks: stimuli each 3 seconds and stimuli each 2 seconds.*

cognitive impairment characteristic of some neurodegenerative diseases such as *Multiple Sclerosis* (MS) in which it is present in 60% of the cases [53]. This pathology shows effects like memory impairment, attention sustained, visuospatial perception and verbal fluency abnormalities, slowing of information processing and difficulties in problem solving and abstract reasoning [66, 53]. These effects are believed to be caused by the loss of connections between different cortical areas due to demyelination and axonal degeneration [66] and the loss of white matter was well-documented in the corpus callosum (CC) of patients even if it was in first stages of the disease [109]. Even if the Magnetic Resonance Imaging (MRI) yielded great conclusions about the neurological patterns of this disease, a connection between that evidences and the cognitive impairment observed were not always consistent, inspiring the need for other neuroscientific approaches [53]. The EEG coherence tool is a natural candidate due its capacity of studying functional relationships among the brain areas.

In this study, the objective is two apply a first analysis of the spectral content and coherence among EEG signals using the algorithm proposed in Chapter 5 and also

a time-frequency coherence approach. The main motivation of using these data is the appliance of some event-related measure of spectrum and coherence, the data of the next Chapter is continuous and does not permit this approach. This chapter is divided three parts: a first section concerning stationary analysis, a second relative to dynamical analysis and a last instance in which I briefly discuss the mains results of this chapter. In both of the two following parts details of the experimental implementation and results obtained are presented.

.

7.2 Stationary Analysis

Analogously to the situation presented with the simulation data, for calculating the spectrum and the coherence it was used the same algorithms, the sampling frequency was also 256 Hz, all the important parameters used were the same. The results concern the analysis of the four conditions and the frequency bands chosen to analyze were $\theta(4-7Hz)$, $\alpha(8-12Hz)$ and $\beta(13-30Hz)$.

7.2.1 Spectral Analysis

The first observation is a visible greater amount of power in the alpha and theta bands than in the subsequent higher band (beta) in all EEG datasets, being that factor a common finding [28].

Comparing the basal condition with eyes open to calculus situation (both stimulus conditions) patent in the figure 7.2, we can see that there is an increasing in power for each of the four electrodes for the alpha and beta bands. Analyzing more quantitatively that variation, the electrode in which the change was higher was the parietal, being the difference slightly more expressive in the situation of the task with 3-second interval stimulus. However, in this situation the peak seems centered only in 10 Hz (alphoid frequency) contrasting with the peak in the task with 2-second interval stimulus that looks more broad in frequency. Notwithstanding, the differences were significant for all electrodes and specially higher for the alpha frequencies, showing a clear relation of this band with the task. Comparing the power in the two task conditions, there are not other qualitative differences among the results. A typical finding was also present: the great decrease of alpha power between the resting states with eyes closed and eyes open reminiscent of alpha blocking phenomenon.

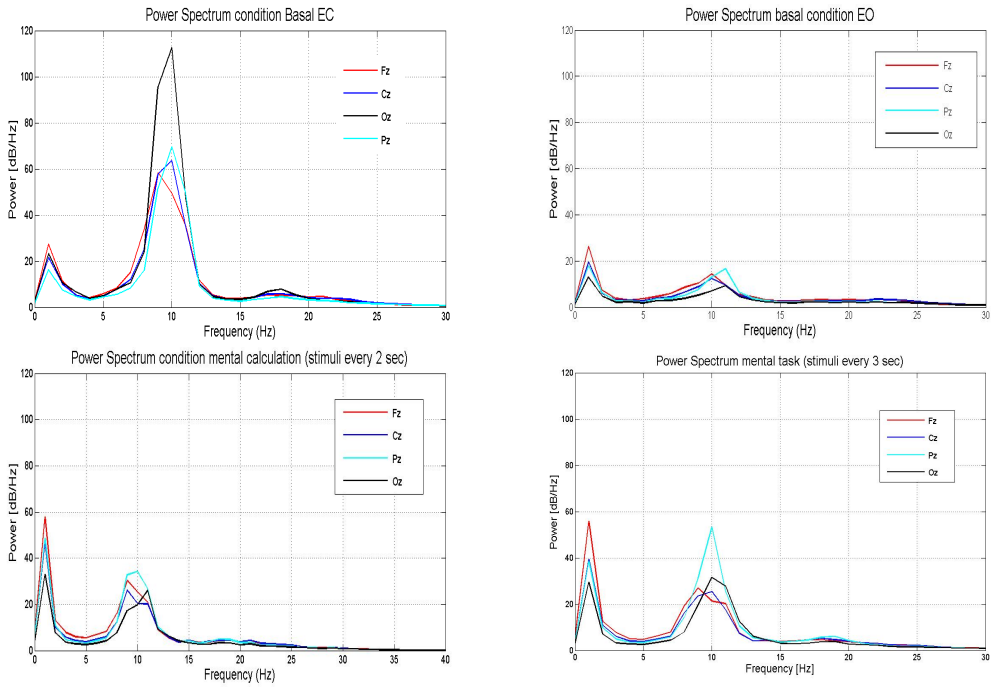

Figure 7.2: *Power spectrum from basal condition to a mental task situation.*

7.2.2 Coherence Analysis

Firstly, I would like to reaffirm a previous assumption for this analysis - in all channel analysis which if we are not comparing a difference between two conditions and only one is concerned, we have to bear in mind that adjacent electrodes have usually higher values of coherence not only because of phase coupling among them but also because they are more exposed to volume conduction problems, this must be present in all analysis of this and the subsequent chapters. The connectivity analysis trough coherence is based on a total of 6 combinations: Fz-Cz, Fz-Pz, Fz-Oz, Cz-Pz, Cz-Oz and Pz-Oz.

Basal Conditions

Analyzing the basal conditions near the region of 10 Hz, we observe in the recording with the eyes open a decrease relatively to the eyes closed in the value of coherence between every electrode except the pair Fz/Cz in the region of the alpha band. This a natural result once the rhythm alpha is almost exclusively present in the posterior part of the brain and is suppressed by visual stimulation [28]. On the other hand, results shown also that the variation of coherence was higher (near 20%) for the pairs Fz/Oz and Cz/Oz

than the approximately 10% variation of Fz/Pz, Cz/Pz and Pz/Oz. For interpretation of this facts, we can take in consideration that the most affected electrode during alpha blocking would be the occipital and so its coherence pairs would show the highest degree of uncoupling, that would explain the 20% variation of Fz/Oz and Cz/Oz. In that case, the fact that the other combination with the occipital channel (Pz/Oz) has an inferior difference though still superior to the Fz/Pz, Cz/Pz pairs is probably consequence of being the only combination where Fz and Cz (unaltered coherence) do not take part.

This preliminary observations are an evidence that oscillatory activity in the frontal region within the alpha band cannot be explained exclusively by the alpha rhythm, almost inexistent in this area, another source should be the cause of the high coherence value of the Fz/Cz channels. This source is possibly the *SMR*, this rhythm involves a band of frequencies partially equal to the alpha zone, which signify we have two different cortical generators working in the same frequency region. Supporting this interpretation is the fact this rhythm is observed strongly in situations where the sensory-motor cortex is idle like the present basal conditions.

Mental Task Conditions

Generally speaking, there is a tendency in all combination electrodes to decrease coherence values in the alpha band when some mental task starts, I noted that in every case of the two modes of stimulation except for the pairs Pz/Oz, here coherence in the alpha band undergoes a tenuous increase in both conditions and specially in the situation of 3-second interval (see figure 7.3).

In the task with 3-second stimulation occurs a small increase in the frontocentral pair in a frequency of the theta region (nearly 7) as we can see on figure 7.4, this is the only significant change in this frequency band.

Considering now the region of 14-15 Hz (traditionally a β region), I tried to look to differences in power that could suggest me the possibility of an increase in coherence for all electrodes in that narrow-band and even if all signals have an increased power, I could not find a pattern of where that increasing is most significant as I explain previously. Regarding now coherence variation in the same band, there is a consistent result of higher coherence in the more frontal pair Fz/Cz (see Figure 7.4). The difference is higher for the stimulation with the 2-second interval.

Apart these findings already reported, the general tendency for both conditions and for all channel combinations is lowering coherence values. Although, in an

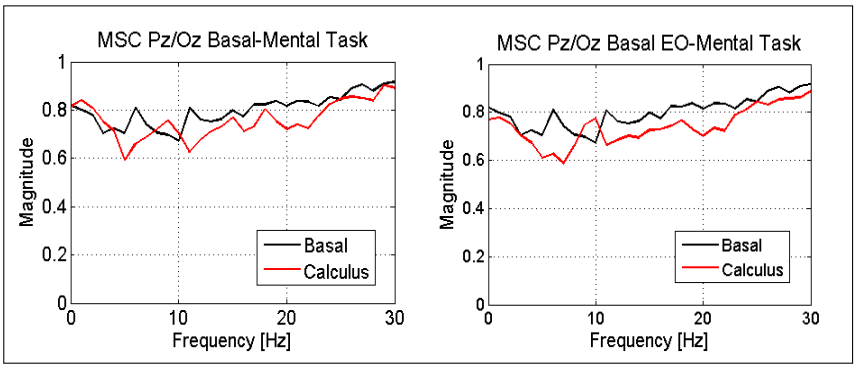

Figure 7.3: *Magnitude Squared Coherence for the pair Pz-Oz contrasted between basal eyes open condition and the two mental tasks: 2-sec interval (left) and 3-second interval (right). Note the alpha peak present in both but slightly higher for the 3-second stimulation.*

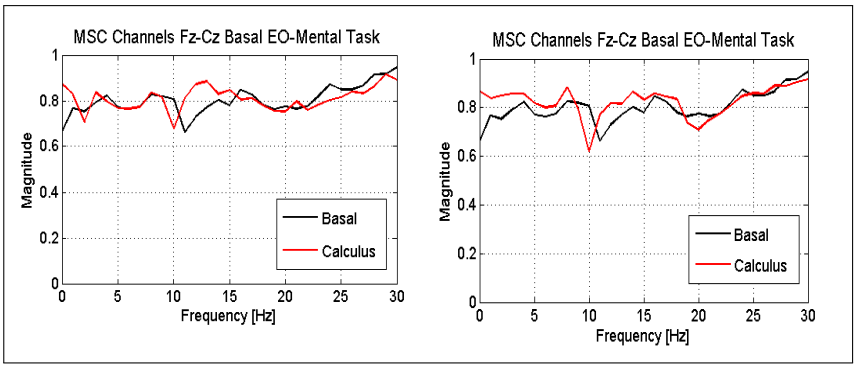

Figure 7.4: *Magnitude Squared Coherence for the pair Fz-Cz contrasted between basal eyes open condition and the two mental tasks: 2-sec interval (left) and 3-second interval (right). Note the increase in coherence in the sub-region of β, nearly 12-16 Hz and a small increase also in the θ region merely for the condition with 3-second stimulation.*

expressive part of the pairs one cannot even tell that exists a significant difference among basal condition with eyes open and task performance as the differences are so low they cannot surpass the confidence level.

Comparing the spectral results with coherence results they do not fully agree, there is a decrease in coherence in alpha for all pairs except the posterior one and results of power show an augment for all electrodes and specially the parietal. Regarding beta rhythm, results of both measures agree in an increase within this region however, looking more attentively, changes of beta power seem more centered near to 20 Hz meanwhile coherence increases in 12-16 Hz. This is not surprising as power spectrum and coherence are independent measures.

7.2.3 Some Conclusions

On a first glance, this analysis suggests that it is possible to relate differences on frequency bands like θ, α and β arising with the mental task though the changes reported are really small. Moreover, power spectrum and coherence offer quite distinct information.

This analysis suggests alpha coherence decreases in all except Pz-Oz pair whereas and beta coherence increase consistently in both conditions in the frontal region. The results between the two mental task conditions were also distinct, in the task with longer period of stimulation theta seems to increase and in the 2-second stimulation exhibits no differences.

A possible explanation for the fact that when the two distinct mental tasks are contrasted, there is a general reduce of coupling in the situation of 3-second stimulus interval is probably due to in this condition more time is conceded to the individual to rest between every calculation and as though this situation should approach more the results found in the rest condition. Or looking in a totally distinct way to the results, the fact that despite the alpha blocking phenomenon we have an increased alpha coherence in pairs (Cz/Oz and Pz/Oz) might relate this frequency band with the calculus task, particularly with a situation the individual had more time to respond.

7.3 Dynamical Analysis

Following the fact that it may be abusive to consider the recordings analyzed stationary, I tried to look for information also on the temporal aspect. The measure to

quantify the spectrum was the Event Related Spectral Perturbation (ERSP) proposed by [7]. The ERSP is an event-related measure which expresses the degree of changes in the spectrogram following task, for the computation the power spectrum is calculated over a sliding window and averaging across all trials performed, all the results are normalized by dividing by the mean baseline spectra immediately precedent to the stimuli events. The deviation is given in the temporal course of the epoch. Considering n trials, the ERSP is represented by the sum across all trials (k) of the temporal and frequency dependent power $F_k(f,t)$ divided by the total number of trials:

$$ERSP(f,t) = \frac{1}{n}\sum_{k=1}^{n}|F_k(f,t)|^2 \tag{7.1}$$

For evaluation of coherence, due to the periodic nature of this experiment's task one may use another estimation: the ITC (Inter-Trial Coherence). It reveals the extent of synchronization of the oscillatory activity at a given pair of latency/frequency to a set of events to which the EEG trials are time locked [7], a total degree of synchronization is represented by the number 1 whereas the absence of it between the recorded data and the time-locked events yields a zero value. One can measure the linear coherence (ITLC) or the phase coherence (ITPC), the main difference lies in the normalization process: in the case of phase coherence normalization to one is done initially to each trial and then the complex average followed (only phase information is passed); instead, in the linear case we only normalize after the average (see equations 7.2 and 7.3). The linear coherence is likewise the version of coherence implemented in the previous section, relying on the Matlab routine *mscohere()*, there is not a clear advantage of the two methods, on one hand performing normalization in each trial may help leading with artifacts (the contribution of one trial is diluted in the whole picture) but on another hand, information may be lost.

$$ITPC(f,t) = \frac{1}{n}\sum_{k=1}^{n}\frac{F_k(f,t)}{|F_k(f,t)|} \tag{7.2}$$

$$ITLC(f,t) = \frac{\sum_{i=1}^{n}F_k(f,t)}{\sqrt{n\sum_{k=1}^{n}|F_k(f,t)|^2}} \tag{7.3}$$

The modulus || represents the complex norm.

This measure was first proposed in 1996 by Tallon-Baudry et all (see [115]) and subsequently followed and extended by many others (e.g [50]) and was then designated "phase-locking factor". The background concepts were highlighted in Chapter 4.

Finally, to evaluate coherence among distinct signals, one can use the Event-Related Cross-Coherence (ERCOH), the principle is the same as in the coherence calculated in the previous section but adapted for two signals, in the linear case it can be represented by the Equation 4.7 and for the phase coherence by the following equation:

$$ERPCOH^{x,t}(f,t) = \frac{1}{n}\sum_{i=1}^{n}\frac{F_k^x(f,t)F_k^y(f,t)^*}{|F_k^x(f,t)F_k^y(f,t)|} \tag{7.4}$$

7.3.1 Experimental Procedure

I used the software EEGLAB v. 6.01b developed by Delorme and Makeig (see reference [7]) to obtain these time-dependent spectral and coherence measures. I will explain briefly the assumptions made and parameters chosen for each measure.

The computations made involved for each channel even-related spectral measure (ERSP) and event-related coherence estimate (ITC), in addition regarding combination pairs cross-coherence was also calculated. The aim was to discuss the potential advantages of this measures in extracting time-frequency features of EEG recordings.

The ERSP measure is implemented utilizing the EEGLAB in-built function *newtime(f)*. I used for spectral decomposition two different ways: DFT decomposition and sinusoidal wavelets. The type of wavelets applied were from the class Morlet variant, cycles were ascending from the lowest frequency to the highest (2 to 12.5 cycles), yielding a varied trade-off at distinct frequencies. In order to compute significance levels, an alpha value equal to 0.5 was applied and surrogation followed, the process used for the surrogation was inversion of the polarity in the ERSP and randomization of the phase (ITC), 100 trials were performed - non significant values are zeroed and plotted in green. I implemented also ITLC and ITPC in order to compare both results.

For calculating the event-related coherence among distinct channels I follow a computation using the EEGLAB function *newcrossf()*, the function I created is reported in Appendix 2. I computed event-related phase coherence for both conditions with fixed-window of 128 samples (500ms) and sinusoidal wavelets with ascending cycles between 2 and 12.5. The determination of levels of significance was identical to procedure made for ERSP and ITC. The possible non redundant combinations are 6. I tried to look for features in one task and compared both tasks.

7.3.2 Main Results

On a first glance, the most prominent conclusion is the intrinsic temporal pattern associated with the tasks. Generally speaking, we can see in the task with 2 seconds stimulation changes post-stimulus centered in a time-scale of some milliseconds until almost one second, while with the 3-second stimulation, the results extend to 2 seconds. A more detailed description will be made for each electrode in further considerations.

Comparing the results of ERSP and ITC, they are not always correlated, sometimes one outlast the other or shows a feature inexistent in the other.

Regarding the comparison between ITPC and ITLC measures, the results were the same for the former in all trials, and for the latter the differences were small, although phase coherence could identify more isolated episodes of ITC in the both cases of DFT and wavelet analysis for the two tasks. Nonetheless, the same episodes could hardly, for the most of the times, reach significance (assessed by the ERP curve in the bottom picture) and a clear gain of one of the approaches is not evident (see Figure 7.5).

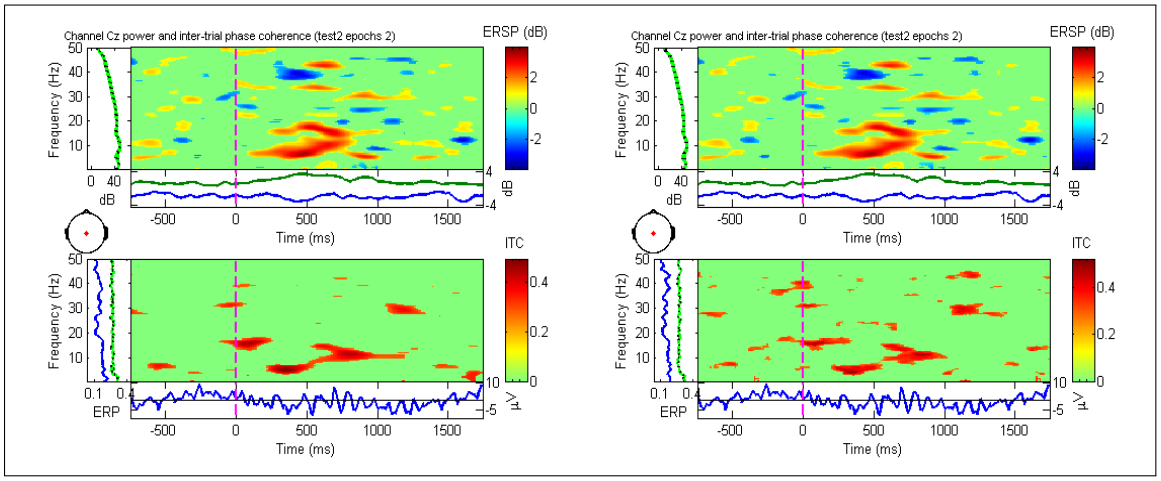

Figure 7.5: *Comparison for the central electrode and the 2-second stimulation task of the ITLC (left) and ITPC (right), using a fixed-window. Note the changes inherent to each mode in the lower panel. Frequencies are plotted trough 0.5-50 Hz.*

In addition, the results also shown some differences among the wavelet and fixed-window approaches followed. In a rough way, the sinusoidal wavelets give significant values in a more diffuse temporal-frequency region, showing that might exist interesting effects in a more expanded region of this two-dimensional space (Figure 7.6 illustrates this finding).

I investigated also what were the concrete findings regarding the tasks, I looked

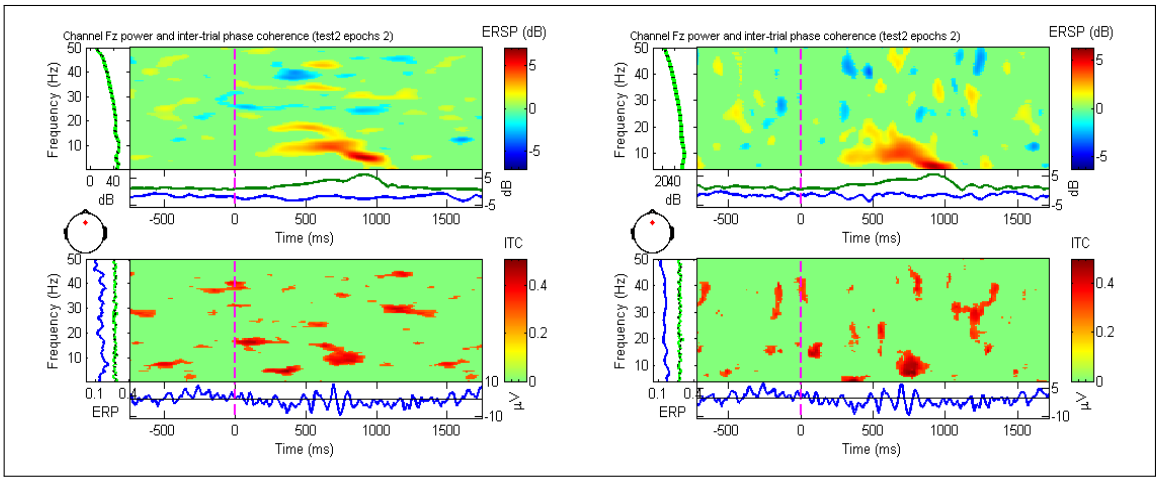

Figure 7.6: *Top: The ERSP for the frontal electrode for the 2-second stimulation task using hanning tapered zero-padded DFT (left) and Morlet variant wavelets (right). The upper left panel shows the baseline mean power spectrum, and the lower part of the upper panel,the ERSP envelope (low and high mean dB values, relative to baseline, at each time in the epoch), the ERSP is depicted trough the color scheme on the right. Bottom: The ITC for the same electrode-condition combination . Frequencies are plotted trough 1-50 Hz(DFT) and 4-50 Hz (Wavelet).*

for the ERSP time-frequency characteristics of both tasks and made a brief comparison among them.

For the task with 2-second interval stimulation, one can depict a spectral event-related change in all three bands (θ, α and β) being inconstant in time. The Table 7.1 shows the changes have a temporal pattern specific of the electrode in question, although for e.g. theta oscillations seem to present in Fz, Cz and Pz (in a smaller scale) in a common period of 800-1000 ms. Changes in alpha occur specially also in Fz, Cz and Pz. The activity in the Oz starts before stimulus and though may be a consequence of prolonged resting state instead of a phenomenon following task. For beta we have a general increasing in 15-17 Hz in a temporal scale that not exceed 1 second, in fact only for theta exist significant alterations in a temporal span higher than one second.

Relatively to the longer task, the scenario is quite similar: regarding theta we have stronger activation nearly 6 Hz for a period between 500-1000 ms between all channels and other changes electrode-specific; alpha oscillations are for all electrodes very brief in time and sparse. There are a lot of beta frequencies (ranging from 13-17 Hz) related with the task and the channels Fz,Cz and Pz are activated in a common time of 1100-1500 ms. Nonetheless there are a lot of spectral changes post-stimulus that outlast this period (see Table 7.2 for details).

Comparing the results for the two tasks, there is not any consistent observation regarding temporal pattern among the both. In the 3-second task one can notice effects

until 2 seconds whereas ERSP does not overcome 1450 ms in the former task. Important effects also seem to start sooner in the 2-second task.

Finally, one should retain that despite the temporal discrepancy among tasks (span 2-second: almost following stimulus $\longrightarrow$ 1 second and span 3-second task: 500ms $\longrightarrow$ 2s) they show a clear activation of theta, alpha and beta regions. All medial channels shown post-stimulus changes, comparatively Oz shows fewer effects in both tasks.

	Fz	**Cz**	**Pz**	**Oz**
Theta	• 6Hz(0.75-1s).	• 6Hz(0.1-0.6 and 0.8-1s). • Small increase (6Hz,1.25-1.45s).	• 6Hz(0.2-0.6s). • Small increase (6Hz,0.8-1s)	• 6Hz(0.25-0.5s).
Alpha	• 10Hz(0.3-0.9s).	• 10Hz(0.25-0.8s).	• 12Hz(0-0.1 and 0.4-0.6s).	• 11Hz(just before the stimulus-0.6s).
Beta	• 17Hz(0.3-0.7s).	• 16Hz(0.25-0.8s).	• 16Hz(0.3-1s).	• 15Hz(0.25-0.9s).

Table 7.1: *Summary of the principal ERSP increasings (frequency and time in seconds) found for all electrodes and bands θ, α and β in the 2-second interval stimulation using fixed-window decomposition. The frequencies and times are reported in a rough manner, the frequency/ies chosen is/are the most representative.*

The analysis of event-related coherence, on its turn, is not much conclusive about a time-frequency coupling structure. Generally, it reveals some inconstancy of coherence in a temporal scale but there is not any clue for synchronization following task.

For the event-related coherence among channel combinations, if the electrodes are adjacent all values are really high and any possible temporal structure is indiscernible in every condition, using fixed or varying-windows. For the remaining three combinations there are variations with time but none is locked with the stimulation. Comparison between the two modes of stimulation across time, permitted to conclude that the task with 3 seconds has a lot more phenomenons of desynchronization among all combination pairs than the task with 2 seconds. Apart that finding, the pattern depicted in both is more or less the same (see details in Figure 7.8).

The results obtained with the dynamical analysis are compared with the previous stationary results and related with state-of-art in mental calculation research in the discussion.

	Fz	Cz	Pz	Oz
Theta	• 6Hz(0.5-1s). •Small increase (6Hz,0.1-02 and 1.6-2.2s)	• 6Hz(0.4-1.2 and 1.4-2s).	• 6Hz(0.45-1.2s). • Small increase (6Hz,1.5-1.9s)	• 6Hz (0.5-1.2,1.6-1.8s).
Alpha	• 10Hz(0.65-0.9s)	•Until 11Hz(0.55-0.9s) • Until 12Hz(0.75-0.9 and 0.1-03s).	• 10 Hz(0.2-0.9 and 1.1-1.9s).	• 10-12 Hz(0.09-0.3,1-1.25 and 1.55-1.9s).
Beta	• 15Hz(0.35-0.55, 1.1-1.5 and 1.85-2s). • Other small activations.	• 14-15 Hz(1-1.6,1.85-2s). • Other smaller activations in higher β frequencies.	• 13-15 Hz(0.15-0.35 and 1.1-2s). • Other smaller activations	• 14-15Hz(1-1.25,1.55-1.9s and some really brief episodes).

Table 7.2: *Summary of the principal ERSP increasings (frequency in hertz and time in seconds) found for all electrodes and bands θ, α and β in the 3-second interval stimulation using fixed-window decomposition.The frequencies and times are reported in a rough manner, the frequency/ies chosen is/are the most representative.*

7.4 Discussion

Previous to start the discussion, an important assumption of this chapter must be highlighted - the primordial purpose is not to establish a pattern that relates coherence with the task of mental calculation, results from merely one subject are naturally limited to draw conclusions. Instead, the main purpose is to analyze some suggestive findings and compare different potentialities of the algorithms used. I will build this conclusion analyzing the three frequency bands, comparing both, the non-dynamical and the temporal and frequency-dependent strategies. I consider that these results may inspire future implementations of this type of protocol in larger populations.

Starting with theta band, the non-dynamical analysis shown its role in the 3-second task, namely in the fronto-central region. Yet, the spectrogram clearly implicated theta in both tasks (2 or 3-second stimulation) in a non constant temporal scale.

Regarding alpha effects induced by the task, in the first analysis we concluded alpha decreased in all combinations and augmented in the posterior one (specially in the 3-second experiment). The ERSP revealed a complexer pattern. There are changes in Oz that clearly show the activation start precedes the onset of the stimulus so it may be not relevant and only due to a continued inactivation of the occipital region. Notwithstanding, all electrodes show other changes, Fz and Cz show an increase in ERSP in nearly the same time (300-800 ms) as well as Pz and Oz (0.4-0.6s) and also their activations seem

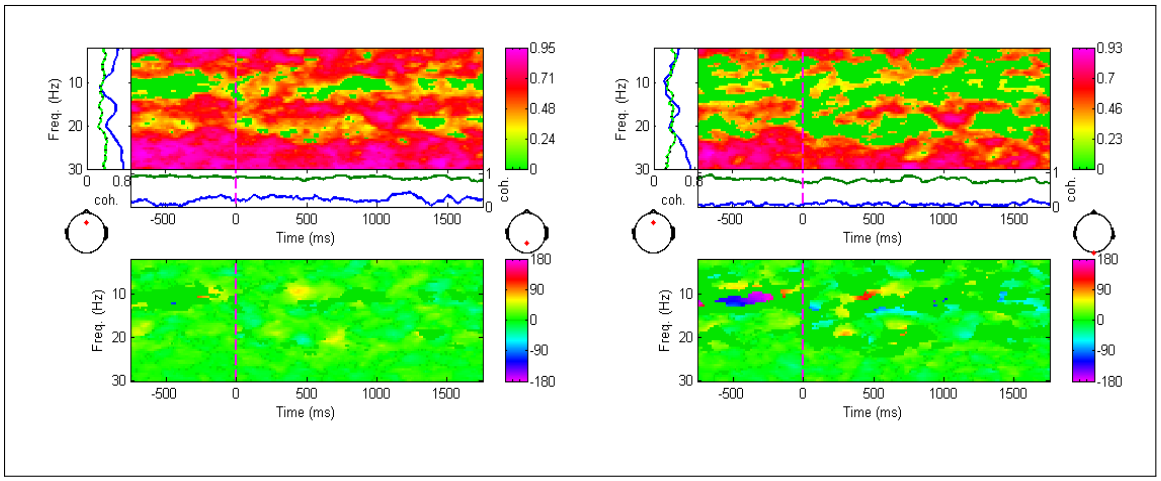

Figure 7.7: *Two example cases of Event-related phase coherence computed with fixed-window in the task with 3-second stimulation.Left: pair Fz/Pz and Right: pair Fz-Oz. The panel on the left on the top image represents the mean baseline coherence among the frequencies. The horizontal panel instead shows coherence maximum (green) and minimum (blue) value in the range of all frequencies.In the inferior plot, phase difference of the two signals is shown for all cases coherence is significant. Frequency span is 2-30 Hz.*

to centered in distinct alpha frequencies.

Finally, the spectral and coherence analysis of beta region shown in a first approach, an augment in the fronto-central region (specially in the task with 2-second stimulation). Activation was expanded to all electrodes and did not exceed one minute (2-second task) or two minutes (3-second task) with the dynamical analysis.

From the analysis with ERCOH in a general way for all bands, one depicts that coupling among distant channels varies with time, namely in the longer task that variation is more present with more phenomenons of uncoupling. An analysis of adjacent electrodes was impossible, they shown always extremely high values of coherence due to volume conduction effects.

The two strategies shown congruently differences among the two mental tasks, not disregarding however they have a basic common pattern. Particularly, both methods demonstrated that roughly, coupling is reduced or has more episodes of reducing in the task with the longer time for alpha and beta frequencies. Regarding theta oscillations and the two mental tasks, theta coherence or spectral content seems to be enhanced predominantly in the longer task (stationary analysis only detects increased theta coherence in this task and in dynamical analysis episodes of ERSP and ITC are more and longer).

Considering the primary goal of infer qualitative comparisons among the diverse strategies, the results suggested the two approaches (stationary and dynamical) can offer distinct information. Moreover, in the dynamical analysis one can sustain that the linear and phase coherence seem to not differ much in the present case. Nevertheless, the

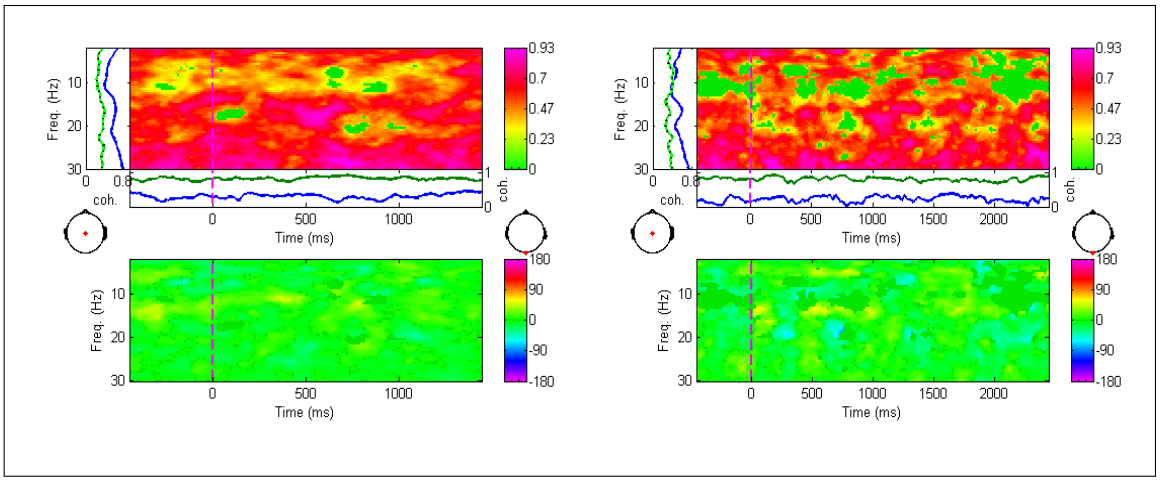

Figure 7.8: *Comparison of Event-related phase coherence computed with varying-window in both tasks for the combination pair Cz/Pz - task 2 seconds (on the left) and task 3 seconds (on the right). Frequencies represented are between 2-30 Hz.*

choice must be highly dependent on the data we are dealing with. Regarding frequency-temporal decomposition, the method with wavelets shown important changes in a greater extension of the bi-dimensional space, at what extent this really reflects more real physiological changes following task is a question that remains unclear, as pointed out by [5] the phase information obtained with wavelet transform is currently not completely understood. Authors like [93] have already found evidences corroborating this superiority of wavelet decomposition. Due to the limitations of the present data, a complete analysis of the ERCOH was not feasible.

One important conclusion is that, even if dynamical analysis revealed more features even in frequency structure, it really offers a lost on the resolution of frequency (implicit trade-off), and accordingly one cannot neglect none of the strategies in order to obtain the maximal information.

The main goal of this chapter is not to establish clear relations but I should say that some results agree with the current theories regarding arithmetical calculation (see Chapter 6). Accordingly, beta spectral or coherence changes seem to increase like in [37] and theta appears related to a longer time to do the calculations, an hypothetically role of theta waves and the longer time the individual had to answer may be explained by the possibility of retrieving known facts from memory to solve the problem and the subsequent role of memory in the process.

Chapter 8

Mental Calculation: Counting backwards task

"Can you do addition?" the White Queen asked. "What's one and one and one and one and one and one and one and one and one?" "I don't know," said Alice. "I lost count." **Lewis Carroll**

8.1 Experimental Protocol

8.1.1 EEG Acquisition and Participants

EEG data were recorded from a 32-electrode cap used in an experiment with 15 healthy volunteers (7 male, aged $23-40$, mean: 31.9 ± 5.3), right handedness was common among all except one volunteer. The electrodes used were FP1, FP2, AF3, AF4, F7, F3, Fz, F4, F8, Fc5, Fc1, Fc2, Fc6, T7, C3, Cz, C4, T8, Cp5, Cp1, Cp2, Cp6, P7, P3, Pz, P4, P8, PO3, PO4, O1 and O2, distributed according to the International 10-20 system, and using averaged reference (see Figure 8.1). The impedance of the electrodes was kept in the worst case below 10 kOhm (for the greatest part of the electrodes and the individuals the values were much lower), being controlled by the amount of conductive gel that was used to establish the contact between the electrodes and the skin. The recordings were sampled at 2048 Hz, and three digital filters were applied to the data: a high-pass filter with a cut-off frequency at 1.6 Hz, a low-pass filter at 60 Hz and a notch (50 Hz). EOG artifacts were removed with a posteriori processing. All these steps were made through commercial versions of *BESA 5.1.8* software and *Biosemi* equipment, the former was used for the preprocessing (artifact rejection, filter appliance...) and the latter controlled

the acquisitions (permitted to establish the sampling rate and see the impedance of the electrodes). The volunteers were a population mainly constituted by university students or teachers, they all declared not having any auditory, visual or neurological problems and only performer 10 is left-handed. Performers 4 and 11 were under medication. The Table 8.1 in the end of the chapter summarizes some details regarding the volunteers.

The individuals started the test in resting state, basal recordings were made with eyes open and eyes closed. Then, the subjects were instructed verbally to start the task which lasted for 3 minutes (details are succinctly explained in the next section). The subjects were not informed previously about the task they would perform so no previous practice is assumed.

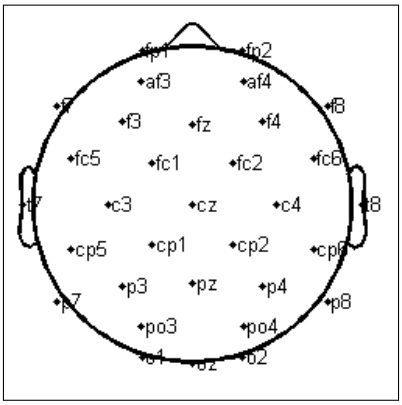

Figure 8.1: *Distribution of the electrodes utilized in the present experience. Electrodes outside the head model account for lateral positions.It was used average reference.*

8.1.2 Cognitive task: Counting Backwards

On this experimental protocol, a simple task was utilized, basically it consisted in with eyes closed, subtract successively from 200 by 3 during 3 minutes. The volunteers were told to repeat the procedure in case they finished the sequence without interrupting. For every 10 subtractions there is a pattern, the last digit of the result is (0,7,4,1,8,5,2,9,6,3) and the first two follow also a logic:

$$\underbrace{200-197-194-191-188-185-182-179-176-173}-$$
$$\underbrace{170-167-164-161-158-155-152-149-146-143}-140...$$

After the 3 minutes of the task, the performs were asked in what number they finished the calculation and what strategy they follow for the execution. From the whole group, only five individuals (performers 2, 3, 4, 7 and 9 - see Table 8.1) declared they used

only the calculation. The others, generally stated they started to use the computation and after discovering the pattern used the two strategies. The greatest part only declared they used the pattern (9,6,3) although confirmed the result in multiples of 30. Only one performer had great difficulties and showed evidence of high grade of mistakes in the task. A control of calculation mistakes was not made because it was hypothesized that occasional mistakes must not have influences on the results and the goal is to evaluate a situation of normal calculation, mentally made with the minimal external confounds. Regarding the speed of calculation, there were 4 individuals which did not overcame one turn of computations i.e. they did not reach zero (they were performers 6, 11, 12 e 15).

This is a task which demands a lot of cognitive effort (as we seen in Chapter 6 does not rely in rote learning), needs a constant use of working memory (WM) [51] and it can be used in individuals with neurological problems [51, 37, 83, 130]. Working memory is the capacity of holding in memory temporarily an amount of information that is often necessary to accomplish a task (see reference [9] for review). A challenging feature of this testing is also that it comprises a double strategic nature, specially when it is executed for a somehow long period (in the present case 3 minutes). Indeed, for performing such a type of test we can always rely on the pure computation or learn the repetitive pattern inherent and retrieve it as a fact from memory without even effectuate the calculation (i.e. real manipulation of the numbers).

8.2 Experimental Paradigm and EEG Processing

8.2.1 Frequency Analysis

Frequency analysis considered the following classical bands: θ (4-8 Hz), α (8-12 Hz), β (13-30 Hz) and γ (above 30 Hz). Due to great variability in the alpha band, a division between lower alpha ($\alpha 1$ between 8-10 Hz) and upper alpha ($\alpha 2$ between 10-12 Hz) was followed. Although, beta band can also be split between sub-bands $\beta 1$ (13-18 Hz) and $\beta 2$ (18-30 Hz) that division was not considered once few differences lay on that subdivision. The gamma region was analyzed but results are not exposed, we consider that due its low or inexistent presence in the power spectrum of the participants, their infrequent episodes of coherence and the limitation of the algorithm shown in the simulation when applied to the γ frequencies, there are not any conditions to accurately analyze this band.

8.2.2 Study of Spectral Power and Coherence

As it was already exposed, EEG power and coherence provide measures of regional activation and interregional connectivity, this two measures are independent but a congruent occurrence of high power and coherence is a strong indication of particular task-related frequency relevance.

The spectral power and coherence were calculated considering Equations 4.6 and 4.7, by the Matlab v 7.1 in-built functions *pwelch()* and *mscohere()*, the segments of data were Hanning tapered and an overlap of 50% applied which are proved to improve the reliability of the estimation [15]. The dimension of window chosen was 4096 samples (2 seconds) before the overlapping. I tried to look for differences with smaller windows (2048 (1 second), 1024 (500 milliseconds)...) but the general tendencies were always equal (see Figure 8.2), once in this experience there is a constant performing of the same task it is not so important to have a detailed information in time and the trade-off between frequency and time must privilege instead a more grainy picture of frequency. The spectral power was studied, analyzing which bands have a significant amplitude contribution in the overall scalp or just in some electrodes for the conditions basal eyes closed and mental calculation. On the other hand, coherence was compared between the previously referred conditions and the recordings during the mental task were also divided in three parts corresponding each one to nearly 1 minute of recording. The intention was to find if there were significant differences between the first minute and the last ones in the cases which the subjects declared they used the memorized sequence instead of doing the arithmetical computation. Results in power and coherence will be compared to possibly identify important relations.

Power spectrum was computed for the whole set of channels, coherence instead, was calculated with all the combinations of channel C3 (precentral left channel) and channel C4 (precentral right channel) making a total of 64 pair combinations for each condition: basal eyes closed, mental task, first minute mental task, second minute mental task and third minute mental task.

In order to account for possible relations between the serial subtraction with bilateral parietal activation because EEG coherence arising from mental calculation may implicate short-range intraparietal connections as suggested by fMRI studies (see Chapter 6) and/or the fact fronto-parietal network was already pointed out as related to working memory system necessary for a task such as the present [87], additionally, I computed coherence also between the electrodes F3, Fz, F4, P3, Pz and P4. The first three represent

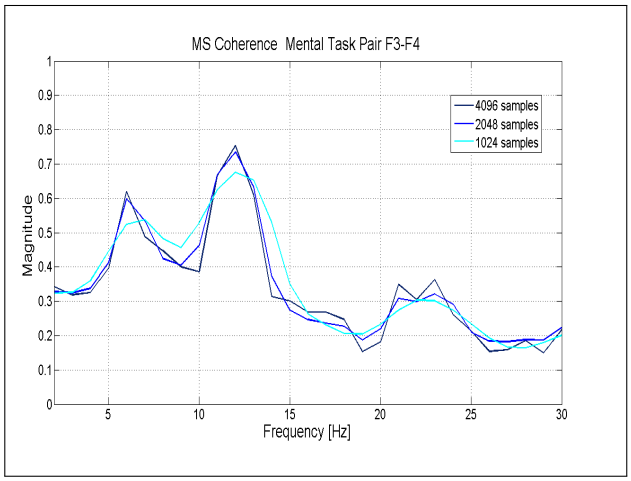

Figure 8.2: *Comparison of the results with progressively smaller windows (4096 samples (2 seconds), 2048 (1 second), 512 (0.5 seconds))- example for the pair F3-F4 (performer 2) during mental calculation. Longer windows produce a more refined picture of frequency but the general tendency is maintained.*

an anterior group of frontal electrodes with short-range connections and the last three a similar symmetric parietal system. Long-range connections are represented by three groups- intra-hemispheric left (F3-Pz, Fz-P3 and F3-P3), intra-hemispheric right (F4-Pz, Fz-P4 and F4-P4) and inter-hemispheric (F3-P4 and F4-P3). The medial pair (Fz-Pz) was also took in consideration. Figure 8.3 illustrates all the pairs analyzed. Totally, there were computed more new 16 coherence graphs for each individual.

. Previously I established some hypothesis that could apply to this results based on previous research in similar matters. The MEG study of [84] found an association between large-scale fronto-parietal α and β synchrony increasing and mental calculation and a study of amplitude related higher alpha power amplitudes during a WM retention period and suppression after it in the parietal domain [85].

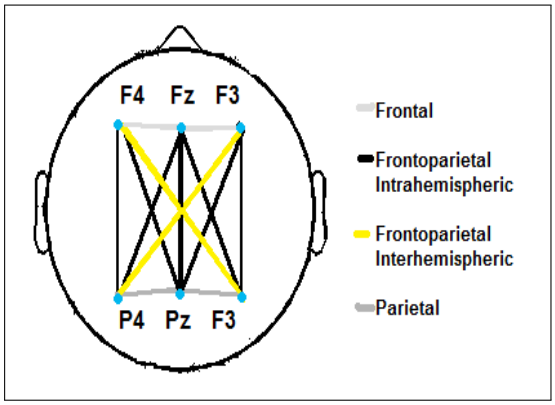

Figure 8.3: *The analyzed channel pairs in frontoparietal study, I investigated short and long range connections, pairs inside one hemisphere or representing coupling among the two hemispheres.*

On the other hand, in the work of [87] and [125] θ coherence was enhanced during the retention period in the frontoparietal network. Still in [87], alpha short-range anterior connectivity decreasing and augmented long-range theta coherence was found in visuo-spatial working memory task. A more pronounced posterior theta coherence may be also related to more memory load.

In posterior and bilateral central regions the alpha upper frequencies were also found to be more coherent with increasing load of WM [81].

Based on this information I will focus this part of analysis in the following hypothesis:

- Theta (θ): 1. may increase during the task in the fronto-parietal network due to the WM need of keeping numbers in mind to proceed with the subtractions. 2. may be higher in the individuals which used the pattern for doing the calculations because the WM load is higher (they retrieve the numbers and the pattern), can augment in such a case also in the posterior areas such as parietal lobe.

- Alpha (α): 1. Possibly augments in the fronto-parietal network and parietal zones and decreases in the frontal areas. 2. Like θ with increasing memory load (individuals that use the pattern) can increase in parietal region. Research up-to-date lacks details that permit a correct analogy between difference experiences.

- Beta (β): may increase in the fronto-parietal network.

8.3 Results

8.3.1 Power Results

There is a great variability in the results of spectral power across the performers, neither in values of amplitude nor in relative change of power between basal and mental task conditions there is an agreement between all participants.

For almost all independent single epochs, alpha was the predominant band, theta shown also consistently a significant spectral content as well as beta, notwithstanding the latter had a relatively smaller representation. The gamma power spectrum was practically inexistent in all observations. Subtracting mental task power from the basal background, the arising pattern reveals a tendency to decrease alpha in 10 individuals and increase beta in 8. An augment in theta was also found, although only in 4 performers. I equally observed that even if alpha generally decreased, the power in the upper alpha band was higher in 6 cases comparing to the basal situation.

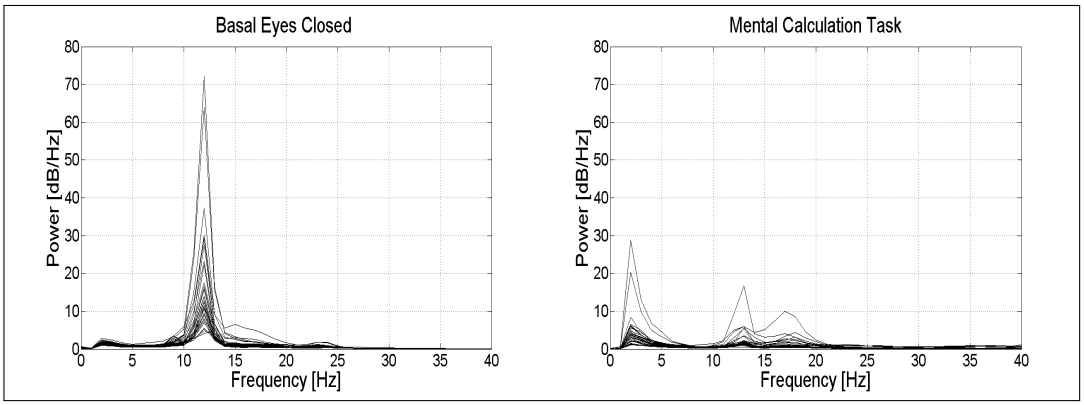

Figure 8.4: *Power spectrum [dB/Hz] of performer 8 for all channels during basal condition eyes closed (left) and mental calculation (right). Note the vanishing of alpha frequency (12 Hz) during mental calculation accompanied by a tenuous increase in frequencies of beta band.*

8.3.2 Coherence Results

Following a preliminary visual inspection, there is a significant variability in the results of coherence between the different subjects. This is expectable once the mental task is complex and even on the basal situation great fluctuations are expected among the subjects [22]. A high variance was found among the analyzed population, inside the same condition and among conditions so, a mean of the results would be fallacious. A more insightful analysis of the results was made for the combinations of the central symmetric electrodes C3 and C4 located in the left and right hemisphere, respectively, with all the other 31 electrodes and, for the pairs in the fronto-parietal network. That sort of analysis contemplates intra and inter-hemispheric, long and short-range relations.

In a general way, a common finding in all subjects and conditions is that episodes of coherence in the slower bands are not so broad in frequency than the ones in the faster bands - beta and gamma. A deepest analysis will be the goal of the next sections.

Comparing Coherence Basal-Mental Task

Comparing the calculus-basal situation, it is possible to underpin a multiplicity of changes, yet only some of them are consistent. In the alpha band, there is a decrease in 11 individuals for at least one of the sub-bands. This diminution is almost always in $\alpha 1$ region and the participants where this decreasing is apparent in the upper alpha band have all presumingly their alphoid in this band. At the same time, we can see related with $\alpha 2$ an increase in some regions of the cortex of the coherence, this is reported in 14 individuals and do not show a clear topographical pattern across the cases.

In the beta band, a consistent increase in linear coupling for all individuals is

present (e.g. Figure 8.5). Among all the possible connections, the ones more frequently enhanced are the left intra-hemispheric of the frontal and/or precentral areas, being this topographical characteristic inherent to 12 participants.

Also in theta there are significant changes, coherence between θ outbounds increases for 12 participants as well, although in some of them the number of combinations in which occur this augmenting is quite small. Furthermore, to this finding it is hard to address a regional constraint although it seems preferentially anterior than posterior.

Comparing the spectral power and coherence results, they coincide only partially for all bands. Namely, in alpha decreasing coherence reported two more cases of diminution than the power changing cases. A more contrasting situation was the augment in $\alpha 2$ in which power was only higher in 7 situations and strengthened coherence was always present except for one case. The same conclusion holds for beta band, a higher coherence is present in every combination and spectral changes only occur in seven participants. For theta, results express even less accordance as spectrum changes only for four individuals and for one them coherence does not increase.

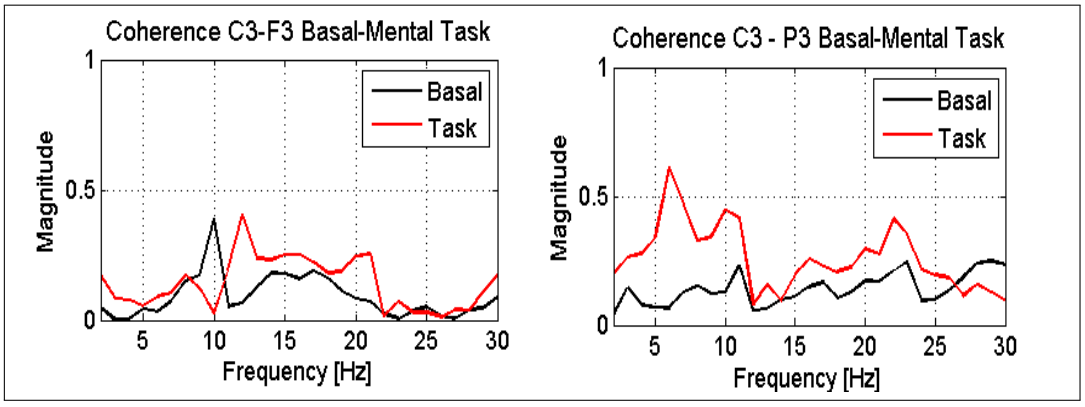

Figure 8.5: *Top: Magnitude squared coherence of subject 9 for precentral and frontal electrodes C3-F3 during basal condition eyes closed (black) and mental calculation (red). Note the increase in a1 frequency (12 Hz) and ß frequencies. Right: Magnitude square coherence of subject 2 in the same conditions but for precentral and parietal electrodes C3-P3. An increase in 6 Hz (θ), α (11 Hz) and β (22 Hz) is shown.*

Coherence Intra-minute Mental task analysis

Evidences of the second part of the analysis (intra-minute analysis) shown an even more complex pattern. On a first glance, there are not any consistent results concerning a specific frequency band or minute. The bands with the most representational increases among the whole population are: alpha (first minute: an increase in 8 individuals; underrepresented in the second and increases in 6 cases in the last minute) and beta (for 6

individuals in the first minute, for the second and the third, 10 and 8 cases, respectively).

A curious feature of increasing beta is that participants never shown an increase in all the three minutes, the phenomenon of increasing beta is exclusive in the first minute for 3 cases, exclusive of second minute for one subject and only occurring in the third minute for two cases. The greatest part of the subjects (the ten left) revealed a progressively increasing beta minute to other in the two first or two last minutes span. For alpha temporal pattern, we can also depict that increases are as well strictly related to just with one minute or two, only a subject shows a constant increase across minutes. Alpha coherence is in 8 cases higher in just only one minute (4 cases in the first minute, 4 cases in the third minute), in 2 cases the tendency is augmenting only in first and third minute and in 1 case the same happens for first and second minutes. Independently, 8 individuals shown an exclusive or no, higher coherence in the first minute (e.g. Fig. 8.6). The fact that for nearly half of the population alpha coherence was enhanced in the first minute is suggestive. The group which presented this characteristic is composed by performers 1,3,5,6,9,13,14 and 15, I searched for a common trait among this group but I could not find one involving all of them.

Considering now theta coherence, once again there is not any clear pattern, differences concern at the maximum 5 subjects. For subjects 1 and 2 coherence increases in the first and third minutes, while for subjects 4 and 13 coherence increases in the second and third minutes. There are 8 cases where changes of coherence depend on the minute but there is not any consistent observation.

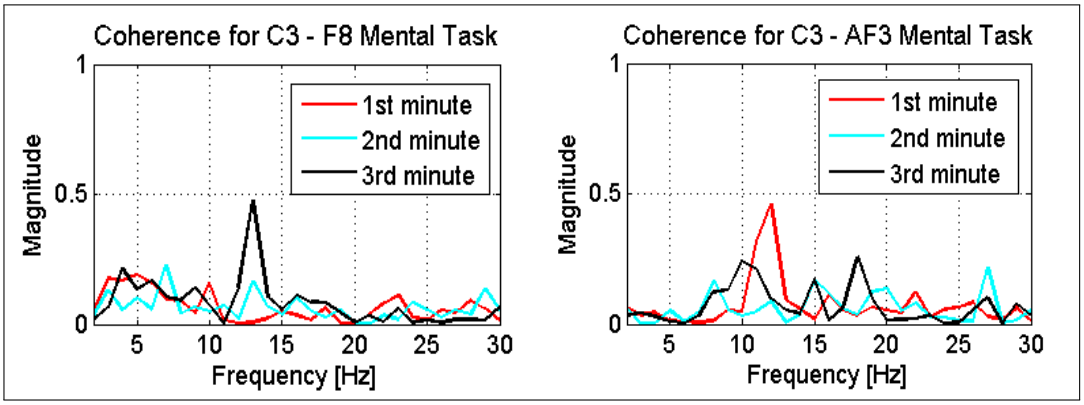

Figure 8.6: *Left: Magnitude squared coherence for the precentral-inferior frontal pair (C3-F8) in each minute in the case of subject 8. Note the 13 Hz frequency peak more pronounced in the third minute. Right: Magnitude squared coherence for the precentral-frontal pair(C3-AF3) in each minute in the case of subject 9. Note that the 12 Hz frequency peak more pronounced in the first minute is a tendency found in 9 cases.*

Study of fronto-parietal network

Accordingly with the experimental paradigm, I investigated also possible task-induced relation in the frontal, parietal and specially fronto-parietal area which the previous analysis could not naturally give any information about. Results from performers 10 and 15 were excluded from this part of the analysis due to the existent artifacts in some channels in study, so we will study a population of 13 individuals with 5 which used only the calculation and 9 which used a combined computation/pattern-retrieval approach. I will expose the main findings in the follow lines.

Frontal region Considering the frontal pairs analyzed, for all type of connections there is a consistent result of diminishing alpha coupling in more than half of the population (inter-hemispheric connections displaying the highest number of cases, 11). This supports the formulated hypothesis of alpha desynchronization in frontal areas. Only performers 11 and 12 had increasings in this band and the results for 11 are somehow questionable once this individual showed much difficulty in executing the task (feelings like math anxiety can produce confounds in the whole picture). For theta, there is not any consistent finding but a greater number of changes (increasings or decreasings) occurs in the right side . Contrasting, beta oscillations does not show any lateralization effect, an increase in all connections is present for 6/7 performers. An enhancing in all channels is common for performers 2, 7, 8, 11 and 13, a group in which I cannot detect any other common feature.In Figure 8.7 we can see an example of the most typical situation.

Fronto-parietal region Regarding θ coherence in all the fronto-parietal connections there is not any consistent finding common to all subjects although in concordance to the hypothesis there is an expressive increasing in the inter-hemispheric connections for 9 individuals (e.g. Figure 8.7) and a right-lateralized augment also in 7 volunteers. Notwithstanding, results did not corroborate the hypothesis of enhancing theta oscillations specially when using also the pattern because two subjects which only used the calculation were present in these groups. It is important to note that all the observations in this band shown differences mainly in the sub-band 5-7 Hz. Results in the alpha band were really complex, they point out mainly for inside each hemisphere coherence decreases in the upper alpha band (right: 9 individuals; left: 7 individuals) and also in the medial pair coherence diminishes in some cases but regarding inter-hemispheric connections nearly half of the population has an increased or decreased alpha coherence. Once again, for beta even though I have hypothesized an augment I did not found a consistent result

supporting that theory.

Parietal region Finally, assuming now parietal coherence changes there is not again any general tendency. For theta waves, results point for changes more on the left hemisphere (P3-Pz) or between the two (P3-P4) though the results are not significant because only relate 5 subjects (in Figure 8.7 we can observe a strong theta coherence activation following task). Inside this five cases, only one is from the group of individuals which did not use the pattern. Regarding alpha, once again there is not a consistent finding - I reported a differential tendency depending on the hemisphere: on the left alpha tends to decrease in 6 individuals and remains the same in the others, on the right we have an inverse tendency (in 6 cases coherence increases). It is important to note that this tendencies are related to different groups of subjects. The former group includes performers 1, 6, 7, 8, 9 and 10 and the latter, performers 2, 4, 5, 11, 12 and 13. I tried to look for other common traits among the groups (such as strategy, speed, age...) but I did not find any reasonable consideration. On the contrary, for beta there is not any lateralization, the most common tendency is increasing or remaining constant in these frequencies in all pairs, though the number of increasing coherence subjects is at maximum 6.

8.4 Discussion of the results

Power spectral and coherence estimation can be used to assess frequency and coupling information in a continuous mental calculation effort. A preliminary conclusion is that coherence results seem to offer partly agreement but also distinct information regarding brain networks and arithmetical calculation when compared to power analysis.

Regarding the specific studies of this chapter, this study permitted to conclude that exists a relationship between alpha, beta and theta rhythms and continuous arithmetical effort. The increase of coherence in beta for all participants summed with the increase in power for nearly half of the cases during the task suggests a role of this frequency in the calculus, or at least is due to sustained attention [37]. The study of [117] shown that beta power was higher in mental calculation than only in sign comprehension task, suggesting more use of mental resources, then one can possibly depict consistent with our results the role of β in arithmetic calculus. The results also shown a pronounced left frontal and precentral intra-hemispheric pattern that was already implicated and is known to be related with linguistic functions and working memory capacity.

On the other hand, alpha did decrease during the task, this can be correlated

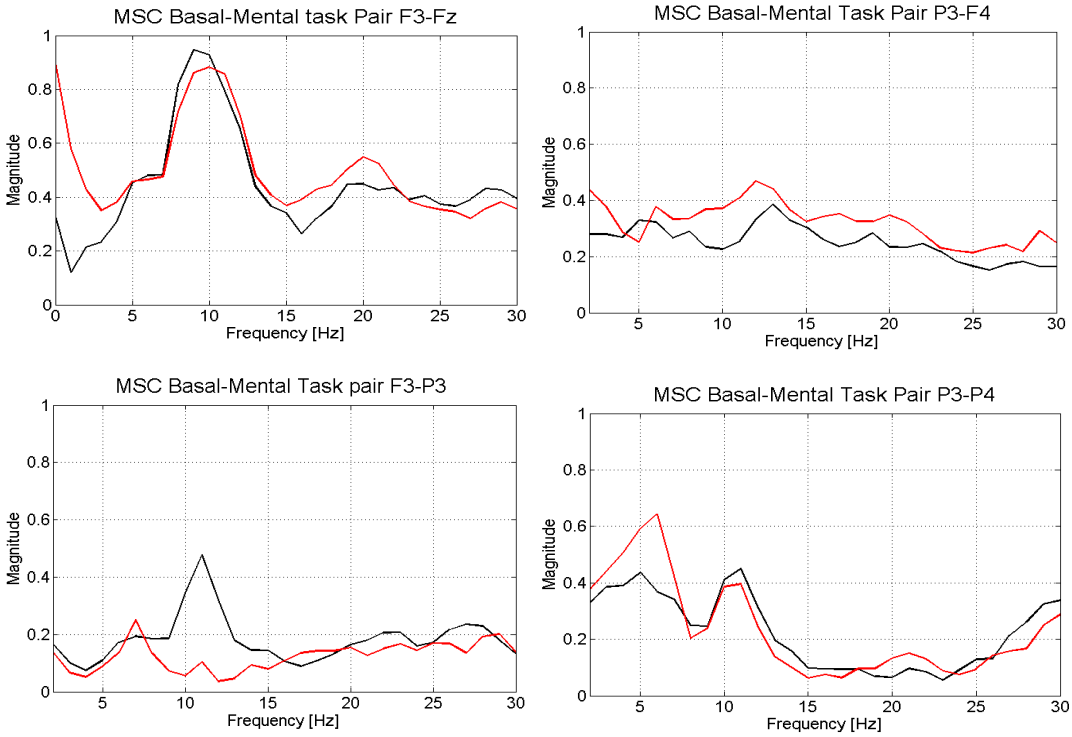

Figure 8.7: *Left Top: Magnitude squared coherence (MSC) for performer 7, pair F3-Fz (left frontal) compared between basal condition with eyes closed and during mental task. Note the slight decrease in upper alpha coherence (nearly 10 Hz) and increase in beta coherence (circa 20Hz). Right Top: MSC for performer 6, pair F4-P3 (inter-hemispheric combination) again in the basal-mental task shift. There is an increasing in θ, α and β bands. Left bottom: MSC for in basal-mental task condition for performer 14 and left intra-hemispheric pair F3-P3. One can depict that alpha coherence almost disappears (a tendency sustained in 9 subjects out of 13), we can also observe a small peak near 6 Hz (θ region), this was common to 5 performers on the left hemisphere. Right bottom: MSC for performer 1 and intra-parietal pair (P3-P4). Results denote a strong increase near 6 Hz (a tendency shared with 5 subjects), alpha seems to decrease slightly as well as beta.*

with the known theory of alpha rhythm as a mechanism associated with an "idling" brain, which disappears when visually stimulated and/or with growing attentiveness or due to selective cortical inhibition (see Ref. [85] for review). Contrasting, the consistent finding of an increased coherence in the upper alpha band reinforced the more recent idea that alpha oscillations do have a role in mental processes. Previous work related with working memory has addressed the same conclusion [87] and emphasized the alpha modulation with memory load, successive increasing of items stored in working memory [81, 37, 117].

Furthermore, theta oscillations increase in a significant part of the population are in concordance with previous studies on mental calculation [62, 61, 117]. A curious

finding is that for the four most slower performers (cases 6, 11, 12 e 15 where the only ones which did not arrive to a second turn of subtractions) spectral power in the θ band was almost inexistent and coherence changes arising from the task really small or also inexistent. The Refs. [113, 62, 57] have found with their work that theta appears during incessant mental calculation but can cease if calculation rate decreases so, theta according with these previous works and also the present, seem to arise during mental calculation dependently on the rate computations are held.

The temporal tripartite analysis evidenced dynamical differences across the three minutes in the frequency bands, evaluating the temporal course of the calculation was insightful as distinct findings were present depending on the minute analyzed. Regarding alpha band, its activity was increased mainly present in the first and third minutes suggesting distinct roles concomitant with time. A significant group (8 performers) had higher values of alpha coherence in the first minute, although I tried to find a special feature common to all subjects that could give a clue on why they all had more alpha coherence in this period I could not draw any conclusion. If this increase is related to cortical inhibition or it really does reflect a mechanism associated with the arithmetical process is hard to unveil.

In theta, I could not find a pattern showing a specific increase or decrease related with time, fluctuations are almost individual-specific. This absence of a temporal pattern should not be considered strange though, holding on the hypothesis advanced in the previous paragraph of theta coherence increasing only if the rate of calculation is high. It is impossible to ensure all individuals maintain a constant mental work during such a long time (3 minutes) and brief hesitations or stopping the calculation for seconds may reflect this variations in the theta band.

For beta distribution among the minutes, I underpinned more changes specially in the two last minutes, 10 individuals had greatest values of coherencies in the second minute.

In summary, a general conclusion of this part of the analysis is the lack of any consistent result which might permit a correlation with the strategy followed in the task. Nonetheless, it permitted to locate temporal constraints for alpha and beta and refined the results obtained comparing the whole period of basal and mental calculation.

Finally, relatively to the study of fronto-parietal network, the main conclusions based on the hypothesis made are resumed for the three bands.

Regarding the analysis of theta, the most part of individuals shown an augment within the fronto-parietal inter-hemispheric connections and for an expressive part combinations on the right side were also obtained, suggesting a lateralization of the theta band role. In the parietal connections though, there are fewer changes on the right side and five

individuals show greater connectivity on the left hemisphere following task. Results are not conclusive but clearly support the hypothesis of parietal regions of both hemispheres being involved in the mental calculation process, this is in agreement with several studies that relate this areas with approximate calculation and quantity representation (like [98], see Chapter 6). Alpha decreased consistently on the frontal pairs as it was expected. Moreover, the results suggest that functions of alpha region related to the task may be multiple, though intra-hemispherically coherence decreases in the most part of the cases, inter-hemispherical connections are increased in half of the cases and decreased in the remaining population. This partly agrees with the hypothesis of upper alpha augment in connectivity in the fronto-parietal connections. In the parietal combinations, alpha increased the right hemisphere and decreased in the left for two different groups of six performers supporting even more the hypothesis of different roles of alpha depending on the region. For beta, the most common tendency above all combinations is to increase specially in the frontal region, fronto-parietal connections did not reveal a clear pattern sustaining the hypothesis of augmenting beta within this network and parietal area shown changes bilaterally (once again, implicating both hemispheres).

Although results partly agreed with the hypothesis, in all cases to address conclusions based on the strategy used was really hard. Indeed, with such a small population and particularly in this case,with merely 5 individuals performing the task only with resource of calculation may be too difficult to overcome the confounds we cannot control with such a small group and drawing major conclusions is impossible.

Another point that is important to refer in the general discussion of this chapter is the fact that two performers possibly have altered mental conditions (though possess a not impaired arithmetic skill). Indeed, performer 3 has OCD (Obssessive-Compulsive Disorder) and performer 10 was depressed. I searched possible confounds related to this pathological states in the literature of coherence studies and I found OCD was correlated with higher theta coherence in fronto-occipital region [91] although in the present study that apparently was not verified in none of the conditions compared to the other performers. On a first analysis, we have no reasons to exclude the results of this individuals but one should assume that may exist other pathology-specific particularities still not well understood in the state-of-art research which can have an influence in the results.

To sum up, results could furnish a preliminary perspective on mental calculation picture, they could relate and made some preliminary analysis on the correlation of the frequency bands θ, α and β with the mental task followed, the patterns of connectivity that were more suggestive and expressive among the whole population may be associated with regional and temporal constraints of arithmetical computation. I will expose in the general discussion what are the most important limitations and propose some changes to

the protocol and analysis that may be helpful in obtaining more precise and consistent results.

Performer	Code	Gender	Age	Strategy for calculus	Final Number	Turns	Academic Level	Notes
1	DRP	M	30	Started to using exclusively calculus, from a certain point used the pattern Confirmed result in the multiples of 30.	72	2	Master, Biology and Geology	
2	RAMC	M	23	Only calculus, tried to use the pattern but quited. Usually visualized the numbers.	170	2	5th year, Physics Engineering	
3	PARS	M	29	Calculus.	167	2	Bachelor, Biology	Obsessive Compulsive Syndrome
4	LMBL	M	37	Only calculus, even after finding the pattern. Usually visualized the numbers like in a list.	200	2	Phd, Informatics	
5	SGS	F	32	Used the pattern 20 in 20. Visualized the results.	185	2	Bachelor, Biology	
6	PASS	M	38	Calculus and occasionally the pattern.	14	1	Master, Physics	
7	OCR	M	40	Used always the calculus, tried to use the pattern but quited.	73	2	Phd, Physics	Native Tongue: Castilian
8	SMMG	F	31	Used the calculus and termination (9,6,3) of the pattern. Started to do quicker the task when using the pattern.	180	2	Bachelor, Biology	
9	MFSA	F	37	Calculus and visualization of numbers.	148	2	Bachelor, English Teaching	
10	CSF	F	31	Calculus and part of pattern (9,6,3).	184	2	Bachelor, Informatics Teaching	
11	CPFRO	F	35	Showed much difficulties. Sometimes subtract 3, others 2. Used numerical termination (7,5,3,0). Great Level of mistakes.	125	1	Bachelor	
12	BTL	F	33	Calculus and part of pattern (9,6,3).	17	1	Master, Physics	Native tongue: French
13	RJGT	M	23	Calculus and termination (9,6,3) of the pattern. Started to do quicker the task when using the pattern. In the zero confirmed the result.	146	2	3rd year, Physics Engineering	
14	SRP	F	29	Calculus and termination (9,6,3). Started to do quicker the task when using the pattern. In the multiples of 30 confirmed the result.	38	2	Phd,Computational Chemistry	
15	LSGA	F	23	Tried to use the pattern.	69	1	4th year, Physics Engineering	

Table 8.1: *Table resuming some details about the volunteers. Performer 10 is the only one who is left-handed. Volunteers 4 and 11 are under medication. All subjects declared they have not any auditive, visual or neurological problem.*

Chapter 9

General Discussion and Conclusion

"The whole is not the sum of the parts." **Aristotle**

This chapter is organized in the following sequence: firstly, it will be discussed what are the main drawbacks and confounds of the experiments of this thesis then, a concise description of the main awards regarding the goals will be made. To finalize, possible extensions of future work will be briefly approached.

9.1 Discussion and Limitations

Initiating in a chronological order of the work planned, in Chapter 5, though the simulated data created made possible qualitative inferences and undoubtedly worked well as a preliminary evaluation of the algorithm for estimation coherence, the creation of more realistic sets of data could accurate the previsions.

In Chapter 7, although I could made some interesting comparisons, results of the dynamical analysis with Event-Related Coherence between adjacent electrodes were somehow limited, I hypothesized this must be due to highest sensibility of coherence to phenomenons of volume conduction that specially affect experiments with mastoid reference, the use of non-cephalic references or averaged reference (like it was used in Chapter 8) should minor a lot this spurious effects [86].

Still, regarding the goal of contrasting stationary and dynamical applications, a main conclusion is this type of dynamical approach as exposed in Chapter 7 seems to be a great way of detecting features induced by a task from the noisy background but a lot more research is needed relatively to the functional significance of the results. In [78]

is studied trough simulated data the polemic question - are the event-related potentials caused by coincident bursts of phasic neural activity or by between-regions synchronization of ongoing oscillatory activity? - the results were somehow inconclusive for either parts. Considering these potential pitfalls, a better control could be made if in the preprocessing of the data, more robust techniques were used to separate neural activity of different sources. Some techniques will be considered in the next section.

Regarding the experiment of Chapter 8, a discussion of the limitations should concern the experimental protocol and the analysis independently. For the former, a greater control of the impedance of the electrodes should be assured (their impedance should be below 5kOhms [26]), although only few had higher impedances and it is really difficult to counterbalance the amount of gel not to loose contact neither increase impedance this can pointed as a further improvement. Relatively to the second, a potential pitfall of a type of analysis that accounts for differences between a basal condition and a task is the fact that considering the new perspectives about brain's resting state as a strongly active network [85], a clear task-induced picture may be hard to depict if it is submersed in a complexer background. In simpler words, an important phenomenon of coupling can be happening in a frequency band although it did not appears relevant because coherence was higher in basal situation. Accordingly, [33] emphasizes a congruent line of thought, saying the signal-to-noise ratio in a mental task recording is very low due to the fact that the EEG amplitudes related with cognitive effort are 10 times smaller than the ones in a spontaneous background EEG and as though, all measures that depend on the amplitude of the signal could fail to determine relevant information. This is a limitation also of the previous experiment of Chapter 7.

In relation to the followed signal processing and analysis there are some implicit drawbacks. The work developed with simulated data in Chapter 5 shown the algorithm developed may not be completely accurate to be used in higher gamma frequencies (above 43 Hz), this results are merely suggestive and do not prove it will not work well on real EEG data. As I started stating in this discussion, for a more accurate validation of the algorithm, sets of data which mimic more faithfully EEG data must be used.

9.2 Contributes of the work done

There are few experiments done using coherence analysis and mental calculation and as though, a lot more work is needed before conclusions can be established. The most part of the experiments concerned merely the use of spectrum and other measures depending merely on the EEG amplitude. As it was concluded in the review by P. Sauseng, W.

Klimesch (2008) [87], EEG amplitude only reflects an unspecific brain activation meanwhile synchronization episodes (of which coherence is a particular case) seem to control the most specific brain processes, in which mental calculation is included. This study shown information of spectral content and coherence can be quite different (for example in Chapter 8 beta spectral significant differences were only present in half of the population meanwhile coherence was higher for all the subjects). In addition, I could draw some main conclusions, I will exemplify some of them in the next paragraphs.

The work in simulated data can be a way of assessing the performance of a certain measure.

Most of all strategies followed in the two chapters with real data furnish important data regarding how mental calculation is processed in the brain.

Both experiments with EEG recordings of mental calculation suggested strongly, relations between this tasks and connectivity within the θ, α and β bands, see details in the discussion of each chapter.

The results were positively concordant with previous studies on mental calculation.

Information on temporal scale of this spectral and coupling changes was also possible trough spectrograms (see Chapter 7 or tripartite analysis of the recordings of Chapter 8).

There are a lot of studies done using coherence, overall this thesis its importance in understanding pathologies or cognitive states was emphasized, particularly, mental calculation was studied experimentally. Understanding arithmetical skills can help in developing new strategies in pathologies such as acalculia and dyscalculia. Furthermore, it may aid improving brain-computer interface systems. Notwithstanding this panoply of applications, it is still a tool misrepresented in clinical practice and more studies urge towards an unification of knowledge that would simplify pragmatical applications.

9.3 Perspectives of future work

I will organize my discussion on the possible future work following two different lines of thought inherent to two distinct but correlated goals of the present dissertation: 1.validating and show the potentialities of the method of EEG coherence following the principals I used to implement it in mental calculation tasks and 2.establishing a view of how this mental processes arise in the brain that can be at least comparable with similar works on the specific field. For the former, I will enumerate some possible extensions and

corrections related to the experimental protocol and the analysis. Further, I will suggest other methodologies that seem promising for the second goal purposes.

Starting with the protocol, even though in the acquisition of data there was a concern to choose selectively a homogeneous group, the totality of performers should be higher to reduce lateral effects. EEG coherence is sensible to phenomenons as gender, handedness and there are even other specific aspects that may act as confounds. An interesting aspect is that certain personality types may account for differences in EEG frequencies, e.g. lesser anxious personalities display more theta oscillations [18]. Additively, to evaluate potential differences regarding different strategies (merely calculation and retrieval of the pattern) one could perform an additional task condition in which subtractions were made constantly to maintain the level of mental effort but with no relation among them (an appropriate sequence should be chosen carefully in order to minimize the possibilities of retrieval of some known facts), comparison among these two tasks could be helpful on this point.

Considering now the analysis, a possible improvement that could give even more significance to the coherence results concerns the preprocessing. It is easily recognizable that techniques such as dipole modeling, Independent Component Analysis (ICA), Principal Components Analysis (PCA) (see [95] and [100] for reference) could be used previously than the computation of coherence. Another interesting approach to minor the effects of volume conduction trough using merely the imaginary part of coherence is suggested by [43].

Still, improvements of the analysis could be to extend the study to gamma analysis, there are some evidences of its role in attentional processes and WM tasks [85] and at least to my knowledge there is not any experiences made using gamma coherence and mental calculation tasks. Nowadays, there is a crescent idea that gamma features are displayed locally and not in a long-range frame [87] so more robust techniques and methods which do not produce much spatial smearing seem more nature candidates to this type of analysis. Also studying delta waves could be interesting, they were already implicated in mental calculation studies [37].

To study higher frequency couplings (such as γ) we will probably need to use a different coherence algorithm, this work shown that coherence relying on the WOSA estimation may be limited. Although [12] criticized potential differences among techniques, the work of Chapter 7 suggested that other spectral decompositions such as the Wavelet Transform may detect a higher number of features. Also another technique to obtain phase information may be used to assess coupling, the Hilbert transform [77] is a measure of the time domain that performs better for narrow band signals. If these techniques are superior to Fourier analysis is still an ingoing debate.

Concerning the studied paradigm, there are further extensions of similar signal techniques that could be followed, it was recognized initially the hypothesis of studying the information contained only in the phase, the idea was analyzing phase delays in order to identify what would be the different stages/regions in the brain having an active role in the task in an chronological space. In this study, I only made analysis of spectral functions of second order such as power and coherence, yet it may also exist coupling among different frequencies and though higher order statistics could give further insights. In the study of [85] cross-frequency phase synchrony increasing was found between α and β bands in an intensive mental calculation task. Exploring also nonlinear coupling information seems also promising [107] and like the study of [1] affirms, linear and nonlinear measures of connectivity only agree in 37%.

Bibliography

[1] A. Meyer-Lindenberg, U. Bauer, S. K.-S. L. K. V. G. S., and Gallhofer, B. The topography of non-linear cortical dynamics at rest, in mental calculation and moving shape perception. *Brain Topography 10*, 4 (1998).

[2] Abeles. Role of the cortical neuron - integrator or coincidence detector. *Israel journal of medical sciences 18* (1982), 83–92.

[3] Abeles, E. S. . M. Applying resampling methods to neurophysiological data. *Journal of Neuroscience Methods 145* (2005), 133–144.

[4] Adam R. Clarke, Robert J. Barry, P. C. H. R. M. M. S. M. K. B. Eeg coherence in adults with attention-deficit/hyperactivity disorder. *International Journal of Psychophysiology 67* (2008), 35–40.

[5] Alexander Klein, Tomas Sauer, A. J., and Skrandies, W. Conventional and wavelet coherence applied to sensory–evoked electrical brain activity. *IEEE TRANSACTIONS ON BIOMEDICAL ENGINEERING, VOL. 53*, ,NO. 2 (February 2006), 266–272.

[6] andG. Pfurtscheller, C. A. Dependence of coherence measurements on eeg derivation type. *Med. & Biol, Eng. & Comput. 34* (1996), 232–28.

[7] Arnaud Delorme, S. M. Eeglab: an open source toolbox for analysis of single-trial eeg dynamics including independent component analysis. *Journal of Neuroscience Methods 134* (2004), 9–21.

[8] Azouz, R. Dynamic spatiotemporal synaptic integration in cortical neurons: Neuronal gain, revisited. *J Neurophysiol 94* (2005), 2785–2796.

[9] Baddeley, A. *Working Memory.* Clarendon Press, Oxford., 1986.

[10] Berger, H. Uber das elektroenkephalogramm des menschen. *Arch. Psychiatr. 87* (1929), 527–570.

[11] Borck, C. Between local cultures and national styles: Units of analysis in the history of electroencephalography. *C. R. Biologies 329* (2006), 450–459.

[12] Bruns, A. Fourier-, hilbert- and wavelet-based signal analysis: are they really different approaches? *Journal of Neuroscience Methods 137* (2004), 321–332.

[13] C. M. Gray P. Konig, A. K. Engel, W. S. Oscillatory responses in cat visual cortex exhibit inter-columnar synchronization which reflects global stimulus properties. *Nature 338* (1989), 334–337.

[14] Caramazza, A., and McCloskey, M. *Mathematical Disabilities. A Cognitive Neuropsychological Perspective.* Lawrence Erlbaum, Hillsdale, 1987, ch. Dissociations of calculation processes., pp. 221–234.

[15] Carter, G. C. Coherence and time delay estimation. In *PROCEEDINGS OF THE IEEE, VOL. 75, NO. 2* (1987).

[16] Challis, R. E. Kitney, R. I. Biomedical signal processing (in four parts) part 3 the power spectrum and coherence function. *Med. & Biol, Eng. & Comput. 29* (1991), 225–241.

[17] Cohen, A., and Kovacevic, J. Wavelets: the mathematical background. *Proceedings of the IEEE 84, no.4* (1996).

[18] Damon J. Mitchell, Neil McNaughton, D. F. I. J. K. Frontal-midline theta from the perspective of hippocampal "theta". *Progress in Neurobiology 86* (2008), 156–185.

[19] Dan-Marius Dobrea, Monica-Claudia Dobrea, M. C. An eeg coherence based method used for mental tasks classification. *IEEE* (2007).

[20] Daubechies, I. The wavelet transform, time-frequency localization and signal analysis. *IEEE TRANSACTIONS ON INFORMATION THEORY 36* (1990).

[21] Daubechies, I. Where do wavelets come from?- a personal point of view. *PROCEEDINGS OF THE IEEE 84, no.4* (1996).

[22] David Balin Chorlian, M. R., and Porjesz, B. Eeg coherence: topography and frequency structure. *Exp Brain Res* (2009).

[23] Dehaene, S., . C. L. Cerebral pathways for calculation: Double dissociation between rote verbal and quantitative knowledge of arithmetic. *Cortex 33(2)* (1997), 219–250.

[24] Dehaene, S. Varieties of numerical abilities. *Cognition 44* (1992), 1–42.

[25] Delorme, A. Statistical methods.

[26] Durka, K. B. . P. *Wiley Encyclopedia of Biomedical Engineering*. John Wiley & Sons, Inc, 2006, ch. Electroencephalography (EEG), pp. 1–15.

[27] Eric R. Kandel, James H. Schwartz, T. M. J. *Principles of Neural Science*, fourth edition ed. H.L. John Butler, 2000.

[28] Ernst Niedermeyer, F. H. L. D. S. *Electroencephalography - Basic Principles, Clinical Applications and Related Fields*. Lippincott Williams and Wilkins, 2004.

[29] Essl, M., and Rappelsberger, P. Eeg coherence and reference signals: experimental results and mathematical explanations. *Medical & Biological Engineering and Computing 36* (July 1998), 399–406.

[30] et al, H. P. Z. Measuring the coherence of intracranial electroencephalograms. *Clinical Neurophysiology 110* (1999), 1717–1725.

[31] et al., J.-P. L. Estimating the time-course of coherence between single-trial brain signals: an introduction to wavelet coherence. *Neurophysiol Clin 32* (2002), 157–74.

[32] et al., J.-S. B. Single-trial multiwavelet coherence in application to neurophysiological time series. *IEEE TRANSACTIONS ON BIOMEDICAL ENGINEERING 54 no. 5* (2007).

[33] et al, L. R. Visualizing cortical activation during mental calculation with functional mri. *Neuroimage 3* (1996), 97–103.

[34] et al, M. K. K. Comparison of stft and wavelet transform methods in determining epileptic seizure activity in eeg signals for real-time application. *Computers in Biology and Medicine 35* (2005), 603–616.

[35] et al, P. L. N. Eeg coherency ii:experimental comparisons of multiple measures. *Clinical Neurophysiology 110* (1999), 469–486.

[36] et al, R. S.-C. Understanding dissociations in dyscalculia - a brain imaging study of the impact of number size on the cerebral networks for exact and approximate calculation. *Brain 123* (2000), 2240–2255.

[37] et al, T. H. Do specific eeg frequencies indicate different processes during mental calculation? *Neuroscience Letters 266* (1999), 25±28.

[38] Francisco Varela, Jean-Philippe Lachaux, E. R., and Martinerie, J. The brainweb: phase synchronization and large-scale integration. *Nature Reviews in Neuroscience 2* (April 2001), 229–239.

[39] G. Tononi, A. McIntosh, D. R. G. E. Functional clustering: identifying strongly interactive brain regions in neuroimaging data. *Neuroimage 7(2)* (1998), 133– 49.

[40] Ganong, W. F. *Review of Medical Physiology*, 21st edition ed. McGraw-Hill, 2003.

[41] GREGORY A. TROUP, J. L. B., and NETTLETON, N. C. The lateralization of arithmetic and number processing: A review. *Intern. J. Neuroscience Vol. 19* (1983), 231–142.

[42] Grossmann, A., and Morlet, J. Decomposition of hardy functions ito square integrable wavelets of constant shape. *SIAM J . Math. Anal. 15* (1984), 723–736.

[43] Guido Nolte, Ou Bai, L. W. Z. M. S. V. M. H. Identifying true brain interaction from eeg data using the imaginary part of coherency. *Clinical Neurophysiology 115* (2004), 2292–2307.

[44] Harriet W. Hanlon, Robert W. Thatcher, M. J. C. Gender differencies in the development of eeg coherence in normal children. *Developmental Neuropsychology 16(3)* (1999), 479–506.

[45] Harris, C. M. The fourier analysis of biological transients. *Journal of Neuroscience Methods 83* (1998), 15–34.

[46] Harris, F. J. On the use of windows for harmonic analysis with the discrete fourier transform. *PROCEEDINGS OF THE IEEE 66 no. 1* (1978).

[47] Hemant Bokil, Keith Purpura, J.-M. S. D. T. P. M. Comparing spectra and coherences for groups of unequal size. *Journal of Neuroscience Methods 159* (2007), 337–345.

[48] Hideo Tohgi, Kou Saitoh, S. T. H. T. K. U. H. Y. K. H. T. S. Agraphia and acalculia after a left prefrontal (f1, f2) infarction. *Journal of Neurology, Neurosurgery, and Psychiatry 58* (1995), 629–632.

[49] Inouye, T., S. K. I. A., and Matsumoto, Y. Localization of activated areas and directional eeg patterns during mental arithmetic. *Electroencephalogr. Clin. Neurophysiol. 86* (1993), 224–230.

[50] J.-P. Lachaux, E. Rodrigues, J. M., and Varela, F. J. Measuring phase synchrony in brain signals. *Human Brain Mapping 8* (1999), 194–208.

[51] J. Sarnthein, A. Morel, A. v. S. D. J. Thalamocortical theta coherence in neurological patients at rest and during a working memory task. *International Journal of Psychophysiology 57* (2005), 87 – 96.

[52] J. Theiler, S. Eubank, A. L. B. G., and Farmer, J. D. Testing for nonlinearity in time series: The method of surrogate data. *Physica D 58* (1992), 77–94.

[53] Javier J Gonzalez-Rosa, Manuel Vazquez-Marrufo, E. V. P. D. M. B. M. A. G. C. M. G., and Izquierdo, G. Differential cognitive impairment for diverse forms of multiple sclerosis. *BMC Neuroscience 7:39* (2006).

[54] Jin'an Guan, Y. C. Single-trial eeg classification using in-phase average for brain-computer interface. *Front. Electr. Electron. Eng. China 3(2)* (2008), 194–197.

[55] John G. Proakis, D. G. M. *Digital Signal Processing - Principles, Algorithms, and Applications*, 3rd ed. 1996.

[56] J.V. Baldo, N. D. Neural correlates of arithmetic and language comprehension: A common substrate? */ Neuropsychologia* - (2006), (In press).

[57] K. Sasaki, H. G. A. N.-S. K. R. M. T. T. Studies on integrative functions of the human frontal association cortex by use of meg. *Electroencephalogr. Clin. Neurophysiol. Suppl. 47* (1996a), 181–190.

[58] Kaiser, D. A. What is quantitative eeg? *Journal of Neurotherapy 10 (4)* (2006).

[59] Kannan Ramchandran, M. V., and Herley, C. Wavelets, subband coding, and best bases. *PROCEEDINGS OF THE IEEE, NO. 4, APRIL 1996 VOL. 84, NO. 4* (1996).

[60] Kawashima, R., T. M. O. K.-I. K. T. N. Y. H. S. T. S. M. W. J. . F. H. A functional mri study of simple arithmetic – a comparison between children and adults. *Cognitive Brain Research 18* (2004), 225–231.

[61] Klimesch, P. S. . W. What does phase information of oscillatory brain activity tell us about cognitive processes? *Neuroscience and Biobehavioral Reviews 32* (2008), 1001–1013.

[62] K.Sasaki, A. Nambu, T. T. R. M. S. K. H. G. Studies on integrative functions of the human frontal association cortex with meg. *Brain Res. 5* (1996), 165–174.

[63] Laine, A. F. Wavelets in temporal and spatial processing of biomedical images. *Annu. Rev. Biomed. Eng. 02* (2000), 511–50.

[64] Landsman, A. S., and Schwartz, I. B. Synchronized dynamics of cortical neurons with time-delay feedback. *Nonlinear Biomedical Physics 1:2* (2007).

[65] Laurent, C. K. . G. Complexity and the nervous system. *Science 284(5411)* (1999), 96–98.

[66] Letizia Leocani, Tiziana Locatelli, V. M. M. R. M. F. M. F. G. M. G. C. Electroencephalographic coherence analysis in multiple sclerosis: correlation with clinical, neurophysiological, and mri findings. *J Neurol Neurosurg Psychiatry 69* (2000), 192–198.

[67] Liu, P. *Wavelets in geophysics.* Academic Press, 1994, ch. Wavelet spectrum analysis and ocean wind waves, pp. p.151–66.

[68] Luca Faes, Gian Domenico Pinna, A. P. R. M., and Nollo, G. Surrogate data analysis for assessing the significance of the coherence function. *IEEE TRANSACTIONS ON BIOMEDICAL ENGINEERING 51 no.7* (2004).

[69] Mallat, S. G. Multifrequency channel decompositions of images and wavelets models. *IEEE TRANSACTIONS ON ACOUSTICS, SPEECH AND SIGNAL PROCESSING 37* (1989).

[70] Margaret G. Funnell, Mary K. Colvin, M. S. G. The calculating hemispheres: Studies of a split-brain patient. *Neuropsychologia 45* (2007), 2378–2386.

[71] Maria G. Knyazeva, G. M. I. Eeg coherence studies in the normal brain and after early-onset cortical pathologies. *Brain Research Reviews 36* (2001), 119–128.

[72] Menon, V., R. S. W. C. E. S. G. G. . R. A. Functional optimization of arithmetic processing in perfect performers. *Cognitive Brain Research 9* (2000), 343–345.

[73] Meyers, S. D., B. G. K., and O'Brien, J. J. An introduction to wavelet analysis in oceanography and meteorology with application to the dispersion of yanai waves. *Mon. Wea. Rev. 121* (1993), 2858–2866.

[74] Michael J. Hogana, Gregory R.J. Swanwicka, J. K. M. R. B. L. Memory-related eeg power and coherence reductions in mild alzheimer's disease. *International Journal of Psychophysiology 49* (2003), 147–163.

[75] MICHAEL RUDOLPH, A. D. Tuning neocortical pyramidal neurons between integrators and coincidence detectors. *Journal of Computational Neuroscience 14* (2003), 239–251.

[76] Michael S. Gazzaniga, Richard B. Ivry, G. R. M. *Cognitive Neuroscience: The biology of the mind.*, 2nd ed. W. W. Norton & Company, Inc, 2002.

[77] Michel Le Van Quyen, Jack Foucher, J.-P. L. E. R. A. L. J. M. F. J. V. Comparison of hilbert transform and wavelet methods for the analysis of neuronal synchrony. *Journal of Neuroscience Methods 111* (2001), 83–98.

[78] Nick Yeung, Rafal Bogacz, C. B. H.-J. D. C. Detection of synchronized oscillations in the electroencephalogram: An evaluation of methods. *Psychophysiology 41* (2004), 822–832.

[79] Nokes, L; Jennings, D. F. T. T. *Introduction to Medical Electronics Applications.* Butterworth-Heinemann, 1995, ch. Chapter 4: Physiological Instrumentation.

[80] Northrop, R. G. *Signals and Systems Analysis in Biomedical Engineering.* CRC Press, 2003.

[81] Ole Jensen, Jack Gelfand, J. K., and Lisman, J. E. Oscillations in the alpha band (9-12 hz) increase with memory load during retention a short-term memory task. *Cerebral Cortex* (2002), 877–882.

[82] P. Goupillaud, A. G., and Morlet, J. Cycle-octave and related transforms in seismic signal analysis. *Geoaploration, vol. 23, p. 85, 1984 23* (1984), 85.

[83] P. Rajna, É. Csibri, I. P. W. S. Task related difference eeg spectrum – a new diagnostic method for neuropsychiatric disorders. *Medical Hypotheses 61(3)* (2003), 390–397.

[84] Palva, J. e. a. Phase synchrony among neuronal oscillations in the human cortex. j. neurosci. 25, 3962–397. *J. Neurosci. 25* (2005), 3962–3972.

[85] Palva, S., and Palva, J. M. New vistas for a-frequency band oscillations. *TRENDS in Neurosciences Vol.30*, No.4 (2007).

[86] Paul L. Nunez, Ramesh Srinivasan, A. F. W. R. S. W. D. M. T. R. B. S. P. J. C. Eeg coherency i:statistics, reference electrode, volume conduction, laplacians, cortical imaging, and interpretation at multiple scales. *Electroencephalography and clinical Neurophysiology 103* (1997), 499–515.

[87] Paul Sauseng, Wolfgang Klimesch, M. S. M. D. Fronto-parietal eeg coherence in theta and upper alpha reflect central executive functions of working memory. *International Journal of Psychophysiology 57* (2005), 97 – 103.

[88] Pesenti, M., Z. L. C. F. M. E. S. D. D. B. S. X. M. B. T.-M. N. Mental calculation in a prodigy is sustained by right prefrontal and medial temporal areas. *Nature Neuroscience 4* (2001), 103–107.

[89] Peter Koenig, A. K. E., and Singer, W. Integrator or coincidence detector? the role of the cortical neuron revisited. *Trends Neurosci. 19* (1996), 130–137.

[90] Pierre Burbaud, Olivier Camus, D. G. B. B. J.-M. C. M. A. A functional magnetic resonance imaging study of mental subtraction in human subjects. *Neuroscience Letters 273* (1999), 195±199.

[91] PUSHPAL DESARKAR, VINOD KUMAR SINHA, K. J., and NIZAMIE, S. H. Subcortical functioning in obsessive-compulsive disorder: An exploratory eeg coherence study. *The World Journal of Biological Psychiatry 8(3)* (2007), 196–200.

[92] Quiroga, R. Q. *Quantitative analysis of EEG signals: Time-frequency methods and Chaos theory.* PhD thesis, Institute of Physiology - Medical University Lubeck and Institute of Signal Processing - Medical University Lubeck, 1998.

[93] R. Saab, M. J. McKeown, L. J. M., and Abu-Gharbieh, R. A wavelet based approach for the detection of coupling in eeg signals. In *Proceeddings of the 2nd International IEEE EMBS-Conference on Neural Engineering* (2005).

[94] Ramesh Srinivasan, William R. Winter, J. D. P. L. N. Eeg and meg coherence:measures of functional connectivity at distinct spatial scales of neocortical dynamics. *Journal of Neuroscience Methods 166* (2007), 41–52.

[95] Ritter, P., and Villringer, A. Simultaneous eeg-fmri. *Neuroscience and Biobehavioral Reviews 30* (2006), 823–838.

[96] Rivera, S.M., R. A. E. M. M. V. Developmental changes in mental arithmetic: Evidence for increased functional specialization in the left inferior parietal cortex. *Cerebral Cortex 15* (2005), 1779–1790.

[97] Ruchkin, D. Eeg coherence. *International Journal of Psychophysiology 57* (2005), 83–85.

[98] S. Dehaene, e. a. Sources of mathematical thinking: Behavioral and brain-imaging evidence. *Science 284* (1999), 970.

[99] S. Laughlin, T. S. Communication in neuronal networks. *Science 301(5641)* (2003), 1870–4.

[100] Saeid Sanei, J. A. C. *EEG Signal Processing.* John Wiley and Sons Ltd., 2007.

[101] Schwilden, H. Concepts of eeg processing: from power spectrum to bispectrum, fractals, entropies and all that. *Best Practice & Research Clinical Anaesthesiology 20 no. 1* (2006), 31–48.

[102] Shaw, J. C. An introduction to the coherence function and its use in eeg signal analysis. *Journal of Medical Engineering & Technology 5:6* (1981), 279 — 288.

[103] Shibasaki, H. Human brain mapping:hemodynamic response and electrophysiology. *Clinical Neurophysiology 119* (2008), 731–743.

[104] Singer, W. Neuronal synchrony: A versatile code for the definition of relations? *Neuron 24* (1999), 49–65.

[105] Smith, S. W. *The Scientist and Engineer's Guide to Digital Signal Processing.* 1997.

[106] Srinivasan, N. Cognitive neuroscience of creativity: Eeg based approaches. *Methods 42* (2007), 109–116.

[107] Stam, C. Nonlinear dynamical analysis of eeg and meg: Review of an emerging field. *Clinical Neurophysiology 116* (2005), 2266–2301.

[108] Stephane A. Roy, K. D. A. Coincidence detection or temporal integration? what the neurons in somatosensory cortex are doing. *The Journal of Neuroscience 21(7)* (2001), 2462–2473.

[109] Stephanie C. Manson, Jacqueline Palace, J. A. F. P. M. M. Loss of interhemispheric inhibition in patients with multiple sclerosis is related to corpus callosum atrophy. *Exp Brain Res 174* (2006), 728–733.

[110] Steven A. Prescott, Stèphanie Ratte, Y. D. K. T. J. S. Nonlinear interaction between shunting and adaptation controls a switch between integration and coincidence detection in pyramidal neurons. *The Journal of Neuroscience 26(36)* (2006), 9084 –9097.

[111] Stevens, V. K. . C. Connectivity optimization and the positioning of cortical areas. *Proceedings of the National Academy of Science USA 100(13)* (2003), 7937–47.

[112] Susanne Reiterer, Claudia Hemmelmann, P. R. M. L. B. Characteristic functional networks in high- versus low-proficiency second language speakers detected also

during native language processing: An explorative eeg coherence study in 6 frequency bands. *Cognitive Brain Research 25* (2005), 566 – 578.

[113] T. Ishihara, N. Y. Multivariate analytic study of eeg and mental activity in juvenile delinquents. *Electroencephalogr. Clin. Neurophysiol. 33* (1972), 71–80.

[114] T. Koenig, D. Studer, D. H. L. M. W. K. S. Brain connectivity at different time-scales measured with eeg. *Phil. Trans. R. Soc. B 360* (2005), 1015–1024.

[115] Tallon-Baudry, C., B. O. D. C. . P. J. Stimulus specificity of phase-locked and non-phase-locked 40 hz visual responses in human. *Journal of Neuroscience 16(13)* (1996), 4240–4249.

[116] Thakor, N. V., and Tong, S. Advances in quantitative electroencephalogram analysis methods. *Annu. Rev. Biomed. Eng. 6* (2004), 453–95.

[117] Thalía Fernández, Thalía Harmony, M. R. J. B. J. S. A. R. E. M. Eeg activation patterns during the performance of tasks involving different components of mental calculation. *Electroencephalography and clinical Neurophysiology 94* (1995), 175–182.

[118] Thomeer, E.C., S. C., and van Woerkom, T. Eeg changes during mental activation. *Clin. Electroencephalogr. 25* (1994), 94–98.

[119] Thomson, D. J. Spectrum estimation and harmonic analysis. *Proceedings of the IEEE 70,no 9* (1982), 1055–1096.

[120] Thomson, R. D. M. . D. J. Robust resistant spectrum estimation. *Proceedings of the IEEE 70,no 9* (1982), 1097–1115.

[121] Tognoli, E., and Kelso, J. S. Brain coordination dynamics: True and false faces of phase synchrony and metastability. *Progress in Neurobiology 87* (2009), 31–40.

[122] Torrence, C., and Compo, G. P. A practical guide to wavelet analysis. *Bulletin of the American Meteorological Society* (1998).

[123] Unser, M., and Aldroubi, A. A review of wavelets in biomedical applications. *PROCEEDINGS OF THE IEEE 84, no.4* (1996).

[124] Van Milligen B, Sanchez E., E. T. H. C. B. B. C. B. Wavelet bicoherence: a new turbulence analysis tool. *Phys Plasmas 2* (1995), 3017–32.

[125] Von Stein, A., S. J. Different frequencies for different scales of cortical integration: from local gamma to long range alpha/theta synchronization. *Int. J. Psychophysiol. 38* (2000), 301–313.

[126] Webster, J. G. *Medical Instrumentation - Application and Design*, 3rd edition ed. John Wiley & Sons, 1998.

[127] Weiss, S., and Mueller, H. M. The contribution of eeg coherence to the investigation of language. *Brain and Language 85* (2003), 325–343.

[128] Yang Zhan, David Halliday, P. J. X. L. J. F. Detecting time-dependent coherence between non-stationary electrophysiological signals— a combined statistical and time–frequency approach. *Journal of Neuroscience Methods 156* (2006), 322–332.

[129] ZHANG Yun-ting, ZHANG Quan, Z. J., and Wei, L. Lateraliy of brain areas associated with arithmetic calculations revealed by functional magnetic resonance imaging. *Chinese Medical Journal 118(8)* (2005), 633–638.

[130] Zoltán Hidasi, Balázs Czigler, P. S. v. C. M. M. Changes of eeg spectra and coherence following performance in a cognitive task in alzheimer's disease. *International Journal of Psychophysiology 65* (2007), 252–260.

Appendix 1

```
%Function to create data for testing the condition of phase modulation with
%a mix spectrum of sines. The noise introduced in the phase is an uniform
%white noise with uniform distribution.


function generate_simulationPM= generate_simulationPM


rand('state',0);
fs = 256; % Sampling frequency
t =(0:fs*120)/fs; % sequence of 2 minutes
m=0;

for m=0:0.1:1 %running trough all the levels of noise

xn = 0.7*sin(2*pi*6*t + (a/pi*e)*rand(size(t)))+ sin(2*pi*10*t +
(a/pi*e)*rand(size(t))) + 0.6*sin(2*pi*14*t + (a/pi*e)*rand(size(t))) +
0.8*sin(2*pi*22*t + (a/pi*e)*rand(size(t)))+ 0.4*sin(2*pi*43*t +
(a/pi*e)*rand(size(t)));
yn=  0.7*sin(2*pi*6*t + (a/pi*e)*rand(size(t)))+ sin(2*pi*10*t +
(a/pi*e)*rand(size(t))) + 0.6*sin(2*pi*14*t + (a/pi*e)*rand(size(t)))
+ 0.8*sin(2*pi*22*t + (a/pi*e)*rand(size(t)))+ 0.4*sin(2*pi*43*t +
(a/pi*e)*rand(size(t)));

xn=xn(:);
yn=yn(:);


end
```

```
filename = sprintf('simulationPM_%1.1d.mat',a);
save(filename,'xn','yn');

-----------------------------//-----------------------------------------------

function [sl,slf,df,F,Coh_matrix] = surrogation1_simulations(file)


%Function to calculate coherence in simulated data with
% significant thresholds calculated through a surrogation
% procedure(FFT surrogates- randomization of the phases).


fs=256;
i=0;
nfft=256;
noverlap=256/2;
global Cxy
sdata1=0;
sdata2=0;
p=0.95
plot_position=1;

Coh_matrix=[ Cxy(:)'; zeros(i-1,length(Cxy))];

 for c1=1:2:size(file,2)

   for  c2=2:2:size(file,2)

         if c1== c2-1

                 cs1=file(:,c1);
                 cs2=file(:,c2);

             [Cxy_normal,F1]=mscohere(cs1,cs2,hann(512),noverlap,nfft,256);
```

```
     for (i=0:99) %starting the cycles i to reach statistical significance

                  display(sprintf('Processing trial number %d',i))


                  N1 = length(cs1); %number of points
                  N2 = length(cs2);
                  r1 = abs(fft(cs1))/(N1/2); %absolute value of the fft
                  r1 = r1(1:N1/2);
                  r2 = abs(fft(cs2))/(N1/2);
                  r2 = r2(1:N1/2);

      if rem(nfft, 2) %multiply by 2 to retain the same amount of energy
%(not multiply the DC or Nyquist components)
              r1(2:end) = r1(2:end)*2;
              r2(2:end) = r2(2:end)*2;
        else
              r1(2:end -1) = r1(2:end -1)*2;
              r2(2:end -1) = r2(2:end -1)*2;
      end

freq = [0:N1/2-1]*fs/N1; %find the corresponding frequency in Hz.

%part 2:surrogation

r1 = r1 + (pi*e)*rand(size(r1));

sdata1 = ifft(r1);
sdata1 = sdata1(:);


sdata2 = r2;
sdata2 = sdata2(:);

[Cxy,F2]=mscohere(sdata1,sdata2,hann(512),noverlap,nfft,256);
```

```
Coh_matrix(i+1,:) = Cxy(:)';

figure
close all

end % loop of the number of trials i.


[n,xx]=hist(Coh_matrix,50);
nc = cumsum(n)
slf = zeros(1,size(nc,2));
for k = 1:size(nc,2)
  [nn,ii] = unique( nc(:,k) );
   slf(k) = interp1( nn, xx(ii), 100*p, 'linear', 0 );
end
sl = mean(slf);

subplot(4,3,plot_position)

axis([0 60 0 1])
plot(F1,Cxy_normal,'g')
hold on
axis([0 60 0 1])
plot(F2,slf)
hold off
title(sprintf('MSC channels  %d %d case %s, ',c1,c2,inputname(1)));
xlabel('Frequency [Hz]');
ylabel('Magnitude');


filename =sprintf('surrogation_data1sim_%s_%d%d.mat',inputname(1),c1,c2);
save(filename,'sdata1','sdata2','Coh_matrix','slf','sl');

plot_position=plot_position + 1;

     end %end of condition if c1==c2-c1
```

```
  end %loop of the channels c1

end %loop of the channels c2
```

Appendix 2

```
%This function implements the Event-related Cross-Phase coherence among
%all channel combinations (excluding redundancies) using the EEGLAB function
%newcrossf(), here it is implemented using wavelet time-frequency decomposition.

function ERphase_coherence = ERphase_coherence(condition)


c1 = [1 2 3 4 ];

c2 = [1 2 3 4];

display(sprintf('Processing Condition %d',condition));

setname = sprintf('test%d_epochs.set', condition);

[ALLEEG EEG CURRENTSET ALLCOM] = eeglab;
EEG = pop_loadset(setname, '\C:\Program Files\MATLAB71\work\');
for cs1 = 1 : length(c1)
for cs2 = 1 : length(c2)

if (c1(cs1) ~= c2(cs2) && (cs1 < cs2))

display(sprintf('Channels %d with %d',c1(cs1),c2(cs2)));
figure

[coh, mcoh] = pop_newcrossf( EEG, 1, c1(cs1), c2(cs2), [-1000 2000], [2 0.5] ,
'winsize',[128],'type','phasecoher', 'topovec', [c1(cs1) c2(cs2)], 'elocs',
EEG.chanlocs,'title','Phase Coherence','alpha',0.05,'padratio', 4,'boottype',
'rand','naccu',100);
```

```
close all

    end
  end
end

filename = sprintf('ERphasecoherence_%d.mat', cond);
save(filename, 'coh', 'mcoh')
```